Universe Beyond Inflation and ΛCDM

by

Hyung Jin Kim

A thesis
presented to the University of Waterloo
in fulfillment of the
thesis requirement for the degree of
Doctor of Philosophy
in
Applied Mathematics

Waterloo, Ontario, Canada, 2021

Examining Committee Membership

The following served on the Examining Committee for this thesis. The decision of the Examining Committee is by majority vote.

External Examiner:	Matteo R. Fasiello IFT Madrid
Supervisor(s):	Ghazal Geshnizjani Florian Girelli
Internal Member:	Achim Kempf Eduardo Martin-Martinez
Internal-External Member:	Latham Boyle Dept. of Physics, University of Waterloo

Author's Declaration

This thesis consists of material all of which I authored or co-authored: see Statement of Contributions included in the thesis. This is a true copy of the thesis, including any required final revisions, as accepted by my examiners.

I understand that my thesis may be made electronically available to the public.

Statement of Contributions

This thesis is written under the supervision of Ghazal Geshnizjani. I was the sole author for the chapter 1 and 6.

The research in chapter 2 is based on a published paper [41], written under supervision of Ghazal Geshnizjani with collaborators Supranta S. Boruah and Michael Rouben. The calculations in section 2.2 were originally done by Ghazal Geshnizjani and Michael Rouben. I did the original calculations in following sections, which were crosschecked with the original calculations by Supranta S. Boruah. I was a main contributor in writing the manuscript with contributions from all coauthors.

I am the sole author of 3, with the manuscript reviewing the works of [50, 27].

The chapter 4 is based on a published paper [20] and a paper in progress. The computations of higher order perturbation terms, numerical computation of the power spectrum, computation of f_{NL} and the parameter space terms are my original computations and codes in sections 4.2 to 4.7. I also have a major contribution in writing the manuscript.

The chapter 5 is based on a published paper [100]. This is a project I did with Arman Shafieloo and Benjamin L'Huillier while I was visiting Korea Astronomy and Space Science Institute (KASI). The original idea was conceptualized by Arman Shafieloo. I contributed in discussions leading to completion of the paper. All of the computations in this chapter were done separately by me and Benjamin L'Huillier, which then were crosschecked with each other.

Abstract

The current paradigm of universe, ΛCDM model with an early phase of inflation, has been quite successful in describing our universe in a simple manner, yet matching well with the observational evidence. This model is a parameterization of the Big Bang theory with the universe composed of the three major components: the Cold Dark Matter (CDM) and the cosmological constant Λ accounting for the dark energy, and ordinary radiation and matter (relativistic and non-relativistic particles from standard model). However, there are some questions and puzzles yet to be solved or addressed. In the aspect of the early universe, the cosmic inflation has been successful in resolving problems such as the horizon problem, flatness problem, yet it fails to answer some other remaining puzzles such as the singularity problem and fitting in standard theory of particle physics. In part I, I explain two different approaches to tackle these issues. First, I will show how singularity can be avoided in a bouncing universe realized through a Cuscuton modification of gravity, without any instabilities. Second, I will demonstrate how the effective field theory of inflation can be extended to include k^6 terms in the dispersion relations. I will also show that there exists regions of parameter space that are allowed by the observational evidence.

In the context of the late universe, one of the challenges ΛCDM model faces is the detection of, or lack thereof, dark matter. Without the existence of cold dark matter, Einstein's theory of gravity fails to explain some of the observed gravitational effects in large scale structures such as rotation curves for galaxies. Furthermore, the measured upper bound to the cosmological constant is much smaller than the theoretical value of zero-point energy suggested by quantum field theory. To resolve such questions, other theories and models of universe such as theories of modified gravity and other dark energy models have been proposed. In the part II, a model-independent approach to constrain cosmological parameters and different expansion histories will be demonstrated. Interestingly, with the precision of current data it seems that the observation favor ΛCDM model.

Acknowledgements

I would like to thank all the people who made this thesis possible.

I would especially thank my supervisor Ghazal Geshnizjani for the support and guidance throughout my PhD.

I would like to thank all my collaborators including Niayesh Afshordi, Amjad Ashoorioon, Supranta Sarma Boruah, Arman Shafieloo, Benjamin L'Hullier.

I would also like to thank my family and my fiancee for always being there for me and supporting me.

Finally, I thank the University of Waterloo, and all the staffs and administrative members of the University. I acknowledge the support of the Natural Sciences and Engineering Research Council of Canada (NSERC) for my research during my PhD program.

Table of Contents

List of Figures

Chapter 1

Introduction and Background

1.1 Introduction

Cosmology, the study of cosmos, has always been a great interest to mankind. It is a field that involves the origin and the evolution of the universe we live in. It is a field that looks into fundamental questions 'where do we come from' and 'how will everything end?' It is a field that has been brought up in mythologies, religions, and philosophy. In ancient times, the universe has been described using mankind's imaginations and by ideas of supernatural forces. However, with the development of scientific methods, mathematical tools, and technology, came more mathematical models and scientific theories of the universe such as Copernicus' suggestion of a heliocentric universe, Kepler's laws, and Newton's theory of gravity. Modern cosmology is considered to begin with Einstein's development of the general theory of relativity (General Relativity or GR) in the early 1900s. Not too long after Einstein's theoretical breakthrough, a major observation of expanding universe set the modern cosmology afoot [141].

The confirmation of the expanding universe and the development of GR lead to the realization that as we go far back into the past, the universe was very hot, dense and compact[81]. This era, the beginning of the universe is called the **Big Bang** era. The early cosmological models of Big Bang era could not address some puzzles. For example, the size of the observable universe that may be inferred from the cosmic microwave background (CMB) observations with the assumption of the Big Bang model is multiple order of magnitude larger than the particle horizon, yet the causally disconnected regions of space were homogeneous and isotropic at the scale of the observable universe. The proposal of cosmic inflation, a phase of accelerated expansion during the very early universe, managed to answer few puzzles of the early Big Bang theory, including the problem mentioned above. However, as we discuss in this thesis, there are still unanswered questions and puzzles in the context of the early universe.

There also remain cosmological puzzles in the context of late universe. Current astrophysical observations indicate that the composition of the visible matter in universe can not account for all of the observed gravitational effects in large scale structures such as galaxy rotation curves [147].

Cosmologists have postulated the existence of cold dark matter (CDM), which are non-relativistic particles that do not interact with electromagnetic waves, but have gravitational effects similar to Baryonic matter can resolve this puzzle. The detection of dark matter particles has become one of the highest priorities of experimental particle physics. Furthermore, the supernovae observation followed by CMB observation have independently show that our universe is currently expanding at an accelerated rate[123, 90]. Since the ordinary energy and matter components of the universe, including dark matter could not account for this acceleration, there must either exist another energy component that causes accelerated expansion, dark energy or Einstein's theory of gravity most be modified at very large scales. The most simple proposal for the identity of dark energy is the cosmological constant, Λ. This set of ideas to explain the dynamics and initial condition of our universe is referred to as the ΛCDM model, and is now the most widely accepted paradigm of modelling our cosmos.

In the first part of this thesis, I will attempt to describe some new approaches in addressing some of the puzzles of the physics of the early universe. In the second part, I will describe a technique in applying observations to constrain different models of dark energy. However, in this chapter, I will briefly review the fundamentals of the theory of GR, basics of cosmology and the inflationary models, which will allow the readers to understand the work done in the following chapters. In chapter 2, our proposal to address the Big Bang singularity, Cuscuton bounce, will be explained. In chapter 3, we switch gear and review a particular strategy to study inflation as an effective field theory. In this approach, the action of cosmological perturbations around inflating Friedmann-Lemaître-Robertson-Walker (FLRW) backgrounds can be obtained by writing the most generic diffeomorphism invariant effective field theory, where time diffeomorphism is spontaneously broken. In chapter 4 we show this theory can be further extended to include dispersion relation $w(k)$ up to $w^2 \propto k^6$. Furthermore, we study the interaction terms for the extended effective field theory of inflation and study the constraints on the theory from the size of non-Gaussianities. In Chapter 5, we shift our focus to late universe. I describe a framework to reconstruct the expansion history of universe from growth rate measurements, and put model-independent constrains on some important cosmological parameters including the matter density parameter, Ω_m.

1.2 Brief Review of Theory of General Relativity

In the early 1900s, Albert Einstein published the Theory of General Relativity (GR) which set a milestone in physics and later cosmology. In this chapter, we review some of the main definitions and tools from General relativity that will be used throughout this thesis. GR posits that the matter and energy curve space time, and the acceleration of particles due to the gravity is enforced by the curvature of space-time. Based on these idea, Einstein's theory of gravity also provides a solid framework to understand the evolution of our cosmos.

In GR, the concept of distance is not only about the spatial distance between two points in space, but also about the time interval between two events. Thus, it introduces the notion of

spacetime infinitesimal interval in the most general form

$$ds^2 = g_{\mu\nu} dx^\mu dx^\nu. \tag{1.1}$$

In its simplest form for flat and static spacetime known as **Minkowski Space** the **line element** is written as:

$$ds^2 = -(cdt)^2 + dx^2 + dy^2 + dz^2. \tag{1.2}$$

where c is a fixed constant that represent a local speed of light and dt,dx,dy,z denote the interval in time and three spatial dimensions respectively[1]. We also take $c = 1$ for the rest of this thesis. We can see that the above line element can be written in a matrix form as

$$ds^2 = \begin{pmatrix} dt & dx & dy & dz \end{pmatrix} \cdot \begin{pmatrix} -1 & 0 & 0 & 0 \\ 0 & 1 & 0 & 0 \\ 0 & 0 & 1 & 0 \\ 0 & 0 & 0 & 1 \end{pmatrix} \cdot \begin{pmatrix} dt \\ dx \\ dy \\ dz \end{pmatrix} = -dt^2 + dx^2 + dy^2 + dz^2. \tag{1.3}$$

The 4 by 4 matrix

$$\begin{pmatrix} -1 & 0 & 0 & 0 \\ 0 & 1 & 0 & 0 \\ 0 & 0 & 1 & 0 \\ 0 & 0 & 0 & 1 \end{pmatrix} \tag{1.4}$$

is the matrix representation of the **metric** of Minkowski space. Clearly, for different type of spacetime, the metric takes a different form. The metric itself has following properties:

- There exists an inverse
- A metric is symmetric

Before I proceed further, I would like to point out that I will use the Latin letters $i, j, k, ...$ to denote the spatial indices ranging from 1 to 3, and the Greek letters $\alpha, \beta, \mu, \nu, ...$ to denote the time and spatial indices ranging from 0 to 3. In this notation, we denote the matrix representation of the metric as $g_{\mu\nu}$ and the inverse of the metric as $g^{\mu\nu}$ and the coordinate vectors as x^μ, such that $t = x^0$ and $\vec{x} = x^i$.

General relativity makes use of tensor algebra in differential geometry. For example, vectors and covectors are rank $(1, 0)$ and $(0, 1)$ tensors respectively, and scalar functions are rank $(0, 0)$ tensors. In general rank (n, m) tensors are multilinear operators that take n number of covectors and m number of vectors to $\mathcal{R}$. Throughout the thesis, a tensor of rank (n, m) will be denoted using n number of lower indices and m number of upper indices. The metric $g_{\mu\nu}$ and its inverse $g^{\mu\nu}$ can be used to lower and raise indices of a tensor. For example, contracting metric as $g^{\mu\nu}$ with a vector V^μ will result into a covector

$$V^\mu g_{\mu\nu} = V_\nu. \tag{1.5}$$

[1]The sign of the components of the spacetime interval has two different conventions $(-, +, +, +)$ or $(+, -, -, -)$. Throughout the paper, we will use the $(-, +, +, +)$ convention

Note that here we have introduced a convenient convention known as the **Einstein Summation Convention** commonly used in physics and GR literature such that when an index is repeated it implies summing over that index. It is important to note that not all objects that can be represented as matrices are tensors. Let us consider coordinate transformation $x^\mu = (t, x, y, z) \to x^{\mu'} = (t', x', y', z')$. Then under these transformations, a tensor $T^{\mu\nu}$ must transform as

$$T^{\mu'\nu'} = \frac{\partial x^{\mu'}}{\partial x^\mu}\frac{\partial x^{\nu'}}{\partial x^\nu}T^{\mu\nu}. \tag{1.6}$$

Now consider an infinitesimal transformation of a vector A^μ from a point x^α to $x^\alpha + dx^\alpha$:

$$dA^\mu = A^\mu(x^\alpha + dx^\alpha) - A^\mu(x^\alpha) = \frac{\partial A^\mu}{\partial x^\alpha}dx^\alpha. \tag{1.7}$$

Then under a coordinate transformation $x^\alpha \to x^{\alpha'}$ the quantity $\partial A^\mu/\partial x^\alpha$ does not act like a tensor even though the vector A^μ transforms like a tensor:

$$\frac{\partial A^{\mu'}}{\partial x^{\alpha'}} = \frac{\partial}{\partial x^{\alpha'}}\frac{\partial x^{\mu'}}{\partial x^\mu}A^\mu = \frac{\partial^2 x^{\mu'}}{\partial x^{\alpha'}\partial x^\mu}A^\mu + \frac{\partial x^{\mu'}}{\partial x^\mu}\frac{\partial A^\mu}{\partial x^{\alpha'}} \tag{1.8}$$

$$= \frac{\partial^2 x^{\mu'}}{\partial x^\alpha \partial x^\mu}\frac{\partial x^\alpha}{\partial x^{\alpha'}}A^\mu + \frac{\partial x^{\mu'}}{\partial x^\mu}\frac{\partial x^\alpha}{\partial x^{\alpha'}}\frac{\partial A^\mu}{\partial x^\alpha}. \tag{1.9}$$

As can be seen by the first term in the equation, the partial derivative acting on a vector (or in general any tensors) is not a tensor. A **covariant derivative** is a derivative that acts as a tensor and is defined as

$$\nabla_\alpha A^\mu = \frac{\partial A^\mu}{\partial x^\alpha} + \Gamma^\mu_{\alpha\beta}A^\beta, \tag{1.10}$$

where $\Gamma^\mu_{\alpha\beta}$ is called a connection coefficient or the Christoffel symbol. Since the connection coefficient determines how a vector changes along the spacetime, the connection contains all the information about the curvature of the spacetime. It happens that there exists an unique connection in our spacetime such that

$$\Gamma^\mu_{\alpha\beta} = \Gamma^\mu_{\beta\alpha} \qquad \nabla_\mu g_{\alpha\beta} = 0. \tag{1.11}$$

Although the connection coefficient contains all the information about the curvature of the spacetime, it is not a tensor. A **Riemann Curvature Tensor**, $R^\alpha_{\beta\rho\sigma}$ is the tensor containing every information about the curvature of the spacetime, and can be written in terms of the connection

$$R^\alpha_{\beta\rho\sigma} = \partial_\rho\Gamma^\alpha_{\beta\sigma} - \partial_\sigma\Gamma^\alpha_{\rho\beta} + \Gamma^\alpha_{\rho\mu}\Gamma^\mu_{\beta\sigma} - \Gamma^\alpha_{\sigma\mu}\Gamma^\mu_{\beta\rho}. \tag{1.12}$$

From the Riemann curvature tensor, we can also obtain the Ricci tensor and the Ricci scalar by contracting indices

$$R_{\mu\nu} = R^\alpha_{\mu\alpha\nu} \qquad R = g^{\mu\nu}R_{\mu\nu} = R^\mu{}_\mu). \tag{1.13}$$

It is also convenient and useful to define the extrinsic curvature of a three dimensional hypersurface embedded in the four dimensional spacetime. An **extrinsic curvature**, $K_{\mu\nu}$ of the hypersurface is

related to the change of a vector normal to the hypersurface. For the normal vector n^α satisfying $n^\alpha n_\alpha = \pm 1$[2], we can obtain the induced metric $h_{\mu\nu}$ on the hypersurface as

$$h_{\mu\nu} = g_{\mu\nu} \mp n_\mu n_\nu. \tag{1.14}$$

Then the extrinsic curvature is defined[3]

$$K_{\mu\nu} = h^\alpha_\mu h^\beta_\nu \nabla_\alpha n_\beta. \tag{1.15}$$

This is particularly useful later on in chapter 4 especially when we choose a specific slicing of the four dimensional spacetime, such as the unitary gauge. This will be further explained in the later chapters.

Now, we relate matter content of the universe and the curvature on the spacetime. This can be done by **Einstein's Field Equation**:

$$G_{\mu\nu} + \Lambda g_{\mu\nu} = \frac{1}{M^2_{\rm pl}} T_{\mu\nu}, \tag{1.16}$$

where $G_{\mu\nu}$ is the **Einstein tensor** defined by

$$G_{\mu\nu} = R_{\mu\nu} - \frac{1}{2} g_{\mu\nu} R, \tag{1.17}$$

and $T_{\mu\nu}$ is the **stress-energy tensor** which conveys information about the density and flux of energy and momentum of energy component in the spacetime. Λ is a constant called the **cosmological constant**. $M_{\rm pl}$ is the reduced Plank mass related to Newton's gravitational constant G by $M^2_{pl} = 1/\sqrt{8\pi G}$. In the context of cosmology and the ΛCDM model, the cosmological constant is associated with the present day acceleration of the expansion of the universe and dark energy. With the understanding of how the curvature in spacetime and matter are related, we can proceed to apply this framework in the context of cosmology and the evolution of universe.

1.3 Background Cosmology and the Early Big Bang Era

One of the principles that the modern cosmology is built around is the cosmological principle. It stems from Copernicus' idea that the observers on Earth are not special observers within our universe. In the context of cosmology, this principle is often stated as: our universe on large scales should look the same from any position (**homogeneity**) and in all direction (**isotropy**). This principle also agrees well with different observations, including those of the cosmic microwave

[2]The sign of n^2 depends on the nature of the hypersurface.

[3]In most GR textbooks, the extrinisic curvature is defined as a three tensor with Latin indices on the hypersurface. In this thesis we use the tangential four tensor field associated with extrinsic curvature. One can go back and forth between the two using the appropriate projections.

background. This allows us to describe the geometry of the spacetime on cosmological scales with the metric which is isotropic and homogeneous to leading order:

$$ds^2 = -dt^2 + a^2(t)\left(\frac{dr^2}{1-\kappa r^2} + r^2(d\theta^2 + \sin^2(\theta)d\phi^2)\right). \tag{1.18}$$

Here, the parameter κ is related to the curvature of the spatial hypersurface[4]. For $\kappa = -1$, the spatial hypersurface is hyperboloid and commonly referred to as **open** by cosmologists[5]. For $\kappa = 1$, the space is elliptic or **closed** and for $\kappa = 0$, the space is **flat**. The function $a(t)$ is the **scale factor**, and it describes how the three dimensional space changes as a function of time t is[6]. The above metric is also known as the **Friedmann-Lemaître-Robertson-Walker (FLRW) Metric**. Using this metric, we can proceed to find different components of the Ricci tensor and then the Einstein tensor. The non-zero components of the Ricci tensor are

$$R_{00} = -3\frac{\ddot{a}}{a} \tag{1.19}$$

$$R_{11} = \frac{a\ddot{a} + 2\dot{a} + 2\kappa}{1-\kappa r^2} \tag{1.20}$$

$$R_{22} = r^2(a\ddot{a} + 2\dot{a}^2 + 2\kappa) \tag{1.21}$$

$$R_{33} = r^2(a\ddot{a} + 2\dot{a}^2 + 2\kappa)\sin^2(\theta). \tag{1.22}$$

Here, the dot above functions denote derivative with respect to time t. The Ricci scalar is then

$$R = \frac{6}{a^2}(a\ddot{a} + a^2 + \kappa). \tag{1.23}$$

Next to obtain the right side of the Einstein equation (1.16), we take perfect fluid approximation[7]. Then the stress-energy tensor for different sources of energy and matter can be approximated as

$$T^{\mu}_{\ \nu}{}^{(i)} = \text{diag}(-\rho^{(i)}, P^{(i)}, P^{(i)}, P^{(i)}), \tag{1.24}$$

where $\rho^{(i)}$ and $P^{(i)}$ are the energy density and pressure corresponding to components labeled with indices i. Similarly we can also define $\rho_\Lambda = M_{pl}^2\Lambda$ and $P_\Lambda = -\rho_\Lambda$. Substituting Ricci scalar and tensor from (1.23) (1.19) and $T^{\mu\nu}$ in (1.24) into (1.16) will lead to two equations known as the **Friedmann equations**

$$\left(\frac{\dot{a}}{a}\right)^2 = \frac{1}{3M_{\text{pl}}^2}\rho^{tot} - \frac{\kappa}{a^2} \tag{1.25}$$

$$\frac{\ddot{a}}{a} = -\frac{1}{6M_{\text{pl}}^2}(\rho^{tot} + 3P^{tot}), \tag{1.26}$$

[4] κ is related to the three dimensional Ricci tensor, but re-scaled with the scale factor a

[5] Note that in the context of cosmology, when cosmologists speak of the universe as open or closed, they often are referring to whether the curvature is negative or positive. These meaning do not have the same definitions as open and closed used in the sense of topology.

[6] The scale factor $a(t)$ is dimensionless, so it cannot tell us the size of the universe by itself. However, if we set $a = 0$ today, then we can say the comoving box at $a = 2$ is twice as big as compared today

[7] This approximation has been tested to be valid to leading order for all the known matter sources

where ρ^{tot} and P^{tot} are the total density and pressure

$$\rho^{tot} = \sum_i \rho^{(i)} \qquad P^{tot} = \sum_i P^{(i)}. \tag{1.27}$$

We now introduce a very important parameter in cosmology and astrophysics,

$$H \equiv \frac{\dot{a}}{a}. \tag{1.28}$$

This parameter is called the **Hubble constant** and it characterizes the expansion rate of the universe. The measurement for H for the current epoch, denoted H_0, is approximately 70 km/sec/Mpc (Mpc stands for mega parsec)[8]. While the local conservation of energy and momentum is automatically satisfied in Einstein's equation, if different matter fields are not strongly interacting with each other, then we can impose the energy-momentum conservation on individual components ($\nabla_\mu T^{\mu\nu} = 0$) to derive the following relations known as the continuity equation:

$$\dot{\rho}^{(i)} + 3H(\rho^{(i)} + P^{(i)}) = 0. \tag{1.29}$$

The Friedmann equations and the continuity equation describes the evolution of the universe on large scales from the very early time to the present.

Essentially, dominant energy components of the universe relevant to cosmology obey a simple **equation of state** relating the density and the pressure given by

$$P^{(i)} = w^{(i)}\rho^{(i)}, \tag{1.30}$$

where $w^{(i)}$ is a parameter characterizing the relations between the density and pressure. We can solve the conservation equation (1.29) using this relation and get

$$\rho^{(i)} \propto a^{-3(1+w^{(i)})}. \tag{1.31}$$

Now, for relativistic particle, $w = 1/3$, and for non-relativistic particles, since they are effectively pressureless, $w = 0$, which gives

$$\rho^{(matter)} \propto a^{-3} \tag{1.32}$$

$$\rho^{(rel)} \propto a^{-4}. \tag{1.33}$$

The different dependence on scale factor tells us that as the universe expands, different periods or phases during the evolution of the universe were dominated by different components of the universe. From observations, the current measurement of the energy density of radiation is very negligible compare to the matter density. Going back in time, without assuming other physics intervening, the scale factor a can approach zero which is referred to as the Big Bang singularity. however, before reaching $a = 0$, the energy density and curvature become too large and go above Planck scales. In this regime the classical description of gravity breaks down.

[8]The precision measurement of H_0 is a very important topic in the field of observational cosmology [121]

From Einstein's equation (1.16), in the absence of matter or radiation, we can take $-\Lambda g_{\mu\nu} = \frac{1}{M_{\rm pl}^2} T_{\mu\nu}^{(vac)}$. Then we have

$$p^{(\Lambda)} = -\rho^{(\Lambda)} \rightarrow w^{(\Lambda)} = -1. \tag{1.34}$$

The energy density from the cosmological constant is independent of the scale factor. But as the density from matter and radiation decreases the universe will be vacuum dominated.

In cosmology it is convenient to write the contribution of each energy content to expansion rate in terms of the **density parameter** and the **critical density**

$$\Omega^{(i)} \equiv \frac{1}{3H^2 M_{\rm pl}^2} \rho^{(i)} \tag{1.35}$$

$$\rho^{(crit)} \equiv 3H^2 M_{\rm pl}^2, \tag{1.36}$$

and

$$\Omega^{(\kappa)} = -\frac{\kappa}{a^2 H^2}. \tag{1.37}$$

The critical density is chosen such that from (1.25)

$$\sum_i \Omega^{(i)} = 1 - \Omega^{(\kappa)}, \tag{1.38}$$

With this parameterization, Friedman equation (1.25) can be written as

$$H^2(a) = H_0^2 \left[\sum_i \Omega_0^{(i)} a^{-3(1+w^{(i)})} + \Omega_0^{(\kappa)} a^{-2} \right], \tag{1.39}$$

where the subscript 0 denote the measurement of the corresponding parameters in the present day.

Then the precision observational measurement of density parameters can tell us whether we live in flat, close, or open universe. The current observation indicate our universe is flat and dark energy dominated with [7]

$$\begin{aligned} \Omega^{(matter)} &= 0.311 \pm 0.0056 \\ \Omega^{(rel)} &= 4.2 \pm 0.1 \times 10^{-5} \\ \Omega^{(\Lambda)} &= 0.6889 \pm 0.0056 \\ \Omega^{(\kappa)} &= 0.0007 \pm 0.0019 \end{aligned}$$

The old theory of cosmology, containing only pressureless matter energy density and radiation was successful in predicting the existence of the cosmic background radiation, or the number of light elements such as helium. However, there were still some unanswered puzzles that physicists had to answer such as the **flatness problem** and the **horizon problem** that lead cosmologists to develop new scenarios to describe early universe in late 1970s [80, 104, 146].

The flatness problem :

The universe in the current state does not seem to have any apparent curvature with $\Omega_0 \simeq 1.02 \pm 0.02$[7]. However, given that $\Omega^{(\kappa)} \propto a^{-2}$, which dilutes much slower than both the matter term and the radiation term. Furthermore, $\sum \Omega^{(i)} + \Omega^{(\kappa)} = 1$ at earlier times means that it should have been extremely smaller than the other two contributions. For example, with the present day constraint of $\Omega_0^{(\kappa)} \lesssim 1$, at the electroweak phase transition, of $a_{\rm ew} \sim 10^{-13}$, the value of the curvature density parameter must be $\Omega_{\rm ew}^{(\kappa)} \lesssim 10^{-26}$. In fact, the actual calculation of the curvature density parameter shows that $\Omega^{(\kappa)} \lesssim 10^{-60}$ within a Planck time after the beginning of the universe. Thus, according to the old cosmological model, our universe requires a very fine tuned value of $\Omega^{(\kappa)}$, and to many cosmologists, this was an unsettling puzzle.

The horizon problem :

The principle of causality states that particles could only have been in causal contact if light could have traveled from one to the other. In this case, these particles are within the particle horizon. The particle horizon in an FLRW universe from some initial time t_i can be calculated in the following way

$$d_{\rm p.hor}(t) = a(t) \int_{t_i}^{t} dt'\, a^{-1}(t') = \int_{a(t_i)}^{a(t)} da\, \frac{1}{a^2 H}. \tag{1.40}$$

Using the equation (1.39) with the current observation of $\Omega^{(matter)} \sim 0.3$, $\Omega^{(rel)} \sim 10^{-4}$, and $H_0 \sim 70$km/s/Mpc, and taking t_i to be the Planck time where in that limit $a = 0$, we can compute that only patches of space within approximately 2 deg of the sky are in causal contact. However, the measurement of the temperature of CMB is isotropic and homogeneous at 10^{-5} level in all directions of the sky which indicates causality on the scale of ~ 10 Gpc. This means that more than about 10^4 different patches of universe had same initial conditions even though they were causally disconnected according to the hot Big Bang theory.

Trying to address these puzzles and a few more, in the late 1970s, a phase of accelerated expansion known as **inflation** was proposed by some cosmologiests [104, 80, 146]. In the inflationary scenarios, the universe is described to be in quasi de Sitter where $a(t) \approx e^{Ht}$. During this phase, the particle horizon is given as

$$d_{\rm p.hor} \approx \frac{e^N}{H}, \tag{1.41}$$

where N is the number of **e-folds** defined as

$$N \equiv \ln \frac{a_{end}}{a_{initial}}. \tag{1.42}$$

Without inflation, the particle horizon will be order of $1/H$, however, with inflation, since energy density and curvature are almost constant while the universe expands, the particle horizon can become much larger than $1/H$ for sufficiently large number of N. Furthermore, the evolution of the curvature density parameter from the onset of inflation to the end of inflation is given by the relations

$$\Omega^{(\kappa)}(a_{end}) \simeq \Omega^{(\kappa)}(a_{initial}) \frac{a_{end}}{a_{initial}} \simeq e^{-2N}. \tag{1.43}$$

This means that even if the curvature density parameter initially was not small, the inflation will 'flatten' the curvature, solving the flatness problem. As it soon turned out that inflation not only answered some of the questions of the early Big Bang model, but also provided a framework to generate the seeds of large scale structure from vacuum quantum fluctuations.

1.4 Inflation

As I mentioned before, inflation is referred to an early phase of accelerated expansion. From the Friedmann equation (1.26), a criteria for the accelerated expansion requires

$$P < -\frac{1}{3}\rho. \tag{1.44}$$

We pointed out earlier that the equation of state for the cosmological constant satisfies the above condition with

$$P = -\rho. \tag{1.45}$$

However, assuming the cosmological constant as the source of onset of inflation leads to the never ending acceleration phase, which does not transition into the radiation dominated era. Also, it is not consistent with observation of anistropies either.

Instead, consider a scalar field ϕ with a potential $V(\phi)$. The action for this field is given by

$$S_\phi = \int d^4x\, \sqrt{-g}\left(-\frac{1}{2}\partial_\mu\phi\partial^\mu\phi - V(\phi)\right). \tag{1.46}$$

We can get the stress-energy tensor for this field by varying the action with respect to the metric

$$T^\phi_{\mu\nu} = \partial_\mu\phi\partial_\nu\phi - g_{\mu\nu}\left(\frac{1}{2}\partial_\sigma\phi\partial^\sigma\phi + V(\phi)\right). \tag{1.47}$$

The energy density and the pressure for this field is then

$$\rho = -T^0{}_0 = \frac{1}{2}\dot\phi^2 + V(\phi), \qquad P = \frac{1}{2}\dot\phi^2 - V(\phi). \tag{1.48}$$

We can see that under the condition $V(\phi) \gg \frac{1}{2}\dot\phi^2$, we can obtain the equation of state

$$P \simeq -\rho. \tag{1.49}$$

The Friedmann equations (1.25, 1.26) then lead to [9]

$$H^2 \approx \frac{1}{3M_{\rm pl}^2}V(\phi), \qquad \dot H \approx -\frac{1}{2M_{\rm pl}^2}\dot\phi^2. \tag{1.50}$$

[9]Here we neglect the curvature term κ for simplicity here, but it is easy to include as well. Throughout this thesis the curvature parameter will be taken to be zero.

It can be shown that the condition that the potential be much bigger than the kinetic energy can be written as the first **slow-roll parameter**

$$\epsilon \equiv -\frac{\dot{H}}{H^2} \ll 1. \tag{1.51}$$

The name slow-roll comes from the fact that the scalar field is 'slowly rolling' down the potential during inflation. There needs to be one more condition so that inflation lasts for sufficiently long enough period. In another words, the change in the kinetic energy needs to be much smaller than the change in the potential energy:

$$\left|\frac{d}{dt}\dot{\phi}^2\right| \ll \left|\frac{d}{dt}V(\phi)\right| \rightarrow |\ddot{\phi}| \ll \left|\frac{\partial}{\partial\phi}V(\phi)\right|. \tag{1.52}$$

From this condition and the Friedmann equations we can define the second slow-roll parameter

$$\eta \equiv -\frac{\ddot{H}}{2H\dot{H}} \ll 1. \tag{1.53}$$

For simple single field inflationary model that we have described above, it is often more convenient to write the slow roll parameters in terms of the potential rather than the Hubble constant:

$$\epsilon_V \equiv \frac{M_{\rm pl}^2}{2}\left(\frac{V'}{V}\right)^2 \ll 1, \qquad \eta_V \equiv M_{\rm pl}^2\frac{V''}{V} \ll 1. \tag{1.54}$$

Here $\epsilon_V = \epsilon$ and $\eta_V = \eta + \epsilon$.

1.5 Quantum Fluctuations in Expanding Universe

The universe is clearly not perfectly isotropic and homogeneous. There are large scale structures (LSS) such as galaxies and cluster of galaxies. Inflationary scenarios can provide the mechanisms and framework in which these LSS are generated from the perturbations at early times. In this section we study how the quantum fluctuations undergoing inflation can seed the generation of the large scale structures and provide connections to present observables via cosmological perturbation theory.

It is more convenient to carry out the analysis of the metric perturbations using the conformal time $d\tau = dt/a(t)$, where the line element for FLRW metric can be written as

$$ds^2 = a(\tau)^2\left[-d\tau^2 + d\vec{x}^2\right]. \tag{1.55}$$

To add perturbatiosn to FLRW metric, we start by introducing ADM formalism. Under the ADM formalism we can break down the spacetime into a foliation of 3-dimensional space-like manifold and a time direction, and then write a general line element as

$$ds^2 = -N^2 d\tau^2 + h_{ij}(dx^i + N^i d\tau)(dx^j + N^j d\tau). \tag{1.56}$$

Here we have introduced three new quantities: N a lapse function, N^i a shift vector, and h_{ij} a 3 dimensional metric [17]. We now write ADM variables in terms of perturbation around the FLRW metric

$$N = a(\tau)(1 + N_1) \tag{1.57}$$
$$N^i = \partial^i \psi + N_T^i \tag{1.58}$$
$$h_{ij} = a(\tau)^2[(1 + 2\zeta)\delta_{ij} + \nabla_i \nabla_j E + \nabla_i F_j + \nabla_j F_i + \gamma_{ij}], \tag{1.59}$$

where δ_{ij} is the Kronecker delta function, and ∇^i is the 3-dimensional covariant derivative associated with the metric h_{ij}. Note that the perturbations can be decomposed into scalar parts, vector parts, and tensor parts by requiring

$$\partial^i F_i = 0, \qquad \nabla_i N_T^i = 0 \tag{1.60}$$
$$\nabla^i \gamma_{ij} = 0, \qquad \gamma^i{}_j = 0. \tag{1.61}$$

Not all of these perturbation variables correspond to actual degrees of freedom. Since GR is diffeomorphism invariant (the change in coordinate should not affect the laws of physics), we can use the coordinate transformation to identify actual degrees of freedom. Consider the transformation

$$x^\mu \to x^\mu + \xi^\mu. \tag{1.62}$$

The translation ξ^μ can be decomposed into ξ^0 and ξ^i. The spatial part can be further decomposed to

$$\xi^i = \xi_\perp^i + \partial^i \xi, \tag{1.63}$$

where $\xi_\perp^i$ is the transverse part such that $\partial_i \xi_\perp^i = 0$.[10] For the scalar perturbations, we can choose specific values of ξ^0 and ξ removing up to two scalar functions for perturbations. This procedure is called fixing the gauge. For the vector perturbations we can fix $\xi_\perp^i$ such that $F_i = 0$.

Now, consider a canonical scalar field minimally coupled to gravity. The action is given by

$$S = \frac{1}{2} \int d^4x \sqrt{-g} \left(\frac{1}{M_{\rm pl}^2} R - g_{\mu\nu} \partial^\mu \phi \partial^\mu \phi - 2V(\phi) \right).[11] \tag{1.64}$$

Taking into account the fluctuation of the scalar field around the homogeneous background, the scalar field can be decomposed as

$$\phi(\tau, \vec{x}) = \phi_0(\tau) + \delta\phi(\tau, \vec{x}). \tag{1.65}$$

We can fix the gauge by choosing specific values of ξ such that $\delta\phi$ in eq. 1.65 and E in eq. 1.57 are set to zero. In this gauge we are taking ϕ constant 3-dimensional hypersurface as space

[10] Every vector v^i can be decomposed into the sum of the transverse part and the gradient of a scalar.

[11] Note that the first term in the action is the Einstein-Hilbert action. Varying this term with respect to the metric, we can obtain the left hand side of the Einstein equation discussed earlier.

foliation. This choice of gauge is known as the unitary gauge or the comoving gauge. Under this choice, we have

$$\delta\phi = 0, \qquad h_{ij} = a(\tau)^2[(1+2\zeta)\delta_{ij} + \gamma_{ij}]. \tag{1.66}$$

The advantage of using ADM formalism is that the equations of motion for N and N^i do not have any time derivatives. So these equations are not dynamical in terms of N and N^i and this leads to two constraints on scalar functions representing perturbations. In the end we are left with only one independent degree of freedom for the scalar perturbation. Solving two constraint equations for the lapse and shift, we can first expand the action 1.64 up to second order in perturbation and then after substituting for lapse and shift we get:

$$S_{(2)} = \frac{1}{2M_{\rm pl}^2}\int d^3x d\tau\ a(\tau)^2 \frac{\phi_0'^2}{\mathcal{H}^2}\left(\zeta'^2 - \partial_i\zeta\partial^i\zeta\right), \tag{1.67}$$

and

$$S_{(2)} = \frac{1}{2M_{\rm pl}^2}\int d^3x d\tau\ a(\tau)^2 \left(\gamma_{ij}'^2 - (\partial\gamma_{ij})^2\right), \tag{1.68}$$

where the prime denote the derivative with respect to the conformal time τ and $\mathcal{H} \equiv a'(\tau)/a(\tau)$. With these equations, the study of perturbations reduces down to a field theory of a single variable. The scalar perturbation ζ is also known as the comoving curvature perturbation and plays a critical role in connecting observable quantities with scalar perturbations.

We can rewrite the second order action for the scalar perturbations in canonical form by introducing an *Mukhanov-Sasaki variable*, v, given by

$$v = a\frac{\phi_0'}{\mathcal{H}M_{\rm pl}}\zeta. \tag{1.69}$$

Then the action looks like that of a canonical single field with a time-dependent mass:

$$S^v_{(2)} = \frac{1}{2}\int d^3x d\tau\ [v'^2 - \partial_i v\partial^i v + \frac{z''}{z}v^2], \tag{1.70}$$

where we have defined

$$z = a\frac{\phi_0'}{\mathcal{H}M_{\rm pl}}. \tag{1.71}$$

To understand this equation in terms of quantum field theory, we first quantize v. The canonical momentum conjugate, p_v, is given by varying the action with respect to v'

$$p_v = \frac{\delta S^v_{(2)}}{\delta v'}, \tag{1.72}$$

which satisfies the commutation relations

$$[\hat{v}(\tau,\vec{x}), \hat{p}_v(\tau,\vec{x}')] = i\delta(\vec{x}-\vec{x}'), \tag{1.73}$$

and

$$[\hat{v}(\tau,\vec{x}),\hat{v}(\tau,\vec{x}')]=[\hat{p}_v(\tau,\vec{x}),\hat{p}_v(\tau,\vec{x}')]=0, \tag{1.74}$$

where the $\hat{}$ denote the quantization of fields as operators. In Fourier mode, we can write

$$\hat{v}(\tau,\vec{x})=\frac{1}{\sqrt{(2\pi)^3}}\int d^3k\left\{\hat{a}_{\vec{k}}v_k(\tau)e^{i\vec{k}\vec{x}}+\hat{a}^\dagger_{-\vec{k}}v_{-k}(\tau)e^{-i\vec{k}\vec{x}}\right\}. \tag{1.75}$$

The operators, $\hat{a}$ and $\hat{a}^\dagger$ are the usual creation and annihilation operators. Time dependent functions v_k satisfy the classical equation of motion

$$v_k''+k^2v_k-\frac{z''}{z}v_k=0. \tag{1.76}$$

In the slow-roll inflationary scenario, we have

$$\frac{z''}{z}\approx\frac{a''}{a}, \tag{1.77}$$

due to the slow-roll condition, and

$$\frac{a''}{a}\approx\frac{2}{\tau^2} \tag{1.78}$$

due to the space being almost de Sitter with $a\sim e^{Ht}\sim\frac{1}{H\tau}$. Requiring the Wronskian normalization condition

$$v_kv_{k'}^*-v_k^*v_k'=2i, \tag{1.79}$$

makes the creation and annihilation operator $\hat{a}^\dagger$, $\hat{a}$ satisfy the continuous limit of commutation relations for each Fourier modes as harmonic oscillator. In the curved spacetime, the typical definition of vacuum state as the lowest energy state is not unique or time independent. However, in the limit that frequencies are varying adiabatically, we can define adiabatic vacuum which remains close to the lowest energy state. In de Sitter background, this leads to the **Bunch-Davis Vacuum**

$$v_k=\frac{1}{\sqrt{2k}}e^{-ik\tau}\left(1-\frac{i}{k\tau}\right). \tag{1.80}$$

and in the limit $k^2\gg z''/z$ it becomes the Minkowski vacuum

$$\lim_{\tau\to-\infty}v_k(\tau)=\frac{1}{\sqrt{2k}}e^{-ik\tau}. \tag{1.81}$$

This vacuum corresponds to the zero particle state in the asymptotic past infinity.

Note that there are three possible regimes for the equation of motion for v_k: *i)* mode functions that stay inside the Hubble radius ($1/(ak)\ll H^{-1}$) from early times all the way to late times, *ii)* the ones that were originally outside (or exit and stay outside) the Hubble radius and *iii)* the ones that exit the Hubble radius during the inflation and re-enter at a later time. The most interesting for understanding the evolution and formation of the LSS are the ones that exit and re-enter the Hubble horizon and generate initial conditions that generate the seeds for the LSS.

1.6 Observational Constraints

Currently, the CMB observation offers the strongest constraints for initial condition of cosmological perturbations. These observational constraints include

- **Amplitude of Scalar the Power Spectrum Δ_ζ:** The size of the fluctuation is characterized by the amplitude of the power spectrum of ζ. The power spectrum P_ζ is given by the two point function for ζ which is the Fourier transform of the power-spectrum

$$\left\langle 0|\hat{\zeta}(\vec{x}_1)\hat{\zeta}(\vec{x}_2)|0\right\rangle = \int d^3k e^{i\vec{k}(\vec{x}_1-\vec{x}_2)}\frac{P_\zeta}{4\pi k^3}. \tag{1.82}$$

  It is conventional to define a dimensionless power spectrum as

$$\Delta_\zeta = \frac{k^3}{2\pi^2}P_\zeta(k), \tag{1.83}$$

  and in slow-roll inflationary models, one can show that

$$P_\zeta(k) \simeq \frac{H^2}{4k^3\epsilon} \Rightarrow \Delta_\zeta = \frac{H^2}{8\pi^2\epsilon M_{\rm pl}^2}. \tag{1.84}$$

  Planck observations on CMB temperature anistropy gives us the amplitude on $\Delta_\zeta \simeq 2.099 \pm 0.029 \times 10^{-9}$[7].

- **Near Scale Invariance, n_s:** Since the Hubble parameter is not exactly constant, but slowly decreasing during the inflation, not all modes exit and re-enter at the same Hubble scale. This means that there is more power on the large scales. Defining

$$n_s - 1 = \frac{d\ln\Delta_\zeta}{d\ln k} = -2\epsilon - \eta, \tag{1.85}$$

  we expect the value of n_s to be close to 1. The CMB data gives us an nearly invariant tilt on the power spectrum with $n_s = 0.9649 \pm 0.0042$[51].

- **The size of non-Gaussianity f_{NL}:** Although CMB observations imply the primordial curvature fluctuations to be almost Gaussian, if there are any primordial non-Gaussianity, and if it is observed, it can give us more information to test different scenarios of the early universe. For Gaussian fields with zero expectation values, n-point functions with odd n should vanish. So to measure deviations from Gaussianity for ζ, we calculate the three point function or its Fourier transformation called the bispectrum $B(\vec{k}_1, \vec{k}_2, \vec{k}_3)$ defined by

$$\left\langle \zeta(\vec{k}_1)\zeta(\vec{k}_2)\zeta(\vec{k}_3)\right\rangle = (2\pi)^3\delta^3(\vec{k}_1+\vec{k}_2+\vec{k}_3)B(\vec{k}_1,\vec{k}_2,\vec{k}_3). \tag{1.86}$$

For the local type non-Gaussianities (NG), you can write ζ as[12]

$$\zeta(\vec{x}) = \zeta_L(\vec{x}) - \frac{3}{5} f_{NL} \zeta_L^2(\vec{x}), \tag{1.87}$$

where f_{NL} is the size of non-Gaussianity, and ζ_L is the linear part of the perturbation. In momentum space we can separate the perturbation into the linear part and the non linear part,

$$\zeta(k) = \zeta_L(\vec{k}) + \zeta_{NL}(\vec{k}). \tag{1.88}$$

For this type of NG, the non-vanishing component of the three point function is

$$\left\langle \zeta_L(\vec{k}_1)\zeta_L(\vec{k}_2)\zeta_{NL}(\vec{k}_3) \right\rangle = -\frac{6}{5}(2\pi)^3\delta^3(\vec{k}_1+\vec{k}_2+\vec{k}_3) f_{NL} \left[P_\zeta(k_1)P_\zeta(k_2) + \text{perm.} \right], \tag{1.89}$$

which is maximized for squeezed limits ($k_1 \sim k_2 \ll k_3$).

In general, the non-Gaussianities do not have to be local. In such cases, the equation (1.89) does not hold. However, one can still write different contributions to the bispectrum as[140]

$$\langle \zeta(\mathbf{k}_1)\zeta(\mathbf{k}_2)\zeta(\mathbf{k}_3) \rangle = (2\pi)^7 \delta^3(\mathbf{k}_1+\mathbf{k}_2+\mathbf{k}_3) \frac{[\Delta(k_1)]^2}{k_1^3 k_2^3 k_3^3} \times \mathcal{A}(k_1, k_2, k_3),$$

and then define f_{NL} through

$$\mathcal{A}(k_1, k_2, k_3) = -\frac{3}{10} f_{NL} \left(k_1^3 + k_2^3 + k_3^3 \right).$$

We can easily check that in the particular case of the local non-Gaussianities, the above agrees with the equation (1.89). The equations (1.86) and (1.90) provide the relation between the three point function, f_{NL} and the power spectrum[13]. Observational constraints on the size of the local-type non-Gaussianity is $f_{NL} \sim -0.9 \pm 5.1$[51]. For different types of f_{NL}, we have equilateral (where f_{NL} is maximized for $k_1 \sim k_2 \sim k_3$), orthogonal (a special template which receives contributions from a wide range of shapes). The Planck constraints on these types of NG are -26 ± 47, -38 ± 24[14].

Tensor to Scalar Ratio: From the equation 1.68, we can also derive the power spectrum of the tensor modes Δ_γ. The ratio of the tensor to scalar power spectrum is given by

$$r \equiv \frac{2\Delta_\gamma^2}{\Delta_\zeta} = 16\epsilon. \tag{1.90}$$

The CMB data from the Planck measurement gives a constraint of $r < 0.11$ [51].

[12] Some literature such as [96] write this in terms of a different metric variable $\Phi = \Phi_L + f_{NL}\Phi_L^2$. The discrepancy comes from the difference of a gauge choice, specifically between the unitary gauge and the longitudinal gauge

[13] The value of f_{NL} is dependent on the shapes of the triangles formed by $\vec{k}_1, \vec{k}_2$ and $\vec{k}_3$

[14] Another widely used shape is enfolded (or flattened where f_{NL} is maximized for $k_1 \sim k_2 \sim k_3/2$).

1.7 Shortcomings of Inflation

Inflation, despite being successful in explaining observations, it is also hard to experimentally prove the since it includes infinite space of models that can fit different observational data. Meanwhile the theory of inflation still has some other shortcomings that need to be addressed. Here, we discuss some of widely known debate of the theory

- **Validity of the Semi-classical Gravity, Effective Theory and Trans-Planckian Problem:** Inflaton, the field responsible for deriving inflation does not fit into the standard model of particle Physics. It can potentially come from the theory of quantum gravity such as string theory once it is established. Until then one can view it as an effective field theory and in the context of semi-classical gravity and as we discuss in chapter 4 the validity and consistency of the effective theory needs to checked. This is also related to trans-Planckian problem. In some models of inflation, some of the scalar modes that seed the large scale structures that we observe today requires physics beyond the Planckian limit. Since the physics beyond the Planckian regimes are unknown, questions such as 'is the framework, such as the quantum field theory in curved spacetime, valid in studying inflation?' need to be addressed.

- **Singularity Problem :** Depending on the models of inflation, it may seem some inflationary models can be past eternal may not require the universe to be arbitrarily dense and hot at the beginning. However, even in such cases, as pointed out by [39], geodesics can still be past incomplete. Therefore the singularity problem is not necessarily resolved in inflation and needs to be addressed separately. This is the motivation behind to topic in chapter 2.

1.8 Summary

In this chapter, I briefly reviewed fundamental physics concepts that are the basic building blocks in understanding the topics of this thesis. General relativity, quantum fields in an expanding spacetime, and inflation are all very successful in describing the physics of the early universe in accordance with current observational data. However, even with their successes, the current paradigm of the early universe seems to have some unanswered questions. Questions such as the singularity problem, initial conditions and developing consistent effective field theory of Inflation ask whether the physics and the frameworks that we use to study the beginning of the universe is valid or not. In part I, I will discuss a bouncing scenario where the singularity problem is avoided in chapter 2, and then in chapters 3 and 4, I will discuss an effective field theory of inflation and its extension to arrive at a better understanding of the inflationary models. In second part I will move to a topic of dark energy and late time acceleration. I will introduce a bottom-up approach where we initially assume minimal framework for dark energy, and then constrain possible frameworks from the observation in the present era.

Part I

Addressing the Puzzles in the Early Universe

Chapter 2

Cuscuton Bounce

2.1 Introduction

The last decade or two has been called the age of precision cosmology. Precise observations of the Cosmic Microwave Background (CMB) radiation and Large Scale Structures (LSS) have provided tight constraints on our cosmological models. Cosmology on theoretical front has also been very successful in building models of early universe that can match these observations. The inflationary paradigm is arguably the most popular among the current models. However, inflationary models do not address all the fundamental questions about the beginning of universe. For instance, it has been argued that inflationary space-times are not past-complete[38]. In other words, inflation doesn't provide a resolution to singularity problem. It is generally posited that quantum gravity effects might lead to the resolution of this problem. However, invoking the unknown powers of quantum gravity to address any initial condition problem that we can not resolve, can be a double-edged sword. For instance, if quantum gravity effects are important, the framework of quantum field theory on curved space-time, which is used to make predictions for inflation becomes invalid at the scales of interest and leads to the so-called trans-Planckian problem [109, 42]. One would hope that if quantum gravity is relevant in the early universe, its effects can be formulated in systematic ways, that can also be tested.

One way in which singularity problem can be evaded is by considering regular bouncing cosmologies, where an initially contracting universe, 'bounces' and starts expanding. Many models of regular bouncing cosmologies have been proposed in the literature [91, 87, 72, 45, 46, 68, 122, 54, 48, 47, 66, 56, 65, 86, 57]. Many of these models share a common feature of possessing scalar field components since scalars provide the simplest framework to describe dynamics. However, the actions for scalar fields differ from each other, depending on which fundamental conjectures they are inspired from. These conjectures can be motivated from phenomenological theories of modified gravity, string theory, loop quantum gravity, etc. One of the obstacles that these scenarios face is that in general relativity, a regular bounce requires the violation of Null Energy Condition (NEC). This generically leads to instabilities or superluminal

speed of sound[1]. There are few proposals in the literature regarding stable ways to violate the NEC. Ghost condensate[54] is one of the early models that was suggested to produce a healthy regular bounce. Later, it was noticed that in the context of late universe cosmology [63], a subclass of Horndeski actions, 'Kinetic Gravity Braiding', can have an healthy null energy condition violation~~NEC~~. This led to the development of more improved versions of the regular bouncing scenarios [68, 122] within Horndeski theories. The stability and superluminal nature of these models has been a subject of interesting debates in literature. Authors in [53, 86, 87] have argued that it is possible to obtain a healthy bounce using Galilean action while [69, 65] argue that when coupling to matter or other regions of phase-space are included, Galilean models have superluminal speed of sound[2].

It is also worth noting that interest in healthy ~~NEC~~ also extends to other areas of gravitational physics, such as traversable wormhole solutions, or models which require universe to be initially static[56]. In the case of traversable wormhole, it has been shown that there are some no-go theorems that apply[128, 127].

In this chapter, we present a new resolution for instabilities associated with ~~NEC~~ scenarios. We show that cuscuton modification of gravity[6, 5] allows for an effective violation of NEC in FRW backgrounds while the actual matter sources satisfy NEC. Note that cuscuton field, mimics the appearance of adding a non-canonical scalar field (cuscuton field) to general relativity. However, the kinetic term of this field is such that it has no dynamical degree of freedom[3] but it modifies gravity in Infrared (IR) regime. Due to its non-dynamical nature, cuscuton models still need other fields to produce dynamics. In other words, cuscuton is instrumental to make the background bounce but the actual dynamical degree of freedom does not violate NEC. Therefore, our model does not fall under the single field $P(X, \phi)$ models that violate NEC and the problems discussed in [148, 70, 61] do not apply to our model.

We would like to also point out that cuscuton terms have previously been shown to be important in having consistent background condition for generating a bounce solution within k-essence models [125] [4] as well as a stable matter bounce scenario in massive gravity models [102].

This chapter is structured in the following way. In Section 2.2, we present a toy model for a cuscuton bounce scenario. In Section 2.3, we analyze the existence of ghosts and other

[1]We refer readers to [66, 133] for further reading and to [126] for a good review on how NEC violation can lead to instabilities, superluminality or possibly unbounded Hamiltonians from below.

[2]Since the literature on this topic is very extensive and still developing, we refer readers to references and citations of the mentioned papers for further details.

[3]"No dynamical degree of freedom" can be interpreted as, equation of motion for cuscuton field does not have any time derivatives. This can be shown explicitly at linear order in flat space-time or around FRW backgrounds. Since action is covariant, that implies there are no local degrees of freedom. For more details, we refer readers to [40]. In [76], authors argue that in Hamiltonian formalism Cuscuton acts as a dynamical field when its inhomogeneities are considered. We suspect that the corresponding equations are not well-posed and the duality of Hamiltonian formalism to Lagrangian formalism is breaking down for Cuscuton. That is an interesting topic that requires further investigation.

[4]There, cuscuton term is part of the single field non-canonical kinetic terms and instabilities discussed in [148, 70, 61] can be applicable.

instabilities in this model. We end with our concluding remarks in Section 2.4.

2.2 A toy model for cuscuton bounce

Consider the following action for a scalar field with a noncanonical kinetic term,

$$S = \int d^4x\sqrt{-g}L(\varphi, X)\,, \tag{2.1}$$

where L is an arbitrary function of the scalar φ and $X \equiv \frac{1}{2}\partial_\mu\varphi\partial^\mu\varphi$ [5].

This action is compatible with a perfect fluid description

$$T_{\mu\nu} = (\rho + P)u_\mu u_\nu - Pg_{\mu\nu} \tag{2.2}$$

assuming

$$u_\mu \equiv \frac{\partial_\mu\varphi}{\sqrt{2X}} \tag{2.3}$$

is time-like. The energy density and the pressure in the comoving fame of u_μ are

$$\rho = T_{\mu\nu}u^\mu u^\nu = 2XL_{,X} - L \tag{2.4}$$

$$P = L. \tag{2.5}$$

We use $_{,X}$ to denote the partial derivative with respect to the variable X.

In a flat FRW background

$$ds^2 = dt^2 - a^2(t)\delta_{ij}dx^i dx^j, \tag{2.6}$$

the homogeneous field equation (2.1) reduces to,

$$(L_{,X} + 2XL_{,XX})\ddot{\varphi}_0 + 3HL_{,X}\dot{\varphi}_0 + L_{,X\varphi}\dot{\varphi}_0^2 - L_{,\varphi} = 0\,, \tag{2.7}$$

where H represents Hubble constant and we denote the time derivative with an overdot. *Cuscuton* modification of gravity is achieved by taking the in-compressible limit of the above perfect fluid such that everywhere on (φ, X) plane

$$L_{,X} + 2XL_{,XX} = 0. \tag{2.8}$$

As we see in that limit, the equation of motion is no longer second order since the second time derivative of φ vanishes (see [6, 5] for more details). A Lagrangian that satisfies the above requirement everywhere in phase space corresponds to

$$L(\varphi, X) = \pm\mu^2\sqrt{2X} - V(\varphi), \tag{2.9}$$

[5] We will use units with $M_p^2 = 1/8\pi G$ and the metric signature is $(+,-,-,-)$.

which is called *Cuscuton* Lagrangian [6]. What is more interesting about this Lagrangian is that when we substitute it in 2.7, not only $\ddot{\varphi}$ dependence vanishes but that $\dot{\varphi}$ dependence cancels as well, leading to the following constraint equation,

$$\pm \text{sign}(\dot{\varphi}) 3\mu^2 H + V'(\varphi) = 0 \, . \tag{2.10}$$

μ can in principle depend on φ but that dependence can be absorbed into a field redefinition such that a new cuscuton action with constant μ and a new potential is obtained.

Since the cuscuton equation is not dynamical, contributions of dynamical matter sources in the universe are necessary to obtain any cosmological evolution. Here, we consider a toy bounce model where the universe consist of a barotropic component $p_m = w\rho_m$ in addition to cuscuton field. A desirable model would initially be a contracting universe where in very early times the cuscuton modifications of gravity are negligible. However, as it gets smaller the cuscuton modification becomes important, causing the universe to bounce into an expanding phase. For simplicity we assume $w = 1$ so $\rho_m \propto a^{-6}$, making cuscuton contributions grow even faster close to the bounce and be dominant over anisotropies. However, this assumption is not fundamental for our result. A simple way to produce such an equation of state from action is to include a minimally canonical scalar field, π, with no potential. That will later allow us to consistently study the behaviour of perturbations during the bounce.

A main feature of a regular bounce ($H \neq \pm\infty$) is that universe goes from a contracting phase ($H < 0$) into an expanding one ($H > 0$) at finite value of scalar factor, a_b. This criteria automatically implies

$$H_b = 0 \tag{2.11}$$
$$\dot{H}_b > 0, \tag{2.12}$$

where b denotes the bounce. In general relativity, the second condition necessitates the violation of NEC for a perfect fluid source.

We now investigate the possibility of a bounce solution in a framework, consisting of cuscuton and a barotropic matter source ρ_m.

The Friedmann and continuity equations can be obtained from action or Einstein's equations

$$H^2 = \frac{1}{3M_p^2}[V(\varphi) + \rho_m] \tag{2.13}$$
$$\dot{H} = -\frac{1}{2M_p^2}[\pm\mu^2\sqrt{2X} + (1+w)\rho_m]. \tag{2.14}$$

Therefore, requiring the energy condition $\rho_m > 0$ and (2.11) be satisfied at the bounce leads to

$$V(\varphi_b) < 0. \tag{2.15}$$

[6] It had been already noted in [111] that this Lagrangian corresponds to the $c_s \to \infty$ limit in a $P(X, \phi)$ theory.

On the other hand, condition (2.12) implies that only the choice of the negative sign for cuscuton kinetic term could lead to a bounce solution. So from here on we only consider

$$L(\varphi, X) = -\mu^2\sqrt{2X} - V(\varphi). \tag{2.16}$$

This in turns, yields Eq. (2.17) becomes

$$-\text{sign}(\dot{\varphi})3\mu^2 H + V'(\varphi) = 0\,, \tag{2.17}$$

which leads to

$$3\mu^2\dot{H} = V''(\varphi)|\dot{\varphi}|. \tag{2.18}$$

Therefore, in the regimes that NEC is valid ($\dot{H} < 0$), cuscuton potential must satisfy

$$V'' < 0, \quad \text{for NEC}, \tag{2.19}$$

but close to the bounce,

$$V'' > 0, \quad \text{for } \cancel{\text{NEC}}. \tag{2.20}$$

In addition, substituting H from Eq. (2.10) back into Eq. (2.13), we arrive at

$$\frac{M_p^2}{3\mu^4}V'^2(\varphi) = V(\varphi) + \rho_m\,. \tag{2.21}$$

This equation demonstrates how for a particular potential $V(\phi)$, the evolution of cuscuton depends on other matter sources in the universe. We can also use this relation to derive further constraints on cuscuton potential. Taking a time derivative of Eq. (2.21), combining it with continuity equation for matter source, $\dot{\rho}_m = -3H(\rho_m + p_m)$, and Eq. (2.10) we get[7]

$$\frac{2M_p^2}{3\mu^4}V''(\varphi) - 1 = -(1+w)\frac{\rho_m}{\mu^2|\dot{\varphi}|} < 0, \tag{2.22}$$

for $w > -1$ or that

$$V''(\varphi) < \frac{3\mu^4}{2M_p^2}. \tag{2.23}$$

This enables us to conclude that while the shape of the potential in the $\cancel{\text{NEC}}$ era (around the bounce) is convex (2.20), its convexity is in this range:

$$0 < V''(\varphi_b) < \frac{3\mu^4}{2M_p^2}. \tag{2.24}$$

However, as we argued before, potential has to become concave, $V''(\varphi) < 0$, in regions where NEC is restored. Setting additional assumptions, such as when far from the bounce, cuscuton

[7]This equation together with (2.21) also demonstrates, how $\dot{\varphi}$ is uniquely determined as a function of φ.

modifications of gravity are negligible, can also be used to obtain additional restriction about the shape of the potential. This assumption can be applied by requiring

$$\lim_{t\to\pm\infty} H^2 = \lim_{t\to\pm\infty} \frac{1}{3M_p^2}\rho_m \to 0, \tag{2.25}$$

$$\lim_{t\to\pm\infty} \dot{H} = \lim_{t\to\pm\infty} -\frac{1+w}{2M_p^2}\rho_m \to 0, \tag{2.26}$$

where $t = 0$ corresponds to the bounce. Using the above conditions in combination with Eq. (2.22), Eq. (2.10) and Eq. (2.21), one can show

$$\lim_{t\to\pm\infty} V'(\varphi_\infty) = 0 \tag{2.27}$$

$$\lim_{t\to\pm\infty} \frac{3\mu^4}{M_p^2}\frac{|V(\varphi_\infty)|}{V'^2(\varphi_\infty)} \ll 1 \tag{2.28}$$

$$\lim_{t\to\pm\infty} V''(\varphi_\infty) \ll -\frac{3\mu^4}{\sqrt{2}M_p^2} \tag{2.29}$$

Note that Eq. (2.24) and Eq. (2.29) imply

$$|V''(\pm\varphi_\infty)|/V''(\varphi_b) \gg 1. \tag{2.30}$$

We now introduce a toy model, where the potential contains a quadratic, an exponential and a constant term, such that it meets all the above conditions:

$$V(\varphi) \equiv m^2(\varphi^2 - \varphi_\infty^2) - m^4[e^{(\varphi^2-\varphi_\infty^2)/m^2} - 1], \tag{2.31}$$

with

$$\frac{\varphi_\infty^2}{m^2} \gg 1. \tag{2.32}$$

The constant term is set to a value that ensures $V(\varphi) = 0$ at $\varphi = \pm\varphi_\infty$ and the large value of φ_∞^2/m^2, guarantees that $|V''(\pm\varphi_\infty)|/V''(\varphi_b) \gg 1$. The viable range for μ consistent with Eq. (2.24) and Eq. (2.29) is then

$$\frac{m^2}{M_p^2} \ll \frac{\mu^4}{M_p^4} \ll \frac{\varphi_\infty^2}{M_p^2}. \tag{2.33}$$

Figure (2.1) displays a schematic shape of a potential where parameters, m and φ_∞ are set to $m = 0.05M_p$ and $\varphi_\infty = 0.25M_p$ so $\varphi_\infty^2/m^2 = 25$. For these choice of parameters the allowed range of μ is $0.22 < \frac{\mu}{M_p} < 0.5$. For the rest of the discussion we keep the values of the parameters in our model to be fixed at $m = 0.05M_p$, $\varphi_\infty^2/m^2 = 25$ and $\mu = 0.3M_p$. Substituting the potential described by Eq. (2.31) into Eq. (2.21), one can derive the evolution of ρ_m and H as functions of φ. Figure (2.2) demonstrates the φ dependence of these quantities, including $\rho_{cus} \equiv V(\varphi)$ and

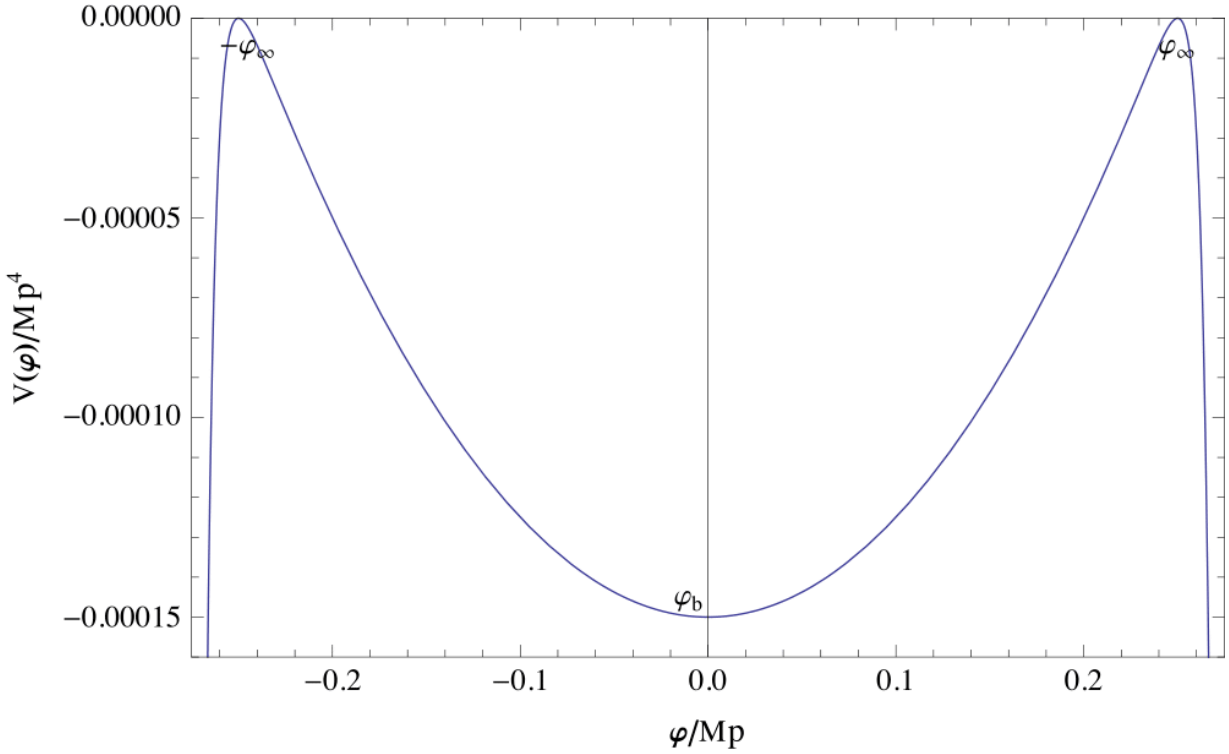

Figure 2.1: $V(\varphi)$ as a function of φ for $m = 0.05M_p$, $\varphi_\infty^2/m^2 = 25$.

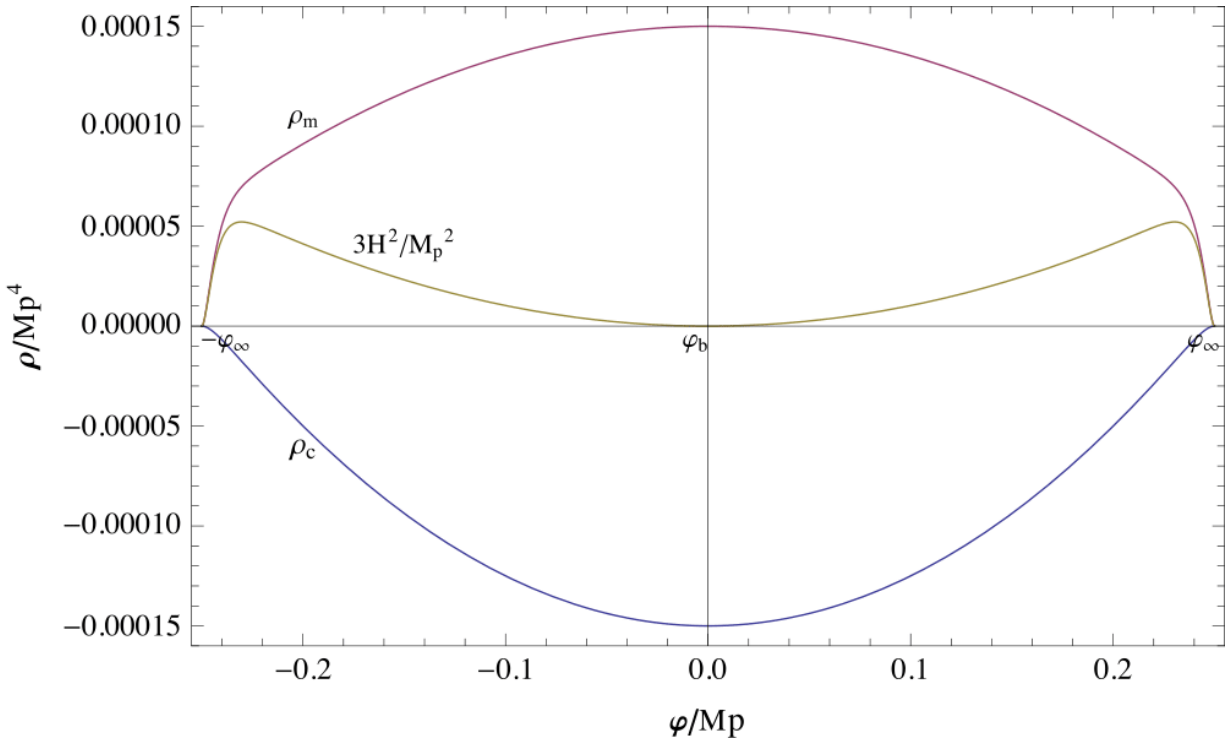

Figure 2.2: Densities and Hubble as functions of φ for $m = 0.05M_p$, $\varphi_\infty^2/m^2 = 25$ and $\mu = 0.3M_p$.

figure (2.3) shows the ratio of ρ_m/ρ_{cus}. As expected the magnitude of ρ_{cus} is negligible far from the bounce and it is always less than ρ_m, except at the bounce where they cancels off in order to yield $\dot{H}_b = 0$.

Assuming $\omega = 1$ ($\rho_m(\varphi) = \rho_b(a/a_b)^{-6}$), one can obtain the evolution of background parameters numerically in terms of cosmic time or conformal time. Figures (2.4) and (2.5) illustrate that the cosmological evolution of Scale factor, $a(t)$, and Hubble constant, $H(t)$, are consistent with our picture for a regular bounce cosmology. Note that for simplicity we have chosen $sign(\dot{\varphi}) > 0$ so $\varphi < 0$ coincides with Hubble parameter being negative and universe contracting. Therefore, when φ evolves into the positive region, the universe undergoes a smooth bounce and enters an expanding phase.

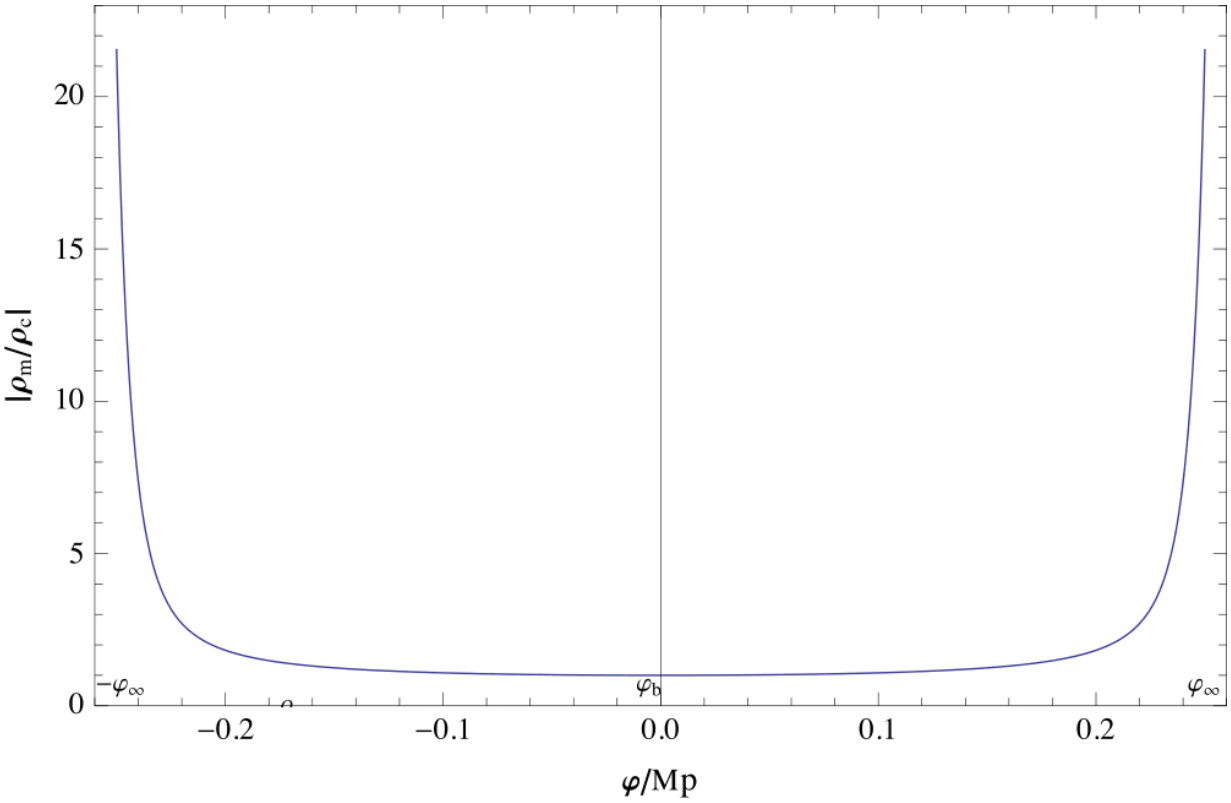

Figure 2.3: Ratio of densities as functions of φ for $m = 0.05M_p$, $\varphi_\infty^2/m^2 = 25$ and $\mu = 0.3M_p$. For this choice for the values of the parameters in the model, ρ_{cus} becomes more than twenty times smaller than ρ_m far away from the bounce.

Having developed a consistent picture of the background bounce, next we study the behaviour of cosmological perturbations around this background.

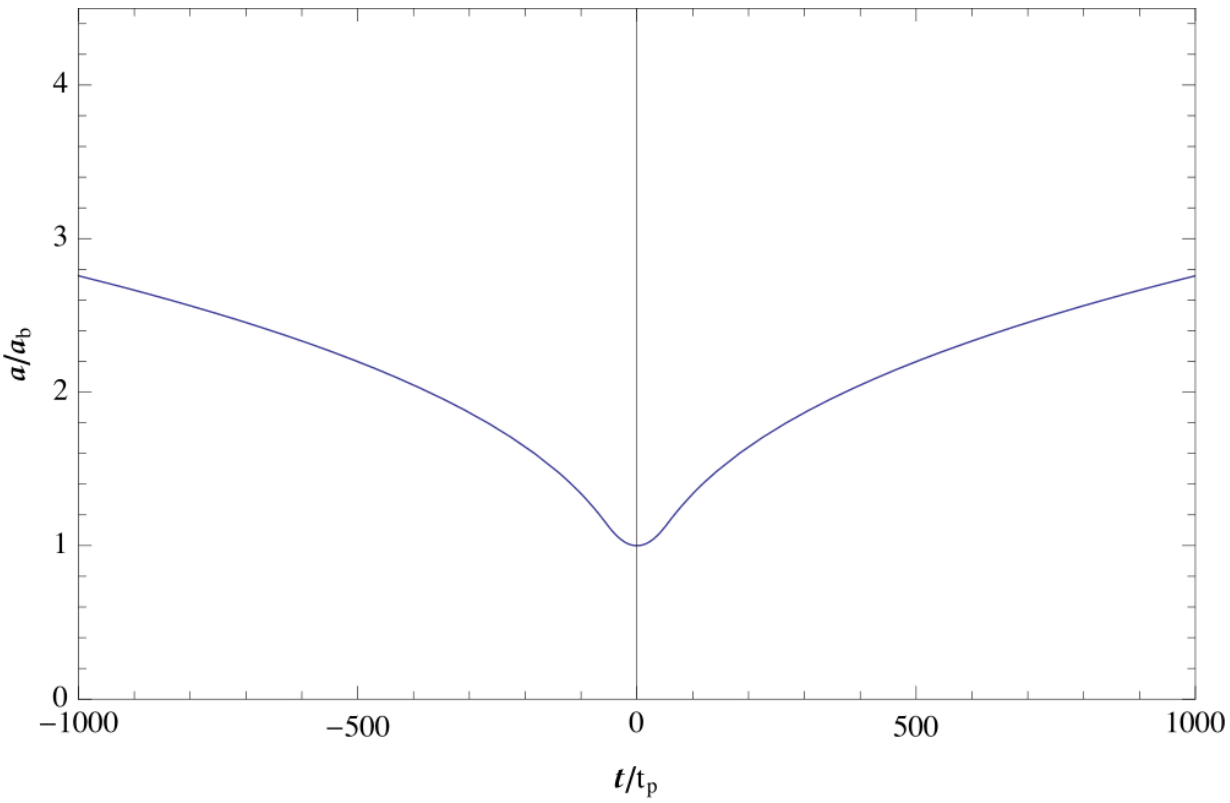

Figure 2.4: The evolution of scale factor, $a(t)$ in time is consistent with universe contracting, undergoing a regular bounce and then expanding.

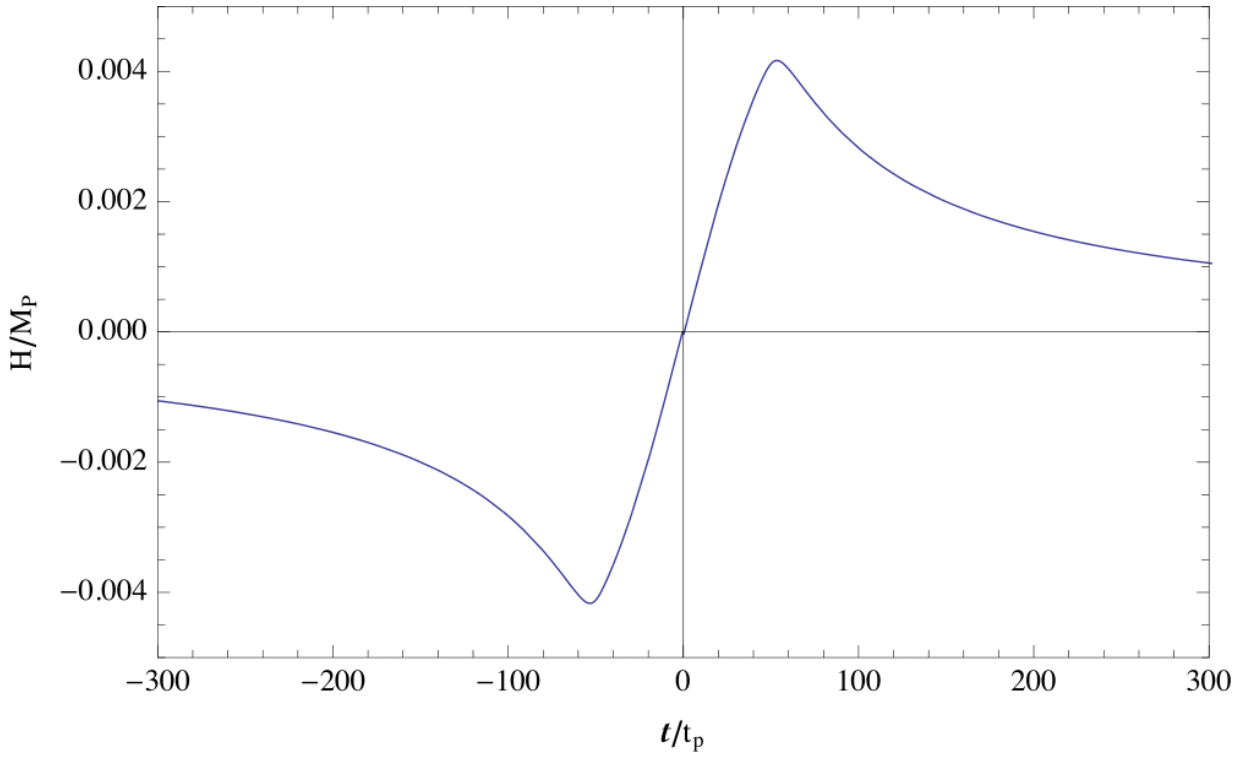

Figure 2.5: The evolution of Hubble constant, H, as a function of time. Hubble constant vanishes at the bounce and far from the bounce and there exists a *NEC* violating region around the bounce where $\dot{H} > 0$.

2.3 Perturbations in cuscuton bounce

2.3.1 Absence of ghosts in cuscuton bounce

One of the generic instabilities that occurs in ~~NEC~~ models is ghost instability. This instability is by definition, a UV instability which can be identified though a wrong sign of kinetic term for excitations around flat space-time. In order to investigate the existence of such an instability in our cuscuton model, we have to study the corresponding action for quantum fluctuations. As we mentioned before, adding a canonical scalar field, π, that doesn't have a potential to cuscuton action, can automatically produce a dynamical source with $\omega = 1$. This allows us to study fluctuation in a framework consistent with the background evolution described in section 2.2.

The full action after including the canonical scalar field is given by,

$$S = \int d^4x\sqrt{-g}\left[\frac{M_p^2}{2}R - \frac{1}{2}D_\mu\pi D^\mu\pi - \mu^2\sqrt{-D_\mu\varphi D^\mu\varphi} - V(\varphi)\right], \tag{2.34}$$

where D_μ denotes Covariant derivatives, φ represents the cuscuton field and π stands for the canonical scalar field.

This action is in fact a subclass of actions that we have studied in [40]. There, we probed the existence of ghosts in cuscuton gravity with a generic canonical scalar field content. We found that in general such models do not contain ghosts. We provide a brief summary of our derivation here as well.

The framework involves the standard way of perturbing action around a flat FRW spacetime. We then used the Unitary gauge fixing[8], where time slices are taken such that π field is the clock and the off-diagonal components of the spatial metric is set to zero. Naively, one would expect two independent scalar degrees of freedom arising from the canonical scalar field and the cuscuton field. However, owing to the non-dynamical nature of cuscuton, we are left with only one independent degree of freedom. We expressed this degree of freedom in terms of ζ, corresponding to curvature perturbations in this gauge. In other words, when expressing the metric in the ADM variables,

$$ds^2 = N^2dt^2 - h_{ij}(dx^i + N^i dt)(dx^j + N^j dt), \tag{2.35}$$

and setting the off-diagonal components of the spatial metric to zero, ζ is defined through $h_{ij} = a^2\delta_{ij}(1 + 2\zeta)$.

Using the Hamiltonian and the momentum constraints, the lapse and the shift can be expressed in terms of ζ and its time derivative. In this gauge, the cuscuton equation turns out to be a constraint

[8]The definition of the Unitary Gauge is not unique when we have more than one field. Here we call the gauge where $\delta\pi = 0$ as the 'unitary' gauge, as π field is the only dynamical field in our theory. Using this point of view, cuscuton can be considered as a non-trivial modification of gravity rather than as an additional field.

equation. That equation can be inverted into the Fourier space to obtain a closed form for $\delta\varphi_k$ in terms of ζ_k and its time derivative as,

$$\delta\varphi_k = \dot{\varphi}_0 \frac{(k/a)^2 H\zeta_k + P\dot{\zeta}_k}{[(k/a)^2 H^2 + (3H^2 + P + \dot{H})P]}, \tag{2.36}$$

where, $P = \frac{1}{2M_p^2}\dot{\pi}_0^2$. Substituting for all the variables in terms of ζ, back in the action, we obtain the quadratics action to be,

$$S^{(2)} = \frac{M_p^2}{2}\int d^3k\ dt\ az^2\left[\dot{\zeta}_k^2 - \frac{c_s^2\ k^2}{a^2}\zeta_k^2\right]. \tag{2.37}$$

$z(k,t)$ and $c_s(k,t)$ are functions that depend on both time and scale and are given by

$$c_s^2 \equiv \frac{(k/a)^4 H^2 + (k/a)^2\mathcal{B}_1 + \mathcal{B}_2}{(k/a)^4 H^2 + (k/a)^2\mathcal{A}_1 + \mathcal{A}_2} \tag{2.38}$$

$$z^2 \equiv 2\,a^2 P\left(\frac{(k/a)^2 + 3P}{(k/a)^2 H^2 + (P)(3H^2 + P + \dot{H})}\right). \tag{2.39}$$

Here, we have introduced the following notation to simplify the relations

$$\mathcal{A}_1 = P(6H^2 + \dot{H} + P) \tag{2.40}$$

$$\mathcal{A}_2 = 3P^2(3H^2 + \dot{H} + P) \tag{2.41}$$

$$\mathcal{B}_1 = P(12H^2 + 3\dot{H} + P) + \dot{H}(2\dot{H} + \frac{H\ddot{H}}{\dot{H}}) \tag{2.42}$$

$$\mathcal{B}_2 = P^2(15H^2 - P + \dot{H}) - P\dot{H}(12H^2 - 2\dot{H} + \frac{3H\ddot{H}}{\dot{H}}) \tag{2.43}$$

As is seen from the quadratic action, (2.37), Cuscuton gravity is free from ghost if the coefficient of the kinetics term, z^2 is positive. The terms, $(k/a)^2$ and P, appearing in the numerator of z^2 are both positive. Hence, positivity of z^2 depends on the sign of the denominator. The denominator can be simplified using the background equation to,

$$(k/a)^2 H^2 + P(3H^2 + \frac{\mu^2}{2M_p^2}|\dot{\varphi}_0|) \tag{2.44}$$

Written in this form, it is apparent that the denominator is always positive. Hence, this class of Cuscuton Gravity, including our bounce model is ghost-free[9]. Furthermore, positivity of denominator and non-vanishing contribution from cuscuton modification, guarantees the absence of any poles in this coefficient regardless of wavelength and at the bounce ($H = 0$).

[9]As discussed in [40] the other class with $+\mu^2$ in the Lagrangian, also turns out to be ghost free.

2.3.2 Absence of dynamical instabilities in cuscuton bounce

We next investigate the dynamical stability of the perturbations in different regimes.

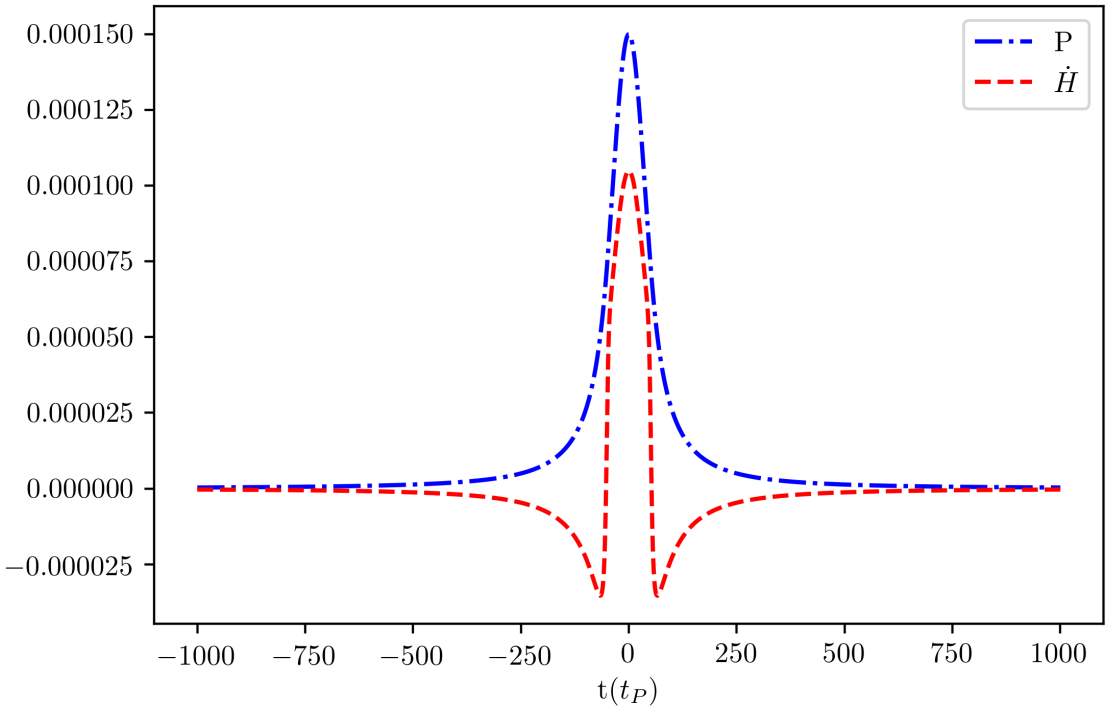

Figure 2.6: The quantities, P, and $\dot{H}$ plotted as a function of time. It can be seen that both quantities are of the same order at the bounce($t = 0$)

As mentioned earlier, the dynamics of the perturbations can be described through the perturbation quantity, ζ. The equations of motion determining the evolution of ζ was derived in [40]. Similar to action, it is convenient to express this equation in the Fourier space

$$\ddot{\zeta}_k + (H + 2\frac{\dot{z}}{z})\dot{\zeta}_k + \left(\frac{c_s^2 k^2}{a^2}\right)\zeta_k = 0, \tag{2.45}$$

where the quantities c_s and z are given in equations (2.38) and (2.39) and we find

$$\begin{aligned} 2\frac{\dot{z}}{z} &= -6H - 2H\left(\frac{((k/a)^2 + 9P)}{(k/a)^2 + 3P}\right) \\ &\quad + \left(\frac{(k/a)^2(2H\dot{H} - 2H^3) + P(\ddot{H} - 12HP - 18H^3)}{(k/a)^2H^2 + P(3H^2 + P + \dot{H})}\right). \end{aligned} \tag{2.46}$$

We would like first to point out, that equation (2.45) does not become singular for any value of k at any time. That's because $P > 0$, $P + \dot{H} = \frac{\mu^2}{2M_p^2}|\dot{\varphi}| > 0$ and c_s^2 is always finite [10].

We now proceed to numerically explore the dynamics of the perturbations for different scales and as they pass through the bounce. Since at the bounce $H_b = 0$ and $\ddot{H}_b = 0$, there are two relevant mass scales in equation (2.45), corresponding to quantities $\sqrt{\dot{H}_b}$ and $\sqrt{P}_b$. Figure 2.6, demonstrates the time dependence of $\dot{H}$ and P for our model. As we see, both $\sqrt{\dot{H}_b}$ and $\sqrt{P}_b$ are comparable and around $\sim 10^{-2}M_p$ at the bounce. Therefore, we can associate a bounce length scale, $l_B \sim 1/\sqrt{\dot{H}_b}$ to this scale and classify our modes with respect to that. We refer to modes as Ultra-Violet (UV)/Infra-Red (IR), if they are shorter/longer with respect to this length scale.

The equation governing the evolution of the perturbations, (2.45) is a second order differential equation, which implies the existence of two independent solutions for each k. We have to check the stability for both of these modes to ensure that perturbations are stable on this bouncing background. To do that, we chose two solutions such that one is non-zero at the bounce but has zero derivative there, while the other is zero at the bounce but has non-zero derivative. Since the Wronskian for these solutions is non-zero at the bounce, they are independent.

To examine the evolution in different regimes, we evolved three wavelength modes, with $\lambda = 0.1l_B, l_B, 10l_B$ numerically. The results of the numerical evolution for the two independent solutions, is shown in Figures 2.7. Our result confirms that there are no instabilities associated with the evolution of modes in different wavelengths scales. As we mentioned before, the value of $\sqrt{\dot{H}_b}$ is $0.01M_{Pl}$. Therefore, the wavelengths we are investigating are of the order of $10\ell_P$, $100\ell_P$ and $1000\ell_P$.

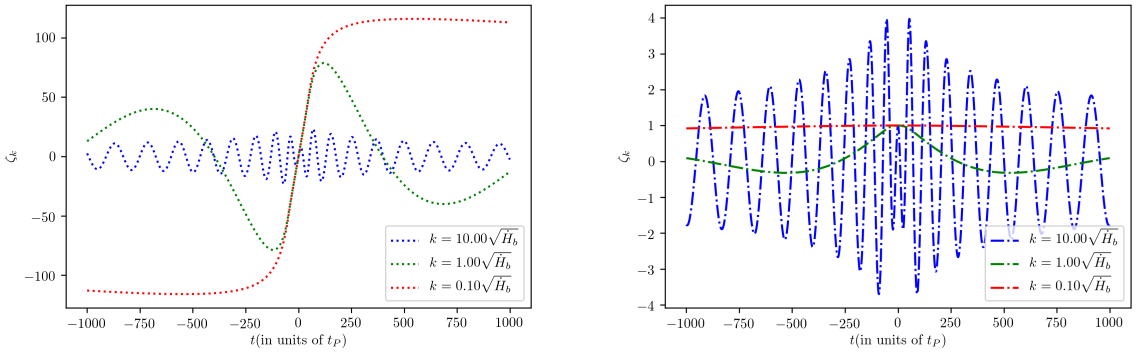

Figure 2.7: Evolution of perturbations at three different length scales, $k/\sqrt{\dot{H}_b} = 0.1, 1.0, 10.0$. The two panels correspond to different initial conditions which leads to linearly independent solutions. The left panel has $\zeta_b = 0, \dot{\zeta}_b \neq 0$. The right panel has $\zeta_b \neq 0, \dot{\zeta}_b = 0$

We conclude that there is no pathology associated with the perturbations at the bounce or at

[10]The denominator of c_s^2 is always positive since the quantities $\mathcal{A}_1$ and $\mathcal{A}_2$ simplify to $\mathcal{A}_1 = P(6H^2 + \frac{\mu^2}{2}|\dot{\varphi}|)$ and $\mathcal{A}_2 = 3P^2(3H^2 + \frac{\mu^2}{2}|\dot{\varphi}|)$.

the transition into ~~NEC~~ region ($|t| \sim 60\, t_p$), neither for UV or IR or intermediate scales.

2.4 Conclusions

In this work, we found a cuscuton bounce solution that has no pathologies associated with ~~NEC~~. Our solution corresponded to a toy model consisting of a cuscuton field, φ, in addition to a dynamical matter source, π. At the background level, we required that away from the bounce (in the contracting or expanding phase) cuscuton density be sub-dominant to matter density. However, we looked for a cuscuton potential such that it would grow faster than matter density as universe contracted and would make the background bounce into expansion. After finding an appropriate potential, we used the cosmological perturbation theory to scrutinize the existence of ghosts and other instabilities in the model. We found that the theory is healthy. We think the underlying reason for absence of instabilities in our model, is that unlike GR, the field which governs the background, i.e. cuscuton, does not have its own dynamical degree of freedom. Therefore, we expect our result can be extended beyond bounce models to more generic classes of solutions with ~~NEC~~, which otherwise suffer from instabilities.

Chapter 3

Review of Effective Field Theory of Inflation (EFToI)

In the previous chapter, I have proposed a model where the universe goes through a bouncing phase, where we do not face the singularity problem. In its formulation, we have deviated away from general relativity by introducing an auxiliary field named Cuscuton. We now return our focus to single field inflationary models and study how we can apply techniques of effective field theories to study inflationary models in one unifying framework [50, 27]. In this chapter, I will briefly review a systemic method to build a general effective action for perturbations in single field inflationary models.

The basic idea is that the background solution for inflation driven by a single scalar $\phi(t, \vec{x})$ has a preferred spatial slicing, where ϕ can be take to be a physical clock. In the unitary gauge, we can realize this slicing by taking

$$\phi(t, \vec{x}) \equiv \phi_0(t) + \delta\phi(t, \vec{x}), \rightarrow \qquad \delta\phi(t, \vec{x}) = 0. \tag{3.1}$$

In this gauge, all degrees of freedom for scalar perturbation is absorbed into metric fluctuations. Furthermore, the time diffeomorphism is spontaneously broken and is no longer a linearly realized symmetry. Due to the reduced symmetry in this gauge, there can be more terms in the action than only four dimensional diffeomorphism invariant terms as all the 3D spatial diffeomorphism invariant terms can also be included.

The terms that can be included are:

- Terms that are invariant under all diffeomorphisms (4-diffs): These are polynomials scalars obtained by contracting polynomials of the Riemann tensor $R_{\mu\nu\rho\sigma}$ and its covariant derivatives.
- Any functions that are purely a function of time and its covariant derivatives.
- Any tensors with free upper indices 0. These include operators such as g^{00} or R^{00}.

- The polynomials of the extrinsic curvature tensor $K_{\mu\nu}$ and its covariant derivatives.

It is convenient and useful to define a unit vector perpendicular to the hypersurface of constant time, $\tilde{t}$:

$$n_\mu = \frac{\partial_\mu \tilde{t}}{\sqrt{-g^{\mu\nu}\partial_\mu \tilde{t}\partial_\nu \tilde{t}}}. \tag{3.2}$$

Then we can also define the induced spatial metric:

$$h_{\mu\nu} \equiv g_{\mu\nu} + n_\nu n_\mu. \tag{3.3}$$

The covariant derivatives of n_μ projected on to the constant time surface gives the extrinsic curvature

$$K_{\mu\nu} = h_\mu^\sigma \nabla_\sigma n_\nu. \tag{3.4}$$

Thus, all polynomials of the covariant derivative of the normal unit vector do not give rise to new terms. Furthermore, the projection of tensors in the action onto the constant time surfaces do not give new terms. For example, the induced 3d Riemann tensor $R^{(3)}_{\mu\nu\rho\sigma}$ can be written in terms of the original 4d Riemann tensor, the induced metric $h_{\mu\nu}$ and the extrinsic curvatures.

According to the above rules, the most general action for a single field theory in curved spacetime can be written as a function $\mathcal{L}$ of allowed operators

$$S = \int dt\ dx^3 \sqrt{-g}\mathcal{L}(R_{\mu\nu\rho\sigma}, g^{00}, K_{\mu\nu}, \nabla_\mu, t). \tag{3.5}$$

While in this gauge, the action (3.5) is only spatial diffeomorphism (3-diff) invariant. To restore the time diffeomorphism invariance, we can apply the Stueckelberg trick. Let us see through a simple example how this process works. Consider the following operators

$$\int dt\ d^3x\sqrt{-g}\left(A(t) + B(t)g^{00}(x)\right). \tag{3.6}$$

Now, to 'free' the unitary gauge and time from being fixed to constant hypersurfaces, we can $t \to \tilde{t} = t + \xi^0(x_\mu)$, $\vec{x} \to \vec{\tilde{x}} = \vec{x}$ Under the time diffeomorphism, the metric transform as

$$g^{\alpha\beta} \to \tilde{g}^{\alpha\beta} = \frac{\partial \tilde{x}^\alpha}{\partial x^\mu}\frac{\partial \tilde{x}^\beta}{\partial x^\nu} g^{\mu\nu}, \tag{3.7}$$

and the integral in terms of $\tilde{x}$ becomes

$$\int d\tilde{t}d^3\tilde{x}\sqrt{-\tilde{g}}\left(A(\tilde{t} - \xi^0(\tilde{x})) + B(\tilde{t} - \xi^0(\tilde{x}))\frac{\partial(\tilde{t} - \xi^0(\tilde{x}))}{\partial x^\mu}\frac{\partial(\tilde{t} - \xi^0(\tilde{x}))}{\partial x^\nu}\tilde{g}^{\mu\nu}\right). \tag{3.8}$$

We can now see that by promoting $\xi^0(\tilde{x})$ in the action above to a field $-\tilde{\pi}(\tilde{x})$, and requiring that it transform as

$$\pi(x) \to \tilde{\pi}(\tilde{x}) = \pi(x) - \xi^0(x), \tag{3.9}$$

the integral becomes invariant under all diffeomorphisms. Note that since under $t \to t + \xi^0$ we get $\delta\phi \to \delta\phi + \dot{\phi}\xi^0$, after time transformation, we no longer expect $\delta\phi = 0$, but rather we have $\pi = \delta\phi/\dot{\phi}_0$.

Now we are interested in this approach in context of slow-roll inflationary models. It can be shown that expanding around FLRW background and using Friedmann equations, the Lagrangian density in (3.5) can be written as[50, 27]

$$\mathcal{L} = M_{\rm Pl}^2 \left[\frac{1}{2} R + \dot{H}\, g^{00} - \left(3\, H^2 + \dot{H}\right)\right] + \sum_{m\geq 2} \mathcal{L}_m(g^{00}+1, \delta K_{\mu\nu}, \delta R_{\mu\nu\rho\sigma}, \nabla_\mu; t)\,, \tag{3.10}$$

with $\mathcal{L}_m$ representing functions of order m in $g^{00}+1$, $\delta K_{\mu\nu}$ and $\delta R_{\mu\nu\rho\sigma}$.[1] The perturbed quantities are given by

$$\delta K_{\mu\nu} = K_{\mu\nu} - K_{\mu\nu}^{\rm FLRW}, \qquad \delta R_{\mu\nu\rho\sigma} = R_{\mu\nu\rho\sigma} - R_{\mu\nu\rho\sigma}^{\rm FLRW}. \tag{3.11}$$

This action is very complicated in general. However, the advantage of using this approach is that, when the generalised slow roll approximation is valid, one can ignore contribution of all the other metric perturbations to scalar perturbations at high energy scales. Basically, if the typical scale of the time dependence of the coefficients in the unitary gauge is much longer than the Hubble time, the theory effectively decouples from gravity and it is possible to compute the scalar power spectrum neglecting metric perturbations in the action.

For instance, under the transformation $t \to t + \pi$ the $M_{\rm pl}^2 \dot{H} g^{00}$ term transform as

$$M_{\rm pl}^2 \dot{H} g^{00} \to M_{\rm pl}^2 \dot{H} g^{00} (1 + \dot{\pi})^2 + \dots. \tag{3.12}$$

Under canonical normalization $\pi_c = M_{\rm pl} \dot{H}^{1/2} \pi$ and $g_c^{00} = M_{\rm pl} g^{00}$, we get

$$M_{\rm pl}^2 \dot{H} g^{00} (1 + \dot{\pi})^2 = \dot{\pi}_c^2 + 2\dot{H}^{1/2} \dot{\pi}_c g_c^{00} + \dot{H} g_c^{00}. \tag{3.13}$$

The second term in (3.13) mixes gravity with the scalar. However, at energies higher than $\dot{H}^{1/2}$, the term $\dot{\pi}_c^2$ dominates the dynamics, so the scalar and gravity decouple.

Now as a simple test we can check what would the action of a simple inflationary model translate to in the unitary gauge:

$$S_\phi = \int d^4x \sqrt{-g} \left(-\frac{1}{2}(\partial\phi)^2 - V(\phi)\right) \to \int d^4x \sqrt{-g} \left(-\frac{\dot{\phi}_0(t)^2}{2} g^{00} - V(\phi(t))\right). \tag{3.14}$$

Now, substituting from the Friedmann equations for the FLRW background gives us the following action at the unperturbed level

$$S_\phi = M_{\rm pl}^2 \int d^4x \sqrt{-g} \left(\dot{H} g^{00} - (3H^2 + \dot{H})\right). \tag{3.15}$$

[1] In the original EFToI formalism [50], only the quadratic operators built out of $\delta K_{\mu\nu} = K_{\mu\nu} - K_{\mu\nu}^{\rm FRW}$ were studied. As we will see, dropping higher order operators is not always necessary and one can extend the EFToI correspondingly.

If we implement the procedure described above for the action (3.15), we obtain

$$\mathcal{L}_{\text{slow-roll}} = -M_{\text{Pl}}^2 \dot{H} \left(\dot{\pi}^2 - \frac{(\partial \pi)^2}{a^2} \right), \tag{3.16}$$

which matches action (3.10) assuming $\mathcal{L}_m = 0$, $m \geq 2$.

Furthermore, one can show, using proper gauge transformations, that π is related to the commonly used conserved quantity for curvature perturbation in literature ζ by $\zeta = -H\pi$. Substituting ζ in the above action reduces it to the standard slow-roll inflationary action for ζ.[2]

Since in many single field inflationary models especially inspired from quantum gravity, we are interested in deviations from the standard canonical scalar field models, one can turn on the coefficients of the operators in $\mathcal{L}_m$ to describe them all.

In the original EFToI study, they investigated inflationary models that can have different speed of sounds as well as dispersion relations up to quartic order. Examples of such corrections had previously been noticed in the community through other approaches. However, the EFToI provide a framework to explore them all generically. The unitary gauge action in this case includes

$$\mathcal{L}_{\text{EFToI}} = \mathcal{L}_{\text{slow-roll}} + \mathcal{L}_2 \,, \tag{3.17}$$

with:

$$\mathcal{L}_2 = \frac{M_2^4}{2!} (g^{00} + 1)^2 + \frac{\bar{M}_1^3}{2} (g^{00} + 1) \delta K^\mu_{\ \mu} - \frac{\bar{M}_2^2}{2} (\delta K^\mu_{\ \mu})^2 - \frac{\bar{M}_3^2}{2} \delta K^\mu_{\ \nu} \delta K^\nu_{\ \mu} \,. \tag{3.18}$$

The first term, $(g^{00} + 1)^2$, is the operator that modifies the speed of sound for scalar perturbations from the speed of light. Noting that $(g^{00} + 1)$ has zero mass dimension, powers of $(g^{00} + 1)^n$ with $n \geq 3$ could also be included which result to more general K-inflationary models. The mass dimension 1 term, $(g^{00} + 1)\, \delta K^\mu_{\ \mu}$, is not symmetric under time reversal, and was already analysed in [50, 28]. Finally $\frac{\bar{M}_2^2}{2} (\delta K^\mu_{\ \mu})^2$ and $\frac{\bar{M}_3^2}{2} \delta K^\mu_{\ \nu} \delta K^\nu_{\ \mu}$ are the operators that lead to Inflationary models with a quartic correction to the dispersion such as those that had been noticed in Ghost Inflation [12, 50].

[2]The correspondence is up to a mass correction in higher orders of slow roll parameters. In quasi de Sitter space, π gets a small mass due to time-dependent background, which has to be taken into account to get the exact correspondence

Chapter 4

Extended Effective Field Theory of Inflation

4.1 Introduction

As we discussed in last chapter, the Effective Field Theory of Inflation (EFToI) [50] provides an alternative picture to understand perturbations in single field driven inflationary models. In this picture, one first fixes the gauge by taking constant time hypersurfaces to coincide with inflaton constant surfaces. In other words, the perturbations of the inflaton field are absorbed into the fluctuations of the metric. The inflaton fluctuations transform non-linearly under the time diffeomorphism but the non-linear sigma model describing it can always be UV completed into the theory of inflation with a linear representation of time diffeomorphism. The Goldstone mode, π, corresponding to breaking time diffeomorphism symmetry, describes the scalar perturbations around the FRW background. Therefore, the most generic action for inflation can be constructed out of the quantities that respect the remaining symmetries, *i.e.* the spatial diffeomorphisms. The coefficients of these terms can be time-dependent in principle.

This means including more terms such as the metric component g^{00} and the extrinsic curvature of constant time hypersurfaces, $K_{\mu\nu}$, which are only spatially diffeomorphism invariant, in addition to standard 4-diffeomorphism invariant terms. It was shown in [50] that, around a FRW background, this reduces to including functions of time, $g^{00}+1$, $\delta K_{\mu\nu}$, $\delta R_{\mu\nu\rho\sigma}$, and covariant derivative.

One can then make the Goldstone mode explicit by applying the Stückelberg technique and study the physics of the Goldstone mode at energies where the mixing with gravity can be neglected. In this framework, the standard slow-roll inflationary model corresponds to adding only operators with time dependence and at most linear in terms of g^{00} (mass dimension zero), before performing the Stückelberg trick. Higher dimensional operators quantify deviations from the standard canonical single field slow-roll inflation. In terms of π and in the decoupling limit, the standard slow-roll Lagrangian is obtained from dimension 4 operators from the kinetic terms

of the canonically normalised π. Including higher order derivatives and mass dimensions can lead to higher order dispersion relations. Due to the non-linear nature of the time diffeomorphism, once it is restored, the spatially diffeomorphism invariant operators will lead to a non-linear dependence on the Goldstone mode. This in turn leads to non-vanishing higher point correlation functions. Therefore, the coefficients of these operators can be constrained by measuring the corresponding correlation functions.

The above approach is borrowed from particle physics since also the Standard Model is described through the lowest dimension operators that are compatible with the symmetries of the system. Then higher dimensional operators describe deviations from the vanilla case and quantify the emergence of new physics. Similarly, in the EFToI, higher dimensional operators can reproduce various interesting inflationary models, such as DBI inflation [11, 140, 139], with speed of sound different from one, or Ghost Inflation [12], with leading spatial gradient term proportional to $(\nabla^2\pi)^2$[50]. In particular, as shown in [50], reducing the speed of sound naturally strengthens the cubic interaction, which in turn enhances the non-gaussianity.

In the EFToI, these higher dimensional operators can also change the dispersion relation. For example, the inclusion of $\delta K^2_{\mu\nu}$ operators modifies the dispersion relation to $\omega^2 \sim k^4$ (similar to Ghost Inflation). Including additional higher dimensional operators of the form $(\nabla^{(s-2)}K_{\mu\nu})^2$ with $s \geq 3$, when they are dominant, would modify the dispersion relation even further to $\omega^2 \sim k^{2s}$.

However, the authors of [50] did not include operators beyond mass dimension 2, since they claimed that these new terms would not be compatible with a sensible EFT description. The reason is the fact that in such theories, when $E \to \Sigma E$, the energy scaling dimension for π would be $\pi \to \Sigma^{-1/2+3/2s}\pi$ and so the scaling behaviour of cubic operators like $\dot\pi(\nabla\pi)^2$ would be $(7-3s)/(2s)$. This would imply that for $s \geq 3$ this operator would become *relevant*, whereas for $s < 3$ it is *irrelevant* at low energies. Hence a theory with a dispersion relation of the form $\omega^2 \sim k^6$ would have an IR strong coupling cut-off Λ_6^{IR} which would in general make this theory not a controllable EFT.

However, we argue here that this may not always be the case. Our reason is that a dispersion relation of the form $\omega^2 \sim k^6$ would not hold up all the way to low energy scales. It is true that the scaling power of $\dot\pi(\nabla\pi)^2$ is $-1/3$, but the scaling power of $(\nabla^2\pi)^2$ and $(\nabla\pi)^2$ are respectively $-2/3$ and $-4/3$. This implies that the dispersion relation would also change from $\omega^2 \sim k^6$ to $\omega^2 \sim k^4$ at some energy scale $\Lambda^{4-6}_{\rm dis}$. Hence, if the coefficients of the higher dimensional operators are tuned such that $\Lambda^{\rm IR}_6 \ll \Lambda^{4-6}_{\rm dis}$, the $\omega^2 \sim k^6$ theory remains weakly coupled throughout its evolution down to low energies. On top of this, one has to require that the scale Λ_4, where the $\omega^2 \sim k^4$ theory becomes strongly coupled, is not below $\Lambda^{4-6}_{\rm dis}$. This is guaranteed if $\Lambda^{\rm IR}_6 \ll \Lambda^{4-6}_{\rm dis} \ll \Lambda_4$. Similarly, one has to require that the standard $\omega^2 \sim k^2$ theory does not become strongly coupled at a scale Λ_2 which is below the scale $\Lambda^{2-4}_{\rm dis}$ where the dispersion relation becomes dominated by the quartic term: $\Lambda^{2-4}_{\rm dis} \ll \Lambda_2$ [30].

Under these conditions, the EFT for the perturbations remains weakly coupled all the way from low energy to the $\omega^2 \sim k^6$ regime. Note that in addition, this framework is only valid on energy scales below Λ_b, where time diffeomorphisms get spontaneously broken by the inflaton

background. Thus, we also need to require $\Lambda_{\rm dis}^{4-6} \ll \Lambda_b$. This is because at Λ_b the scalar perturbations become of the same order of magnitude of the background which, therefore, cannot be integrated out to leave an EFT for the fluctuations only. The cut-off of the EFT for the fluctuations $\Lambda_{\rm cutoff}$ is therefore the minimum between Λ_b and the UV strong coupling scale of the $\omega^2 \sim k^6$ theory, $\Lambda_6^{\rm UV}$, associated with some higher derivative operators which remain irrelevant.

Strictly speaking, the cosmological experiment is done at energies of order the Hubble scale H where horizon exit takes place. Hence, in order for the EFT approach to be under control, one would need just to require $H \ll \Lambda_{\rm cutoff}$ and a horizon crossing that occurs in the region where the dispersion relation takes the standard quadratic form. However, the goal of this chapter is to provide a consistent theoretical framework to motivate the emergence of modified dispersion relations which, as previously shown, can lead to (super-excited) non-Bunch-Davis initial conditions with interesting implications for CMB observations [21]. Thus we need to control the EFT also in the high energy $\omega^2 \sim k^6$ regime which describes the behavior of the perturbations deep inside the horizon. These perturbations are born in the vacuum of k^6 theory but then become excited states due to the transitions to the quartic and finally to the standard quadratic regime for the dispersion relation which happen before horizon crossing. Therefore, in order to be able to describe consistently the whole evolution of these modes from deep inside the horizon to super-horizon scales, we need to be able to trust the EFT for the fluctuations up to the $\omega^2 \sim k^6$ regime.

In this chapter we shall therefore include higher order corrections which in the unitary gauge correspond to operators with mass dimension 3 and 4 that were so far neglected in the literature. Hence, we shall call this framework Extended Effective Field Theory of Inflation (EEFToI). As explained above, these higher dimensional terms modify the dispersion relation and, depending on the sign and magnitude of their coefficients, can have important implications for scalar perturbations. We shall focus only on modifications of the equation of motion that lead to interesting dispersion relations for π by higher order terms, and so we shall consider operators which include at least one factor of $\delta K_{\mu\nu}$ in their expression. One can write down other operators with the same mass dimensions as the one we focus on below, which would not affect the two point function for scalar perturbations. We also drop operators of the form $(1+g^{00})^n$ with $n \geq 3$ since, contrary to $(1+g^{00})^2$, they do not change the speed of sound for π.

The outline of this chapter is as follows. In Sec. 4.2, we present the EEFToI by writing down all operators with mass dimension three and four that can add a correction proportional to k^6 in the dispersion relation. In Sec. 4.3, we discuss the implications of these higher dimensional operators for tensor and scalar perturbations. In particular, after identifying the allowed operators, we focus on the healthy region of parameter space for π and explore various scenarios that can arise. We study the scalar power spectrum in these scenarios, depending on the sign of the coefficients of the quartic and sextic corrections to the dispersion relation. We also analyse the implications for the tensor-to-scalar ratio. In Sec. 4.4, we comment on the cut-off of the EEFToI and the size of non-Gaussianity. In Sec. 4.5 and 4.6 we will study the bispectrum and the non-Gaussianity of the theory and compute the constraints on EEFToI parameter space including the size of the non-Gaussianity. In Sec. 4.7, we conclude and give directions for future research.

4.2 Extended EFT of inflation

4.2.1 Lagrangian of the Extended EFT of inflation

We know proceed to introduce the Lagrangian of the EEFToI. We supplement the unitary gauge action of the EFToI with operators of mass dimension 3 and 4 constructed out of $\delta K^{\nu}_{\ \mu}$, ∇_μ and g^{00} so that the Lagrangian of the EEFToI (again keeping only terms which contribute to quadratic action for π) becomes

$$\mathcal{L}_{\rm EEFToI} = \mathcal{L}_{\rm EFToI} + \mathcal{L}_{2,d3} + \mathcal{L}_{2,d4}\,, \tag{4.1}$$

with:

$$\begin{aligned}\mathcal{L}_{2,d3} + \mathcal{L}_{2,d4} \;=\; & \frac{\bar{M}_4}{2}\nabla^\mu g^{00}\nabla^\nu \delta K_{\mu\nu} - \frac{\delta_1}{2}\,(\nabla_\mu \delta K^{\nu\gamma})(\nabla^\mu \delta K_{\nu\gamma}) - \frac{\delta_2}{2}\,(\nabla_\mu \delta K^{\nu}_{\ \nu})^2 \\ & -\frac{\delta_3}{2}\,(\nabla_\mu \delta K^{\mu}_{\ \nu})(\nabla_\gamma \delta K^{\gamma\nu}) - \frac{\delta_4}{2}\,\nabla^\mu \delta K_{\nu\mu}\nabla^\nu \delta K^{\sigma}_{\ \sigma},\end{aligned} \tag{4.2}$$

where M_i, $\bar{M}_i$ and δ_i's are free (time dependent) coefficients and the sign of each term is also a priori free. We remark that the mass dimension 3 operator $\nabla^\mu g^{00}\nabla^\nu \delta K_{\mu\nu}$ is not symmetric under time reversal and δ_i's are the coefficients of dimension 4 operators.

Our motivation for adding such operators is that they lead to sixth order corrections to the dispersion relation. The reason advocated in [50] for discarding these operators is that sixth order corrections to the dispersion relation would make higher derivative operators relevant, signaling the presence of an IR strong coupling regime. However, as explained in Sec. 4.1 and as we will discuss in more depth in Sec. 4.4, one can still have a sensible EFT description if the IR strong coupling scale of the $\omega^2 \sim k^6$ theory is below the scale $\Lambda^{4-6}_{\rm dis}$ where the dispersion relation becomes dominated by the quartic term.

We emphasise here that in this EFT approach to inflation, the Lorentz symmetry is not preserved. In particular, the mass dimension and energy scaling dimension of the operators depending on δK do not match. We should also add that we have only kept terms that can modify the action for scalar perturbations at second order. There are other operators, e.g. proportional to $\bar{M}\,\delta K^3$, that do not contribute to the linear equation of motion of the Goldstone boson π. For reasons that will become clear momentarily, we first focus on the implications of the mass dimension 3 and 4 operators on the action for tensor perturbations. Then we will get back to the action for the Goldstone mode π derived from the unitary gauge action in the EEFToI.

4.3 Perturbations in the extended EFT of inflation

4.3.1 Tensor perturbations

To study the tensor perturbations, we perturb the spatial part of the metric as follows

$$g_{ij} = a^2(\delta_{ij} + \gamma_{ij})\,, \tag{4.3}$$

where γ_{ij} is transverse and traceless (summation over the repeated index i is assumed),

$$\gamma_{ii} = 0\,, \qquad \partial_i \gamma_{ij} = 0\,, \tag{4.4}$$

and we will expand the action (4.1) up to second order in γ_{ij}. As pointed out in the original EFToI paper [50], from the mass dimension zero up to mass squared operators, only $-\frac{\bar{M}_3^2}{2}\,\delta K^{\mu}_{\ \nu}\,\delta K^{\nu}_{\ \mu}$ affects the equation of motion for γ_{ij}, and adds the following contribution to the action for tensor perturbations

$$S^{\bar{M}_3^2} = -\frac{\bar{M}_3^2}{8}\int a^3 dt\, d^3x\; \partial_0\gamma_{ij}\partial_0\gamma_{ij}\;. \tag{4.5}$$

The action (4.5), together with the terms describing the usual massless scalar field contribution for tensor perturbations,

$$S_{\rm EH} = \frac{M_{\rm Pl}^2}{8}\int dt\, d^3x\, a^3\left(\partial_0\gamma_{ij}\partial_0\gamma_{ij} - a^{-2}\partial_l\gamma_{ij}\partial_l\gamma_{ij}\right)\,, \tag{4.6}$$

produces the following modified equation of motion for tensor perturbations,

$$p_k'' + \left(c_{\rm T}^2 k^2 - \frac{a''}{a}\right) p_k = 0\,, \tag{4.7}$$

where $p_k \equiv a\,\gamma_k$, the subscript k refers to the Fourier transform of the two helicities of the gravitons, and

$$c_{\rm T}^2 = \left(1 - \frac{\bar{M}_3^2}{M_{\rm Pl}^2}\right)^{-1}\,. \tag{4.8}$$

In order to avoid superluminal propagation for tensor perturbations, one must then have $\bar{M}_3^2 \leq 0$. Larger values of $|\bar{M}_3|$ correspond to smaller speed of sound and, for $|\bar{M}_3| \to M_{\rm Pl}$, the speed of gravitational waves $c_{\rm T} \to 1/\sqrt{2}$.

For $\bar{M}_3^2 > 0$, the speed of gravitation waves is superluminal. Lorentz invariant EFTs with this property have been argued to be non-local and not embeddable in a local quantum field theory or string theory [1]. However, [26] argues that such models, despite having superluminal propagation, do not lead to any violation of causality. If $\bar{M}_3^2 > 0$ is taken as a legitimate choice, larger values of $\bar{M}_3^2$ increase the value of speed of sound and in fact this value diverges for $\bar{M}_3^2 \to M_{\rm Pl}^2$.

Now let us focus on the new operators with mass dimension 3 and 4. The term $\frac{\delta_1}{2}\,(\nabla_\mu \delta K^{\nu\gamma})(\nabla^\mu \delta K_{\nu\gamma})$, up to second order in γ_{ij}, yields

$$\frac{\delta_1}{2}\left[-\frac{H^2}{2}\left(\partial_0\gamma_{ij}\right)^2 + \frac{1}{4a^2}\left(\partial_{0m}^2\gamma_{ij}\right)^2 - \frac{1}{4}\left(\partial_0^2\gamma_{ij}\right)^2\right]\,, \tag{4.9}$$

where i, j and m are spatial indices and summation over m is assumed. Other operators do not contribute to the Lagrangian of tensor perturbations once the transverse traceless condition on

γ_{ij} is imposed. The appearance of $\partial_0^2\gamma_{ij}$ in the Lagrangian density (4.9) leads to ghost instability for the tensor perturbations. Thus the requirement of having no ghosts in the tensor sector of the theory translates into

$$\delta_1 = 0\,. \tag{4.10}$$

Therefore, dispersion relation of the primordial tensor fluctuations remains resilient to changes in the scalar and gravitational sector in the EEFToI, like it was shown originally in [52].

4.3.2 Scalar perturbations

The Goldstone boson can explicitly appear in the action via the Stückelberg trick. In this procedure, the variation of the metric with broken time diffeomorphism, $t \to \tilde{t} = t + \xi^0(x)$, $x \to \vec{\tilde{x}} = \vec{x}$, is obtained and $\xi^0(x(\tilde{x}))$ is everywhere replaced by $-\tilde{\pi}(\tilde{x})$ in the transformed action. Then $\pi(x)$ is assumed to transform non-linearly to $\tilde{\pi}(\tilde{x}) = \pi(x) - \xi^0(x)$, which guarantees that the action remains invariant under diffs to all orders [50]. Evaluating the action explicitly for π in Fourier space, Ref. [28] found out that, in the decoupling limit corresponding to $\dot{H} \to 0$ while $M_p^2\dot{H}$ is fixed, the EFToI Lagrangian (3.17) in the unitary gauge leads to the following second order Lagrangian in the π-gauge:

$$\begin{aligned}\mathcal{L}^{(\pi)}_{\rm EFToI} &= M_p^2\dot{H}(\partial_\mu\pi)^2 + 2M_2^4\dot{\pi}^2 - \bar{M}_1^3 H\left(3\dot{\pi}^2 - \frac{(\partial_i\pi)^2}{2a^2}\right) - \frac{\bar{M}_2^2}{2}\left(9H^2\dot{\pi}^2 - 3H^2\frac{(\partial_i\pi)^2}{a^2}\right.\\ &+ \left.\frac{(\partial_i^2\pi)^2}{a^4}\right) - \frac{\bar{M}_3^2}{2}\left(3H^2\dot{\pi}^2 - H^2\frac{(\partial_i\pi)^2}{a^2} + \frac{(\partial_j^2\pi)^2}{a^4}\right)\,,\end{aligned} \tag{4.11}$$

whereas, following the same procedure, the mass dimension 3 parity-violating operator in (4.2) in the same limit $\dot{H} \to 0$ yields

$$\mathcal{L}^{(\pi)}_{2,\,d_3} = \frac{\bar{M}_4}{2}\left(\frac{k^4 H\pi^2}{a^4} + \frac{k^2H^3\pi^2}{a^2} - 9H^3\dot{\pi}^2\right)\,. \tag{4.12}$$

This operator only yields a quartic correction to the dispersion relation. On the other hand, the mass dimension 4 operators in the EEFToI action (4.1) written in Fourier space [1]

[1] In [21], in the definition for $\delta K_{\mu\nu} \equiv K_{\mu\nu} - K^{(0)}_{\mu\nu}$, we had mistakenly subtracted the FRW result $K^{(0)}_{\mu\nu} = -a^2H\delta_{ij}\delta^i_\mu\delta^j_\nu$ from the extrinsic curvature of constant t spatial surfaces. However, this would not produce a tensorial structure for $\delta K_{\mu\nu}$. Following [50], one has to instead subtract $K^{(0)}_{\mu\nu} = -Hh_{\mu\nu}$, which reduces to the FRW result when the perturbations vanish and guarantees that $\delta K_{\mu\nu}$ is covariant. The difference in the obtained results for the action of Goldstone boson is due to this. We thank P. Creminelli for clarification of this issue to us. We take the opportunity to correct the mistake/typo in [50] in defining $K^{(0)}_{\mu\nu}$ as $a^2Hh_{\mu\nu}$. There seems to be an extra factor of $-a^2$ in their expression.

$$
\begin{aligned}
\mathcal{L}^{(\pi)}_{2,\,d_4} \;=\; & -\frac{1}{2}\delta_1\left(\frac{k^6\pi^2}{a^6}-\frac{3H^2k^4\pi^2}{a^4}-\frac{k^4\dot\pi^2}{a^4}+\frac{4H^4k^2\pi^2}{a^2}-6H^4\dot\pi^2-3H^2\ddot\pi^2\right)\\
& -\frac{1}{2}\delta_2\left(\frac{k^6\pi^2}{a^6}+\frac{H^2k^4\pi^2}{a^4}-\frac{k^4\dot\pi^2}{a^4}+\frac{6H^4k^2\pi^2}{a^2}-9H^2\ddot\pi^2\right)\\
& -\frac{1}{2}\delta_3\left(\frac{k^6\pi^2}{a^6}+\frac{3H^2k^4\pi^2}{a^4}+\frac{H^2k^2\dot\pi^2}{a^2}-9H^4\dot\pi^2\right)\\
& -\frac{1}{2}\delta_4\left(\frac{k^6\pi^2}{a^6}+\frac{H^2k^4\pi^2}{2a^4}+\frac{9H^4k^2\pi^2}{2a^2}+\frac{3H^2k^2\dot\pi^2}{a^2}+\frac{27}{2}H^4\dot\pi^2\right)\,.
\end{aligned}
\tag{4.13}
$$

The terms $-\frac{\delta_1}{2}(\nabla_\mu\delta K^{\nu\gamma})(\nabla^\mu\delta K_{\nu\gamma})$ and $-\frac{\delta_2}{2}(\nabla_\mu\delta K^{\nu}_{\ \nu})^2$ produce $\ddot\pi^2$. According to Ostrogradski's theorem [117], higher time derivatives usually lead to ghost instabilities. In principle such a ghost term could be avoided if $\delta_1 = -3\,\delta_2$. Furthermore, note that in the context of an effective field theory, ghosts are not necessarily a pathology if they are small corrections and under control. This is because ghosts maybe an artifact of the truncations and the effective theory is only meant to capture the relevant features of the full theory [44]. However, as noticed in the previous section, one has to set $\delta_1 = 0$ in order to avoid superluminal propagation in the tensor sector, which enforces

$$
\delta_1 = \delta_2 = 0\,. \tag{4.14}
$$

Therefore, for simplicity on this work we only keep the terms $\frac{\delta_3}{2}\nabla_\mu\delta K^{\mu}_{\ \nu}\nabla_\gamma\delta K^{\gamma\nu}$ and $\frac{\delta_4}{2}\,\nabla^\mu\delta K_{\nu\mu}\nabla^\nu\delta K^{\sigma}_{\ \sigma}$.

We shall now derive the equation of motion for π using the total EEFToI Lagrangian in the π language and in the decoupling limit, which is the sum of (4.11), (4.12) and (4.13),

$$
\mathcal{L}^{(\pi)}_{\rm EEFToI} = \mathcal{L}^{(\pi)}_{\rm EFToI} + \mathcal{L}^{(\pi)}_{2,\,d_3} + \mathcal{L}^{(\pi)}_{2,\,d_4} \tag{4.15}
$$

Before that, we briefly discuss the equation of motion corresponding to the EFToI Lagrangian. Variation of $\mathcal{L}^{(\pi)}_{\rm EFToI}$, yields the same equation of motion previously derived in [28],

$$
A_0\,\ddot\pi_k + (B_0 + 3HC_0)\,\dot\pi_k + \left(E_0\frac{k^4}{a^4} + D_0\frac{k^2}{a^2}\right)\pi_k = 0 \tag{4.16}
$$

with

$$
\begin{aligned}
A_0 &= -2M_{\rm Pl}^2\dot H + 4M_2^4 - 6\bar M_1^3 H - 9H^2\bar M_2^2 - 3H^2\bar M_3^2\\
B_0 &= -6\bar M_1^3\dot H - 18\dot H H\bar M_2^2 - 6\dot H H\bar M_3^2\\
C_0 &= -2M_{\rm Pl}^2\dot H + 4M_2^4 - 6\bar M_1^3 H - 9H^2\bar M_2^2 - 3H^2\bar M_3^2\\
D_0 &= -2M_{\rm Pl}^2\dot H - \bar M_1^3 H - 3H^2\bar M_2^2 - \bar M_3^2 H^2\\
E_0 &= \bar M_2^2 + \bar M_3^2\,,
\end{aligned}
\tag{4.17}
$$

where the mixing with gravity has been neglected. Noting that the canonical $\pi_c \sim \sqrt{A_0}\,\pi$ and $\delta g_c^{00} \sim M_{\rm Pl}\,\delta g^{00}$, the mixing energy between gravity and the Goldstone mode π can be neglected at energies

$$E > E_{\rm mix} \sim \frac{\sqrt{A_0}}{M_{\rm Pl}}\,, \tag{4.18}$$

which is known as the equivalence theorem. Namely, the perturbations of the longitudinal mode decouple from the perturbations of the metric at energies higher than $E_{\rm mix}$. Being able to compute the correlation functions at horizon crossing corresponds to assuming $H > E_{\rm mix}$. In the regime where $M_{\rm Pl}^2\dot{H}$ is bigger than the other contributions to A_0, $E_{\rm mix} \sim \epsilon^{1/2}H$, and so the decoupling limit is guaranteed by the slow-roll condition $\epsilon \ll 1$. On the other hand if M_2^4 is bigger than the other parameters in A_0, $E_{\rm mix} \sim M_2^2/M_{\rm Pl}$, and decoupling happens if $M_2^2 < M_{\rm Pl}\,H$. These conditions were obtained in [50] too. Other limiting cases suggest $\bar{M}_1^{3/2} < M_{\rm Pl}\,H^{1/2}$, $\bar{M}_2 < M_{\rm Pl}$ and $\bar{M}_3 < M_{\rm Pl}$.

In terms of the conformal time, $d\tau \equiv dt/a$ and through a change of variable $u_k = a\pi_k$, the equation of motion (4.16) takes the following form

$$u_k'' + \frac{B_0 + 3HC_0 - 3A_0H}{A_0}\,au_k' + \left(\frac{D_0}{A_0}k^2 + \frac{E_0}{A_0}k^4a^2 - \frac{a''}{a}\right)u_k = 0\,. \tag{4.19}$$

Noting that $B_0 + 3HC_0 - 3A_0H = -6\dot{H}(\bar{M}_1^3 + 3H^2\bar{M}_2 + H\bar{M}_3^2)$, in the limit $\dot{H} \to 0$, this equation is reduced to

$$u_k'' + \left(\frac{D_0}{A_0}k^2 + \frac{E_0}{A_0}k^4a^2 - \frac{a''}{a}\right)u_k = 0\,. \tag{4.20}$$

which has the same form derived in [28].

If we now include the higher dimensional corrections $\mathcal{L}^{(\pi)}_{4,\,d_3}$ and $\mathcal{L}^{(\pi)}_{4,\,d_4}$ to the total Lagrangian (4.15), the equation of motion for π becomes

$$A_1\,\ddot{\pi}_k + B_1\,\dot{\pi}_k + \left(C_1\frac{k^6}{a^6} + D_1\frac{k^4}{a^4} + F_1\frac{k^2}{a^2}\right)\pi_k = 0\,. \tag{4.21}$$

Defining

$$F_0(k,\tau) = \frac{9}{2}\delta_3 - \frac{27}{4}\delta_4 - \frac{k^2}{2a^2H^2}(\delta_3 + 3\delta_4) - \frac{9}{2H}\bar{M}_4\,, \tag{4.22}$$

the coefficients of the equation of motion (4.21) read

$$\begin{aligned}
A_1 &= A_0 + 2H^4F_0(k,\tau)\,,\\
B_1 &= B_0 + 3HC_0 + H^5\left[6F_0(k,\tau) + \frac{2k^2}{a^2H^2}\,(\delta_3 + 3\delta_4)\right]\,,\\
C_1 &= \delta_3 + \delta_4\,,\\
D_1 &= E_0 + H^2\frac{\delta_4}{2} + 3H^2\delta_3 - \bar{M}_4H\,,\\
F_1 &= D_0 + 3H^4\left(\delta_3 + \frac{3}{2}\delta_4\right) - \bar{M}_4H^3\,,
\end{aligned} \tag{4.23}$$

where we have assumed that the time-dependence of the coefficients is slow compared to the Hubble time. This means that the terms coming from the Taylor expansion of the coefficients are small.

Expressing the equation of motion for $u_k = a\,\pi_k$, in conformal time and again in the limit $\dot{H} \to 0$, we obtain

$$u_k'' + \frac{2k^2H^3(\delta_3+3\delta_4)}{aA_1}\,u_k' + u_k\left(\frac{C_1}{A_1}\frac{k^6}{a^4} + \frac{D_1}{A_1}\frac{k^4}{a^2} + \frac{F_1}{A_1}k^2 - \frac{a''}{a}\right) = 0\,. \tag{4.24}$$

In a de Sitter space, where $a = -1/(H\tau)$, the above equation reads

$$\begin{aligned} u_k'' \;+\; & \frac{G_3\tau k^2\delta_4}{G_1+G_2\tau^2k^2}\,u_k' + u_k\left(\frac{F_2}{G_1+G_2\tau^2k^2}k^2 + \frac{D_2k^2}{G_1+G_2k^2\tau^2}k^2\tau^2\right. \\ & \left. +\; \frac{C_2k^2}{G_1+G_2\tau^2k^2}k^4\tau^4 - \frac{2}{\tau^2}\right) = 0 \end{aligned} \tag{4.25}$$

where

$$\begin{aligned} G_1 &\equiv A_0 + 9H^4\left(\delta_3 - \frac{3}{2}\delta_4\right) - 9\bar{M}_4H^3 \\ G_2 &\equiv -H^4\,(\delta_3+3\delta_4) \\ G_3 &\equiv -2H^4\,(\delta_3+3\delta_4) = 2G_2 \\ F_2 &\equiv F_1 \\ D_2 &\equiv D_1H^2 \\ C_2 &\equiv C_1H^4 \end{aligned} \tag{4.26}$$

and

$$A_1(k,\tau) = G_1 + G_2k^2\tau^2\,. \tag{4.27}$$

The speed of propagation of the perturbations in the intermediate IR, i.e. for $1 < \kappa\tau < \sqrt{G_1/G_2}$, can now be read out from eq. (4.25) to be

$$c_s^2 = \frac{F_2}{G_1}\,. \tag{4.28}$$

In terms of a dimension less variable, $x \equiv k\tau$, the equation of motion (4.25) takes the form

$$\frac{d^2u_k}{dx^2} + \frac{G_3x}{G_1+G_2x^2}\frac{du_k}{dx} + \left(\frac{F_2}{G_1+G_2x^2} + \frac{D_2x^2}{G_1+G_2x^2} + \frac{C_2x^4}{G_1+G_2x^2} - \frac{2}{x^2}\right)u_k = 0\,. \tag{4.29}$$

In general, due to non-polynomial scale dependence of the dispersion relation, the sound wave analogy does not necessarily apply. A variety of scenarios can in principle arise, depending on the size and sign of various coefficients. For example, if G_1 and G_2 are positive, the modes start with $c_s^2 \sim 0$ in infinite past and gradually, achieve a constant c_s^2 given by F_2/G_1 as they finally exit the horizon for $|k\tau| \ll 1$. If one of G_1 or G_2 (but not both) is negative, there could be a

singular time in the evolution of each mode from inside the horizon when the speed of sound becomes infinite. It is also possible that both the speed of sound and the coefficient of the quartic correction to the dispersion relation are negative. These instabilities can in principle be avoided in the UV by a positive sextic correction to the dispersion relation. Even though such scenarios are all interesting, we will not focus on them in this paper.

In the following, we set $\delta_3 = -3\,\delta_4$, so that the equation of motion (4.29) simplifies to [2]

$$\frac{d^2u_k}{dx^2} + \left(\frac{F_2}{G_1} + \frac{D_2}{G_1}x^2 + \frac{C_2}{G_1}x^4 - \frac{2}{x^2}\right)u_k = 0\,. \tag{4.30}$$

If $F_2/G_1 > 0$, as assumed here, our definition of the speed of sound for scalar perturbations (4.28) is real and well-defined:

$$c_s^2 = \frac{F_2}{G_1}\,. \tag{4.31}$$

If $F_2/G_1 < 0$, one deals with the sort of dispersion relation that comes up in Ghost Inflation-like scenarios [12, 135]. This will not be something that we focus on in this investigation. Moreover, in order to avoid potential issues related to superluminal propagation in the IR and a unitary UV completion, we assume that [1]

$$0 \leq c_s^2 \leq 1\,. \tag{4.32}$$

The first inequality could be satisfied if F_2 and G_1 have the same sign. Note that it is also possible to have $c_s^2 = 1$ if

$$4M_2^4 - 5\bar{M}_1^3 H - 6H^2\bar{M}_2^2 - 2H^2\bar{M}_3^2 - 9H^4\delta_4 - 8\bar{M}_4H^3 = 0 \tag{4.33}$$

eventhough, higher-point interactions will not be zero. This shows that, although in the EFToI one tries to quantify the deviations from the standard slow-roll model with the operators $\mathcal{L}_m$ in (3.10), there is still the possibility that one flows back close to the regime of slow-roll inflation with $c_s = 1$ via appropriate tuning of the coefficients of the various higher dimensional operators. This result was also true in the EFToI with δK^2 terms in the unitary gauge Lagrangian. Although one expects to see an enhancement in the non-gaussianity amplitudes due to the modified dispersion relation.

Defining $x' \equiv c_s\,x$, the equation of motion (4.30) reduces further to

$$\frac{d^2u_k}{dx'^2} + \left(1 + \alpha_0 x'^2 + \beta_0 x'^4 - \frac{2}{x'^2}\right)u_k = 0\,, \tag{4.34}$$

where

$$\alpha_0 \equiv \frac{D_2}{G_1 c_s^4} = \frac{D_2 G_1}{F_2^2} \qquad \beta_0 \equiv \frac{C_2}{G_1 c_s^6} = \frac{C_2 G_1^2}{F_2^3}\,. \tag{4.35}$$

[2] With $\delta_3 \neq -3\,\delta_4$, the mixing between gravity and the Goldstone boson becomes time-dependent for each mode. Even though at horizon crossing, one can tune the parameters to make $H > E_{\rm mix}$, when the physical momentum of the mode $k/a > M_{\rm Pl}(\delta_3 + 3\delta_4)^{-1/2}$, the mixing with gravity cannot be neglected. At such momenta the theory of General Relativity also breaks down and in absence of a quantum theory of gravity the predictions of the theory becomes unreliable.

In order to have a stable vacuum in the deep UV, where the dispersion relation is dominated by the k^6, we consider $\beta_0 > 0$[3]. If Hubble crossing takes place when $\omega^2 \sim k^2$, transitions between regions with a different dispersion relation can lead to excited initial states [21]. In this case, if $\alpha_0 < 0$, one can have relatively large corrections, much bigger than one, compared to the standard inflationary predictions for the two point function. This can happen even if the dispersion relation has a single turning point, *i.e.* a single horizon crossing is assumed to occur.[4] The latter scenario is possible if $D_2/G_1 < 0$ and $C_2/G_1 > 0$ [5].

One should note that the coefficients $\bar{M}_i$'s, with $i = 1, 2, 3$, in (3.18) can appear with either sign. In fact, as noticed in the previous section about tensor perturbations, one has to assume $\bar{M}_3^2 < 0$ in order to avoid superluminal tensor perturbations. Noting that

$$D_2 = (\bar{M}_2^2 + \bar{M}_3^2 + H^2\frac{\delta_4}{2} - \bar{M}_4 H)H^2 \,, \tag{4.36}$$

using the definition (4.35), the condition $\delta_3 = -3\delta_4$ and the expressions (4.26) for C_2 and G_1, it is not difficult to show that

$$D_2 = -\frac{2\alpha_0}{\beta_0 c_s^2}\delta_4 H^4 \,. \tag{4.37}$$

As stated before, to achieve the stability in the UV, one has to assume that $\beta_0 > 0$, and hence, D_2 and $\alpha_0\delta_4$ must have opposite signs. If $\delta_4 > 0$, noting that $C_2 = -2\delta_4 H^4$ will be negative, one has to assume $G_1 < 0$ to obtain a positive β_0. Assuming $\dot{H} < 0$, that puts an upper bound on how large the first slow-roll parameter ϵ can be in this scenario. Then in order to achieve $\alpha_0 < 0$, one has to assume that $D_2 > 0$. This combined with that $\bar{M}_3^2 < 0$ for tensor perturbations to be subluminal, means

$$|\bar{M}_3|^2 < \bar{M}_2^2 + \frac{\delta_4}{2}H^2 - \bar{M}_4 H \,. \tag{4.38}$$

On the other hand, if $\delta_4 < 0$, one has to assume $D_2 < 0$ and the reverse of the above equality should hold and, conversely, a lower bound on ϵ is found under the assumption that $\dot{H} < 0$. One should emphasize that the value of α_0 and β_0 are not solely determined by c_s. There are other variables involved in these parameters and even for the choice $c_s \approx 1$, α_0 and β_0 can be substantial. Of course, with $c_s \ll 1$, the values of these parameters will get larger, but a reduced sound speed is not necessary to have large corrections to the dispersion relation. For $c_s \approx 1$, since non-gaussianities are usually determined by factors $1/c_s^2$, one expects at least not to get an enhancement from speed of sound. Nonetheless the non-linear evolution of the mode inside the horizon due to the non-linear dispersion relations, may enhance the value of the non-gaussianity and bring it potentially to a value that can be observed. In fact, if, as in [21], the evolution of the modes inside the horizon can be mapped into excited states with large occupation

[3]Dispersion relations dominated by the k^6 term can also be motivated from studies in the context of condensed matter physics applied to black holes [89].

[4]We are referring to $1 + \alpha_0 x'^2 + \beta_0 x'^4 \sim \frac{2}{x'^2}$ as horizon crossing.

[5]In solid state physics, the perturbations that appear close to the minimum of the dispersion relations at large k's are known as *rotons*, the ones that are close to the maximum of the dispersion relation are called *maxons* and the ones that are in the linear regime of the dispersion relation are *phonons*. In the cosmological setup, starting from deep inside the horizon, each mode in principle can undergo all three phases until it exits the horizon.

numbers at horizon crossing, it is expected that, even for $c_s = 1$, equilateral [8, 24] and flattened non-gaussianity configurations [82, 25] will get enhanced. Whether such an equivalence holds and how higher dimensional operators in the EEFToI contribute to the bispectrum shapes and amplitude is something that we plan to investigate in near future.

4.3.3 Scalar power spectrum

In this section we investigate the effect of the modified mode equation (4.34) on the scalar power spectrum for different scenarios, corresponding to different signs and magnitudes of the coefficients of the quartic and sextic corrections to the dispersion relation. In general, overall correction to standard the Bunch-Davies power spectrum can be expressed as a multiplicative factor

$$\Delta_s = \gamma_s \, \Delta_s^{\rm B.D.} = \gamma_s \, \frac{H^2}{8\pi^2 c_s \epsilon} \, . \tag{4.39}$$

If both $\alpha_0 > 0$ and $\beta_0 > 0$, the mode evolution inside the Hubble patch remains oscillatory throughout, and unless the parameters α_0 and β_0 are of order one, one does not expect to see a significant modification to the Bunch-Davies power spectrum. We solve the mode equation (4.34) numerically, from the positive frequency WKB mode in the infinite past,

$$u_k(x' \to -\infty) \simeq \frac{1}{2} \left(-\frac{\pi}{3} x'\right)^{1/2} H^{(1)}_{\frac{1}{6}} \left(-\frac{\sqrt{\beta_0}}{3} x'^3\right) \, , \tag{4.40}$$

and then read off the power spectrum when the mode exits the horizon, $x' \to 0$. We have computed the factor γ_s for several values of α_0 and β_0. For example, for $\alpha_0 = \beta_0 = 0.2$, one has $\gamma_s \simeq 0.717$, for $\alpha_0 = \beta_0 = 0.5$, $\gamma_s \simeq 0.53$ and for $\alpha_0 = \beta_0 = 1$, $\gamma_s = 0.4$. It seems that in this case, $\gamma_s < 1$ in most of the parameter space. In fact, solving and plotting the power spectrum for different values of α_0 and $0.01 < \beta_0 < 2$ confirms this conjecture. The larger the values of α_0 and β_0, the more suppressed the power spectrum. However, this suppression is at most of order a few tenths. For $\alpha_0 = \beta_0 \sim 2$, the modulation factor $\gamma_s \approx 0.3$ (see Figs. 4.1 and 4.2). Noting that, in the case of positive quartic correction to the dispersion relation, enhancement of the coefficient of the quartic term suppresses the power spectrum too [22], one is tempted to deduce that positive higher order corrections to the dispersion relation will in general reduce the amplitude of the power spectrum.

On the other hand, if $\alpha_0 < 0$, there could be large modulation factors on the power spectrum. In [21], we focused on the range of parameters for α_0 and β_0 such that

$$z \equiv \frac{\beta_0}{\alpha_0^2} \geq \frac{1}{4} \, . \tag{4.41}$$

This requirement was coming from the fact that the dispersion relation should not become tachyonic for any physical momentum in flat spacetime. If we allow for $z < 1/4$, the quantum modes will get amplified while they are still inside the horizon, which will increase the resulting

power spectrum exponentially. However, such a large enhancement for the scalar power spectrum will probably come about at the price of enhancing the size of non-gaussianity, and may thus clash with experimental bounds on them. The issue of non-gaussianity with such modified dispersion relations is something that we plan to return to in the next work. As for the power spectrum itself, we examined this regime numerically. We have plotted in Figs. 4.3 and 4.4 the factor γ_s, with β_0 in the range $\frac{\alpha_0^2}{5} < \beta_0 < \frac{\alpha_0^2}{4}$, for several values of α_0. As can be readily seen, when β_0 goes below $\alpha_0^2/4$, the power spectrum grows substantially. With the decrease of the parameter α_0, the interval of time the mode spends under the influence of negative quartic contribution and possibly becomes tachyonic while still inside the horizon, increases and one sees a larger amount of enhancement for γ_s. In fact, for $\alpha_0 = 0.01$, and $\beta_0 = \alpha_0^2/5$, γ_s can reach values as large as 1000 (see Fig. 4.4). One other point that may be worth highlighting is that for large values of β_0 for each α_0, the maximum enhancement in this case seem to occur at $\alpha_0 \sim 0.2$. As we will see, in the interval $1/4 < z < 1/3$, the same pattern repeats itself.

In [21], we had also assumed that the mode never becomes lighter than the Hubble parameter up until the last horizon crossing. That would mean that the equation $\omega^2 = 2H^2$ has only one solution. For

$$z > \frac{1}{3}\,, \tag{4.42}$$

this equation automatically has only one solution. For values of α_0 and β_0 such that

$$\frac{1}{4} \leq z \leq \frac{1}{3}\,, \tag{4.43}$$

having only one solution imposes one of the following conditions

$$\begin{aligned} \alpha_0 &\leq \frac{9z - 2 - 2(1-3z)^{3/2}}{54z^2} \\ \text{or} \quad \alpha_0 &\geq \frac{9z - 2 + 2(1-3z)^{3/2}}{54z^2}\,. \end{aligned} \tag{4.44}$$

The requirement of having one solution was to show that the gluing technique becomes ineffective in capturing the modification to the power spectrum from the sextic dispersion relation. In that case, since $\omega^2 = 2H^2$ had only one solution, calculating the power spectrum analytically required the gluing procedure only once. In this paper, we do not distinguish between multiple and single horizon crossings. What matters to us is the amplitude of the power spectrum when the wavelength of the mode is much larger than the Hubble length or, more quantitatively, when $x' \ll 1$. Therefore, when investigating the $z > 1/4$ region, we allow for $z > 1/3$ as well. Plots of γ_s for different values of α_0 and β_0 for $z > 1/4$ are presented in Figs. 4.5, 4.6 and 4.7. In all cases, the factor γ_s is bigger than one. As one moves away from $\alpha_0 = 0.2$ in both directions, the amount of enhancement in the power spectrum decreases.

Finally, in the case $z = 1/4$, as noted in [21], for $\alpha_0 \sim 0.2$ and $\beta_0 = \alpha_0^2/4$, one can achieve $\gamma_s \simeq 14.774$.

4.3.4 Tensor-to-scalar ratio and consistency relation

Having modified spectra for both tensor and scalar fluctuations, it is expected that the tensor-to-scalar ratio be modified as well. For general modified equations of motion for scalar and tensor perturbations, the tensor-to-scalar ratio is given by

$$r = 16\epsilon \, \frac{c_s}{c_{\rm T}} \frac{1}{\gamma_s} \, . \tag{4.45}$$

Therefore, a departure of any of the parameters, c_s, $c_{\rm T}$ and γ_s from one, will bring about changes in the tensor-to-scalar ratio in comparison with the slow-roll counterpart. It is well known that the majority of kinetic term dominated inflationary models, known as K-inflation [13], would lower r. However, the possibility of enhancing r by allowing for c_s to be bigger than one has also been entertained in [112]. As mentioned before, whether superluminal propagation in EFTs is necessarily an indication of any pathology is still a topic of debate in the community [78].

Depending on the sign of the operator $-\frac{\bar{M}_3^2}{2}\,\delta K^{\mu}_{\ \nu}\delta K^{\nu}_{\ \mu}$, which contributes to the speed of sound for gravity waves, one encounters two branches. In the *superluminal* branch, with $\bar{M}_3^2 > 0$, gravitons propagate faster than light during inflation, $c_{\rm T} > 1$. In the *subluminal* branch, with $\bar{M}_3^2 < 0$, the speed of gravity waves is less than the speed of light. Were one to drop the superluminal branch because of superluminality and causality considerations, the effect of departure from the speed of light is always to enhance r. As $\bar{M}_3$ cannot be pushed beyond $M_{\rm Pl}$ in an EFT treatment, the gravity wave speed during inflation, is bounded from below by $1/\sqrt{2}$, and thus one at most would get an enhancement of $\sqrt{2}$ in r in the subluminal branch. Otherwise, in the superluminal branch, r can be significantly suppressed as $\bar{M}_3^2$ gets larger.

To summarize, in this section we showed that the effect of the EEFToI on scalar perturbations is to change their dispersion relation, not only by modifying the speed of sound but also by including higher order corrections. If the coefficients of the dispersion relation are all positive, the amplitude of the scalar power spectrum gets suppressed by a factor $\gamma_s \lesssim 1$. This would enhance r by a factor of order one. However, if the quartic term of the dispersion relation is negative, the evolution of the modes involves an intermediate phase with negative group velocity, or tachyonic phase, which can in fact enhance the amplitude of scalar perturbations considerably with respect to the Bunch-Davies result, picking up a factor of $\gamma_s \gg 1$. If one allows for the tachyonic evolution of the mode inside the horizon, r can get suppressed by a large factor. On the other hand, if only one allows for having a negative group velocity without a tachyonic phase, the maximum one can achieve is $\gamma_s \approx 14.7$, which suppresses r by a factor of ~ 0.06. This is achieved by $\alpha_0 \sim 0.2$ and $\beta_0 = \alpha_0^2/4$ which was studied in [21] as a dispersion relation that realises super-excited states with large occupation numbers. The mode equation has one turning point for such values of parameters, corresponding to a single horizon crossing.

One can also easily verify that the consistency relation [145, 101]

$$n_{\rm T} = -\frac{r}{8} \tag{4.46}$$

is modified to

$$n_{\rm T} = -\frac{c_{\rm T}\gamma_s}{c_s}\frac{r}{8}. \tag{4.47}$$

This implies that for a given r, we will have a much redder tensor spectrum for $\gamma_s \gg 1$.

4.4 Cut-off and non-gaussianity

As explained in the introduction, the EEFToI can provide a controlled description of the perturbations around a quasi de Sitter background from low energy up to the UV regime where the dispersion relation becomes $\omega^2 \sim k^6$, provided the coefficients of the higher dimensional operators are tuned such that the theory remains always weakly coupled in this energy range. This means that the scattering of Goldstone bosons does not violate perturbative unitarity at any scale below the point where the dispersion relation becomes dominated by the sextic term.

The strong coupling scale can be easily estimated in the π language from the size of the coupling of the interactions described by higher dimensional operators [50]. In order to perform this estimate, let us first note that the canonically normalised Goldstone boson π_c has a time kinetic term of the form

$$\int dt\, d^3x\, \frac{1}{2}\,\dot{\pi_c}^2\,,$$

and so the dimension of π_c, denoted as $[\pi_c]$, is

$$[\pi_c] = k^{3/2}\,\omega^{-1/2}\,. \tag{4.48}$$

The energy dimension of the coefficient c of a generic operator $\mathcal{O}$,

$$\int dt\, d^3x\, c\,\mathcal{O}\,,$$

can be inferred by imposing

$$\frac{c\,[\mathcal{O}]}{\omega k^3} = 1\,, \tag{4.49}$$

where $[\mathcal{O}] = k^s\omega^m[\pi_c]^p$ is the dimension of $\mathcal{O}$. Combining (4.48) and (4.49), we end up with

$$[c] = \omega^a k^b \qquad \text{where} \qquad a = 1 - m + \frac{p}{2} \qquad \text{and} \qquad b = 3 - s - \frac{3p}{2}\,.$$

If we now use the dispersion relation $\omega^2 \sim k^{2n}$ we find

$$[c] = \omega^q \qquad \text{with} \qquad q = 1 - m + \frac{1}{n}\,(3-s) + \frac{p}{2}\left(1 - \frac{3}{n}\right). \tag{4.50}$$

Let us now consider, as illustrative examples, three different operators: $\mathcal{O}_1 = \dot{\pi}_c\,(\partial_i\pi_c)^2$, $\mathcal{O}_2 = (\partial_i\pi_c)^4$ and $\mathcal{O}_3 = \dot{\pi}_c^2\,(\partial_i\pi_c)^2$ whose coefficients c_i have energy dimensions $[c_i] = \omega^{q_i}$ with $i = 1, 2, 3$. Different forms of the dispersion relation then give different energy scalings of these coefficients:

- $n = 1 \quad \Rightarrow \quad q_1 = -2 \quad q_2 = -4 \quad q_3 = -3$
- $n = 2 \quad \Rightarrow \quad q_1 = -\frac{1}{4} \quad q_2 = -\frac{1}{2} \quad q_3 = -\frac{5}{4}$
- $n = 3 \quad \Rightarrow \quad q_1 = \frac{1}{3} \quad q_2 = \frac{2}{3} \quad q_3 = -\frac{2}{3}$

Interestingly, for $n < 3$ we get $q_i < 0 \, \forall \, i = 1, 2, 3$, while q_1 and q_2 become positive for $n = 3$. This implies that all three operators are *irrelevant* when the dispersion relation is at most dominated by the quartic term. This behaviour can be shown to hold for all higher derivative operators. Hence the $\omega^2 \sim k^2$ and $\omega^2 \sim k^4$ theories have only UV strong coupling scales which we will denote respectively Λ_2 and Λ_4. On the other hand, for $\omega^2 \sim k^6$, O_1 and O_2 become *relevant*, while O_3 remains *irrelevant*. This implies that the $\omega^2 \sim k^6$ theory features both a UV and an IR strong coupling scale which we will indicate respectively with $\Lambda_6^{\rm UV}$ and $\Lambda_6^{\rm IR}$. The scale $\Lambda_6^{\rm UV}$ is associated with operators like O_3 whose coupling grows when the energy increases, whereas $\Lambda_6^{\rm IR}$ is related to operators like O_1 and O_2 whose strength grows when the energy decreases. In general, this behaviour is a signal of an inconsistent EFT description.

However, one can still have a sensible EFT for the fluctuations if $\Lambda_6^{\rm IR}$ is below the transition from the $\omega^2 \sim k^4$ to the $\omega^2 \sim k^6$ regime that happens at the scale $\Lambda_{\rm dis}^{4-6}$, provided the $\omega^2 \sim k^4$ theory is always weakly coupled in its regime of validity. Thus we need to tune the coefficients of the higher dimensional operators such that $\Lambda_6^{\rm IR} \ll \Lambda_{\rm dis}^{4-6} \ll \Lambda_4$. On top of this, the theory should not become strongly coupled at lower energies when the dispersion relation still takes the standard quadratic form. Hence we need also to require that Λ_2 is above the scale $\Lambda_{\rm dis}^{2-4}$ which denotes the transition from the $\omega^2 \sim k^2$ to the $\omega^2 \sim k^4$ regime: $\Lambda_{\rm dis}^{2-4} \ll \Lambda_2$.

The strong coupling scale Λ_2 can be estimated from the coefficient of the four-leg interaction term O_2. Given that $q_2 = -4$ in the deep IR where the dispersion relation is $\omega^2 = c_s^2 k^2$, the coefficient c_2 scales as $c_2 \sim 1/\Lambda_2^4$, where it can be shown that [50]

$$\Lambda_2^4 = c_s^7 \Lambda^4 \qquad \text{with} \qquad \Lambda^4 = \frac{2 M_p^2 \dot{H}}{c_s^2 \left(1 - c_s^2\right)} \, . \tag{4.51}$$

This strong coupling scale goes to infinity for $c_s \to 1$ but for $c_s \ll 1$, which is for example a regime interesting for large non-gaussianities, it can become very small. However, as noted in [30], similarly to particle physics, new physics is expected to appear before reaching the strong coupling regime. In turn, this new physics pushes the strong coupling region to higher energies. As explained above, in our case, new physics corresponds to a change in the dispersion relation from linear, $\omega^2 = c_s^2 k^2$, to non-linear, $\omega^2 = k^4/\rho^2$, at the energy scale $\Lambda_{\rm dis}^{2-4} = c_s^2 \rho$. This happens before the $\omega^2 = c_s^2 k^2$ theory becomes strongly coupled if $c_s \, \rho^4 \ll \Lambda_4$. Moreover, in the region where the dispersion relation is quartic, the new strong coupling scale becomes $\Lambda_4^4 = \Lambda^4 (\Lambda/\rho)^{28}$ [30]. Hence the condition $c_s \, \rho^4 \ll \Lambda^4$ guarantees also that this strong coupling scale is indeed larger than the one in the case with a linear dispersion relation.

As noted in [50], the strong coupling scale can also be quantified in terms of the size of non-gaussianities, since

$$\frac{\mathcal{L}_3}{\mathcal{L}_2} \equiv f_{\rm NL} \zeta \, . \tag{4.52}$$

Thus perturbation theory breaks down when this ratio becomes of order one. Given that $\zeta \sim 10^{-4}$, this happens when $f_{\rm NL} \sim 10^4$. Notice however that CMB observations set a stronger upper bound on equilateral non-gaussianities of the order $f_{\rm NL} = -42 \pm 75$ [2]. The relation between non-gaussianities and strong couplings becomes even more manifest by noting that (4.52) can also be rewritten as [30]

$$\frac{\mathcal{L}_3}{\mathcal{L}_2} \sim \left(\frac{H}{\Lambda_2}\right)^2 , \tag{4.53}$$

and so $f_{\rm NL} \sim 10^4$ when horizon exit takes place in the strong coupling region, i.e. $H \sim \Lambda_2$. Given that $f_{\rm NL} \sim c_s^{-2}$, large non-gaussianities emerge when $c_s \ll 1$. From (4.51) it is clear that small values of the speed of sound imply also a low strong coupling scale Λ_2. However if horizon exit occurs in a region where the dispersion relation is dominated by the quartic term, i.e. when $\Lambda_{\rm dis}^{2-4} \ll H \sim \Lambda_2 \ll \Lambda_4$, the theory should be weakly coupled. In fact, the ratio (4.52) takes an expression different from (4.53) when evaluated in the $\omega^2 = k^4/\rho^2$ region

$$\frac{\mathcal{L}_3}{\mathcal{L}_2} \sim \left(\frac{H}{\Lambda_4}\right)^{3/4} . \tag{4.54}$$

Given that $H \sim \Lambda_2 \ll \Lambda_4$, the theory is still weakly coupled even if $c_s \ll 1$. This implies also that $f_{\rm NL}$ should be smaller. In fact, the expression for $f_{\rm NL}$ in the quartic regime gets modified to $f_{\rm NL} \sim \left(\Lambda_{\rm dis}^{2-4}/H\right) c_s^{-2}$ which is suppressed with respect to its expression in the quadratic regime since $\Lambda_{\rm dis}^{2-4} \ll H$. Hence we conclude that even a theory with small speed of sound and large non-gaussianities close to the edge of detectability can remain weakly coupled if the dispersion relation changes before hitting its strong coupling regime.

Notice also that, as explained in Sec. 4.3.3, large non-gaussianities might arise also in the case where the coefficients of the higher dimensional operators are chosen such that $c_s \simeq 1$. In fact, in this case the transitions inside the horizon between regions with modified dispersion relations would give $f_{\rm NL} \sim \gamma_n/c_s^2$ with γ_n which could potentially be large. This case might also be interesting to keep the EEFToI weakly coupled since both Λ_2 and Λ_4 tend to infinity for $c_s \to 1$ (one would however still need to ensure that $\Lambda_6^{\rm IR} \ll \Lambda_{\rm dis}^{4-6}$).

One can insist on pushing the strong coupling scale to even higher energies via the appearance of new physics again before reaching Λ_4. In this case, the new physics would correspond to a change in the dispersion relation from quartic to sextic at the scale $\Lambda_{\rm dis}^{4-6}$ but we argued above that the $\omega^2 \sim k^6$ regime features both an UV and IR strong coupling scale. Hence a sensible EFT description all the way up to the the sextic region requires to have also $\Lambda_6^{\rm IR}$ below $\Lambda_{\rm dis}^{4-6}$.

In addition to the scale where perturbative unitarity is lost, another fundamental scale for the EFT of the perturbations around a quasi de Sitter background is the scale Λ_b where time diffeomorphisms are spontaneously broken by the background. Ref. [30] showed that, for the standard slow-roll case with $c_s = 1$, $\Lambda_b = \dot{\phi}^{1/2} \ll \Lambda_2$, while for $c_s \ll 1$, $\Lambda_2 \sim c_s \Lambda_b \ll \Lambda_b$. Moreover Λ_b controls the size of the perturbations with respect to the background since

$$k^3 P_\zeta(k) = \frac{1}{4}\frac{H^2}{M_{\rm Pl}^2\, \epsilon\, c_s} \sim \left(\frac{H}{\Lambda_b}\right)^4 , \tag{4.55}$$

and so at energies around the symmetry breaking scale the background cannot be integrated out anymore to leave a theory for the fluctuations only. Hence we conclude that the cut-off of the EEFToI should be identified as the minimum between $\Lambda_6^{\rm UV}$ and Λ_b. As an illustrative example, a possible hierarchy of scales which would make the EEFToI valid for the entire energy range up to the $\omega^2 \sim k^6$ region would be

$$\Lambda_{\rm dis}^{2-4} \ll \Lambda_2 \ll \Lambda_6^{\rm IR} \ll \Lambda_{\rm dis}^{4-6} \ll \Lambda_4 \ll \Lambda_6^{\rm UV} \ll \Lambda_b \,. \tag{4.56}$$

We finally stress that cosmological observations are performed only at horizon crossing which occurs at energies of order H where the dispersion relation might take the standard linear expression. Hence, strictly speaking, the only requirement to have a sensible EFT is $H \ll \Lambda_{\rm cutoff}$. However, we are demanding more since we want to provide a consistent theoretical framework for the picture described in [21]. In fact, we want to be able to trust our EEFToI also in the high energy region which determines the behaviour of modes deep inside the horizon. We want these modes to be originally in the adiabatic vacuum of the $\omega^2 \sim k^6$ theory, so that the standard $\omega^2 \sim k^2$ theory features non-Bunch-Davis initial conditions due to the transitions between regions characterised by a different dispersion relation. In turn, these excited initial states can have very interesting implications for cosmological observables.

4.5 Three Point Function Estimation and Calculation

In the previous section, we explored some interesting regions of the parameter space that start with modified dispersion relation through their impact on primordial power spectrum. The computation of three point functions, and thus the computation of non-Gaussianity of EEFToI can help us further explore or constrain these corners of the theory. A rigorous calculation of the non-Gaussianity can be obtained by computing the vacuum expectation value of the three point function of ζ. The three point function in the interaction picture is given by

$$\langle \zeta_{\mathbf{k}_1}(t)\zeta_{\mathbf{k}_2}(t)\zeta_{\mathbf{k}_3}(t)\rangle = -i\int_{t_0}^{t} dt' \,\langle [\zeta_{\mathbf{k}_1}(t)\zeta_{\mathbf{k}_2}(t)\zeta_{\mathbf{k}_3}(t), H_{int}(t')]\rangle, \tag{4.57}$$

where $\zeta = -H\pi$. The interaction Hamiltonian is given by $H_{int} = -L_{int}$ which includes terms beyond quadratic order in action[50].[6]

Before we do a robust computation of the three point functions, let us perform a simple analysis to see how the interaction terms in the action act under the energy scaling when the dispersion relation is governed by $\omega^2 \propto k^6$. Re-scaling energy by a factor of Σ, $E \to \Sigma E$, means that $t \to \Sigma^{-1} t$ and from the dispersion relation $x \to \Sigma^{-1/3} x$. The kinetic term in the action for π after taking the simplification of $\delta_3 = -\delta_4$ has the following form

$$S = \int dt\; d^3x [\frac{1}{2} A_1 \dot{\pi}^2], \tag{4.58}$$

[6]The details of the calculations can be found in the appendix

where A_1 is now simplified to $A_1 = -2M_{\rm Pl}^2\dot{H}+4M_2^4-6\bar{M}_1^3H-9H^2\bar{M}_2^2-3H^2\bar{M}_3^2+\frac{27}{2}H^4\delta_3-9H^3\bar{M}_4$. In the slow-roll limit A_1 variation in time variables is negligible so the dimension scaling implies for the kinetic term to remain invariant, π must scale as $\pi \to \pi$.

We now check the scaling of a generic term in action, $\int dtd^3x\ \mathcal{M}_{m,s,p}$ where m denotes the number of *time* derivatives, s number of *spatial* derivatives and p the overall powers of π. Since $x \to \Sigma^{-1/3}x$, the spatial derivative goes as $\partial_i \to \Sigma^{1/3}\partial_i$ so the contribution to action scales as

$$\mathcal{M}_{m,s,p}\ dt\ dx^3 \to \Sigma^{-2+m+s/3}\mathcal{M}_{m,s,p}\ dt\ dx^3. \tag{4.59}$$

When $m + s/3 < 2$, this term diverges in the low energy limit of $\Sigma \to 0$ and becomes relevant. Note the powers of π cannot be more that the number of derivatives, as the time diffeomorphism invariance of the action does not allow Goldstone boson to be produced without derivatives. This gives us the relations $p \leq s + m$. Also, $p = 1$ corresponds to linear terms, which cancel out for on-shell solutions. Therefore, we only need to examine the relevance of these operators for $2 \leq p \leq s + m$, while $m + s/3 < 2$.

Furthermore, the spatial diffeomorphism invariance enforces s to be even. So with all these constraints taken into account, the only possible combinations of (m, s, p) that remain are $(0, 4, 2)$, $(0, 4, 3)$, $(0, 4, 4)$, $(1, 2, 2)$, and $(1, 2, 3)$[7]. However, note that $\mathcal{M}_{1,2,2} \propto \partial\dot{\pi}\partial\pi = \frac{1}{2}\frac{\partial}{\partial t}\ (\partial\pi)^2$ term becomes $\mathcal{M}_{0,2,2} \propto (\partial\pi)^2$ after integrating by parts, which can be absorbed into the canonical kinetic term. Finally, if we set the restriction $p = 3$ for the purpose of studying the size of non-Gaussianity, we are left with $(0, 4, 3)$, and $(1, 2, 3)$, which are

$$(\partial\pi)^2\dot{\pi} \tag{4.60}$$

$$\partial^2\pi(\partial\pi)^2. \tag{4.61}$$

These terms are also produced from the terms included in the EFToI as well [28]:

$$O_1 = \frac{1}{2}M_2^4(g^{00}+1)^2 \xrightarrow{\{o(\pi^3)\}} -2M_2^4\dot{\pi}(\partial_i\pi)^2/a^2 \tag{4.62}$$

and

$$\begin{aligned} O_3 \ &= -\tfrac{1}{2}\bar{M}_1^3(g^{00}+1)\delta K_\mu^\mu - \tfrac{1}{2}\bar{M}_2^2\delta K^\mu{}_\mu^2 - \tfrac{1}{2}\bar{M}_3^2\delta K^\mu{}_\nu\delta K^\nu{}_\mu \\ &\xrightarrow{\{o(\pi^3)\}} -\tfrac{1}{2}\left(\bar{M}_1^3+\bar{M}_2^2H+2\bar{M}_3^2H\right)\partial_i^2\pi(\partial_j\pi)^2/a^4. \end{aligned} \tag{4.63}$$

Under scaling $E \to \Sigma E$ these two terms go as

$$O_1{}^{\{o(\pi^3)\}} \to \Sigma^{-1/3}O_1{}^{\{o(\pi^3)\}} \tag{4.64}$$

$$O_2{}^{\{o(\pi^3)\}} \to \Sigma^{-2/3}O_2{}^{\{o(\pi^3)\}} \tag{4.65}$$

[7]This exercise can be done for any $\omega^2 \propto k^{2n}$ and there are always finite number of relevant operators.

These cubic terms get additional contributions in the extended theory. The detailed calculation can be found in the appendix A and the new contributions when we set $\delta_1 = \delta_2 = 0$ and $\delta_3 = -3\delta_4$ are the following

$$\left(\delta_3 \nabla^\mu \delta K_{\nu\mu} \nabla^\nu \delta K^\sigma{}_\sigma + \delta_4 \nabla_\mu \delta K^\mu{}_\nu \nabla_\gamma \delta K^{\gamma\nu}\right)^{\{o(\pi^3)\}} \rightarrow \frac{\delta_3 \partial_i^2 \pi (\partial_j \pi)^2 H^3}{3a^4} - \frac{\dot{\pi}(\partial_i \pi)^2 \delta_3 H^4}{a^2} \tag{4.66}$$

and

$$\bar{M}_4 \nabla^\mu \delta g^{00} \nabla^\nu \delta K_{\mu\nu}{}^{\{o(\pi^3)\}} \rightarrow \frac{9\bar{M}_4 H^3 \dot{\pi}(\partial\pi)^2}{a^2}. \tag{4.67}$$

One way of avoiding any potential strong coupling or even large non-Gaussianities, is to fine tune the parameters of EFToI and EEFToI such that

$$-\delta_3 H^4 + 9\bar{M}_4 H^3 - 2M_2^4 = 0, \tag{4.68}$$

and

$$\frac{1}{3}\delta_3 H^3 - \frac{1}{2}\left(\bar{M}_1^3 + \bar{M}_2^2 H + 2\bar{M}_3^2 H\right) = 0. \tag{4.69}$$

Then we will not need to worry about these terms.

We can also perform a preliminary approximation to check the strenght of non-Gaussianity of the concerned terms. Around freezing we have $\omega \sim H$ and $k \sim H/c_s$ and approximating $\dot{\pi} \sim \omega\pi$, the ratio of contributions of these cubic terms to the second order Lagrangian can be estimated as

$$\begin{aligned}
\frac{\mathcal{L}_{\dot{\pi}(\partial\pi)^2}}{\mathcal{L}_2} &\sim (-\delta_3 H^4 + 9\bar{M}_4 H^3 - 2M_2^4)\frac{\dot{\pi}(\partial\pi)^2}{A_1 \dot{\pi}^2} \sim (-\delta_3 H^4 + 9\bar{M}_4 H^3 - 2M_2^4)\frac{\omega k^2 \pi^3}{A_1 \omega^2 \pi^2} \\
&\sim (-\delta_3 H^4 + 9\bar{M}_4 H^3 - 2M_2^4)\frac{H\pi(\frac{H^2}{c_s^2}\pi^2)}{A_1 H^2 \pi^2} \sim (-\delta_3 H^4 + 9\bar{M}_4 H^3 - 2M_2^4)\frac{H}{A_1 c_s^2}\pi, \\
&\sim \frac{(-\delta_3 H^4 + 9\bar{M}_4 H^3 - 2M_2^4)}{A_1 c_s^2}\zeta \sim \left(9\frac{\bar{M}_4}{H} + -\delta_3 - 2\frac{M_2^4}{H^4}\right)\frac{\Delta_\zeta}{c_s}\zeta
\end{aligned} \tag{4.70}$$

$$
\begin{aligned}
\frac{\mathcal{L}_{(\partial\pi)^2\partial^2\pi}}{\mathcal{L}_2} &\sim \left(\frac{1}{3}\delta_3 H^3 - \frac{1}{2}\left(\bar{M}_1^3 + \bar{M}_2^2 H + 2\bar{M}_3^2 H\right)\right)\frac{\left(\frac{H}{c_s}\pi\right)^2\left(\frac{H}{c_s}\right)^2\pi}{A_1 H^2\pi^2} \\
&\sim \left(\frac{1}{3}\delta_3 H^3 - \frac{1}{2}\left(\bar{M}_1^3 + \bar{M}_2^2 H + 2\bar{M}_3^2 H\right)\right)\frac{H^2}{A_1 c_s^4}\pi \\
&\sim \left(\frac{1}{3}\delta_3 H^3 - \frac{1}{2}\left(\bar{M}_1^3 + \bar{M}_2^2 H + 2\bar{M}_3^2 H\right)\right)\frac{H}{A_1 c_s^4}\zeta \\
&\sim \frac{\left(\frac{1}{3}\delta_3 H^3 - \frac{1}{2}\left(\bar{M}_1^3 + \bar{M}_2^2 H + 2\bar{M}_3^2 H\right)\right)H}{A_1 c_s^4}\zeta \\
&\sim \left(\frac{1}{3}\delta_3 - \frac{1}{2}\frac{\left(\bar{M}_1^3 + \bar{M}_2^2 H + 2\bar{M}_3^2 H\right)}{H^3}\right)\frac{\Delta_\zeta}{c_s^3}\zeta
\end{aligned}
\tag{4.71}
$$

The perturbation theory breaks down when the ratio $\frac{\mathcal{L}_3}{\mathcal{L}_2}$ becomes of order one, while as we discuss later CMB observations set a much stronger constraints on this ratio due to contribution to the non-Gaussianity. However, as we see given that amplitude of curvature perturbation are of order 10^{-5} implying $\zeta\Delta_\zeta \sim 10^{-15}$, then it is reasonable to expect that there is a viable window of parameter space where strong coupling is avoided.

To see the restrictions on the size of non-Gaussianity from the CMB observations, we go back to more rigorous calculation of non-Gaussianity. As we can see from the equation (4.57), we will first need to expand the original action and obtain the cubic term in perturbations to compute the three point functions, and the size of non-Gaussianity [8]. Using the standard technique of quantum field theory we promote ζ_k to an operator in terms of the creation and annihilation modes, $a_{\mathbf{k}}^\dagger$, $a_{-\mathbf{k}}$ and the mode function $f(\mathbf{k}, t)$

$$
\zeta(\mathbf{k}, t) = a_{-\mathbf{k}} f(-\mathbf{k}, t) + a_{\mathbf{k}}^\dagger f^*(\mathbf{k}, t). \tag{4.72}
$$

The annihilation and the creation operators satisfy the canonical commutation relations $[a_{\mathbf{k}}, a_{\mathbf{k}}^\dagger] = (2\pi)^3\delta^3(\mathbf{k} - \mathbf{k}')$. The mode function $f(\mathbf{k}, t)$ satisfies the Wronskian condition $\dot{f}(\mathbf{k}, t)f^*(\mathbf{k}, t) - \dot{f}^*(\mathbf{k}, t)f(\mathbf{k}, t) = 2i$. Note that the Lagrangian and the action are writtin in terms of π, and we are interested in the comoving curvature perturbation, $\zeta = -H\pi$, and its bispectrum

$$
< \zeta^3 > . \tag{4.73}
$$

We first transform the terms $H_{int}(\pi) \rightarrow H_{int}(\zeta)$ and also for convenience switch to conformal time τ instead of t. As we pointed out earlier, the most dangerous contributions from H_{int} or L_{int} are coming from terms $\dot{\pi}(\partial_i\pi)^2$ and $\partial_i^2\pi(\partial_j\pi)^2$. In terms of ζ, these terms become

$$
\dot{\pi}(\partial\pi)^2 \rightarrow -\frac{1}{H^3}\zeta'(\partial\zeta)^2 \tag{4.74}
$$

$$
\partial^2\pi(\partial\pi)^2 \rightarrow -\frac{1}{H^3}\partial^2\zeta(\partial\zeta)^2. \tag{4.75}
$$

[8] Refer to the Appendix (A) for the full list of terms

Now, to numerically compute the bispectrum, we need to carry out the computation in terms of the variable $u_k = -\sqrt{A_1}\frac{a}{H}\zeta_k(\tau)$ as a function of the dimensionless variable $x = c_s k\tau$. Under these changes of variables, contributions from these terms to three point function are obtained as following,

1. contributions from the $\dot{\pi}(\partial\pi)^2$ term to $\langle\zeta(\mathbf{k}_1)\zeta(\mathbf{k}_2)\zeta(\mathbf{k}_3)\rangle$:

$$= -i(2\pi)^3\delta^3(\mathbf{k}_3+\mathbf{k}_2+\mathbf{k}_1)\frac{1}{A_1^3\sqrt{c_s^6\lambda^2\theta^2}}\frac{H^8x_f^3}{(c_s\theta)^5}\frac{1}{k_1^6}\left(-\delta_3H^4+9\bar{M}_4H^3-2M_2^4\right)\int_{-\infty}^{x_f}(x_3')^2dx_3' \tag{4.76}$$

$$u_{k_3}(x_f)u_{k_3}^{*\prime}(x_3')u_{k_2}(\frac{\lambda}{\theta}x_f)u_{k_2}^*(\frac{\lambda}{\theta}x_3')u_{k_1}(\theta^{-1}x_f)u_{k_1}^*(\theta^{-1}x_3')(\theta^2-1^2-\lambda^2)\cdot 2+c.c \tag{4.77}$$

$$-i(2\pi)^3\delta^3(\mathbf{k}_3+\mathbf{k}_2+\mathbf{k}_1)\frac{1}{A_1^3\sqrt{c_s^6\lambda^2\theta^2}}\frac{H^8x_f^3}{(c_s\theta)^5}\frac{1}{k_1^6}\left(-\delta_3H^4+9\bar{M}_4H^3-2M_2^4\right)\int_{-\infty}^{x_f}(x_3')dx_3' \tag{4.78}$$

$$u_{k_3}(x_f)u_{k_3}^*(x_3')u_{k_2}(\frac{\lambda}{\theta}x_f)u_{k_2}^*(\frac{\lambda}{\theta}x_3')u_{k_1}(\theta^{-1}x_f)u_{k_1}^*(\theta^{-1}x_3')(\theta^2-1^2-\lambda^2)\cdot 2+sym. \tag{4.79}$$

2. contributions from the $\partial^2\pi(\partial\pi)^2$ term to $\langle\zeta(\mathbf{k}_1)\zeta(\mathbf{k}_2)\zeta(\mathbf{k}_3)\rangle$:

$$= -i(2\pi)^3\delta^3(\mathbf{k}_3+\mathbf{k}_2+\mathbf{k}_1)\frac{1}{A_1^3\sqrt{c_s^6\lambda^2\theta^2}}\frac{H^8x_f^3}{c_s^7\lambda\theta^5}\frac{1}{k_1^6}\left(\frac{1}{3}\delta_3H^4-\frac{1}{2}\left(\bar{M}_1^3H+\bar{M}_2^2H^2+2\bar{M}_3^2H^2\right)\right)\int_{x_0}^{x_f}(x_3')^3dx_3' \tag{4.80}$$

$$u_{k_3}(x_{fn})u_{k_3}^*(x_3')u_{k_2}(\phi x_{fn})u_{k_2}^*(\phi x_3')u_{k_1}(\theta^{-1}x_{fn})u_{k_1}^*(\theta^{-1}x_3')(3\theta^2-1-\lambda^2)+c.c+sym, \tag{4.81}$$

where we have defined parameters $\lambda \equiv \frac{k_2}{k_1}$ and $\theta \equiv \frac{k_3}{k_1}$ and $\phi \equiv \lambda/\theta$ which determine the shape of the triangles formed by $\mathbf{k}_1$, $\mathbf{k}_2$ and $\mathbf{k}_3$.

In early analysis of CMB data the *local* non-Gaussinaity corrections for curvature perturbation were expressed in terms of the quantity f_{NL}, as [96]

$$\zeta = \zeta_L - \frac{3}{5}f_{NL}\zeta_L^2, \tag{4.82}$$

where ζ_L is the linear approximation of the perturbation. For $n_s - 1 \ll 1$, this assumption, which only considers local contributions to non-Gaussianities, leads to the following relationship between the three point function and the dimensionless power spectrum of ζ,

$$\langle\zeta(\mathbf{k}_1)\zeta(\mathbf{k}_2)\zeta(\mathbf{k}_3)\rangle = (2\pi)^7\delta^3(\mathbf{k}_1+\mathbf{k}_2+\mathbf{k}_3)\frac{\Delta_\zeta^2}{k_1^3k_2^3k_3^3}\times\left\{-\frac{3}{10}f_{NL}\left(k_1^3+k_2^3+k_3^3\right)\right\}. \tag{4.83}$$

As we saw earlier, the calculation of the three point function for different interactions, in a top down approach does not necessarily lead to the local form above. However, one can still define

a quantity which is similar and reduces to this definition above for local form. In general writing contributions to bispectrum as

$$\langle\zeta(\mathbf{k}_1)\zeta(\mathbf{k}_2)\zeta(\mathbf{k}_3)\rangle = (2\pi)^7\delta^3(\mathbf{k}_1+\mathbf{k}_2+\mathbf{k}_3)\frac{\Delta_\zeta^2}{k_1^3k_2^3k_3^3}\times\mathcal{A}(k_1,k_2,k_3), \tag{4.84}$$

we can then define f_{NL} through this relation

$$\mathcal{A}(k_1,k_2,k_3) = -\frac{3}{10}f_{NL}\left(k_1^3+k_2^3+k_3^3\right)$$

Therefore the relationship between f_{NL} and bispectrum can be derived from following relations:

$$\langle\zeta_{\mathbf{k}_1}(t)\zeta_{\mathbf{k}_2}(t)\zeta_{\mathbf{k}_3}(t)\rangle = (2\pi)^3\delta^3(\mathbf{k}_1+\mathbf{k}_2+\mathbf{k}_3)B_I(k_1,k_2,k_3), \tag{4.85}$$

which leads to

$$f_{NL} = -\frac{10}{3}B_I(k_1,k_2,k_3)\frac{1}{(2\pi)^4\Delta_\zeta^2}\frac{\prod k_i^3}{\sum k_i^3}. \tag{4.86}$$

Now, to connect to our numerical calculations, we further define

$$\tilde{q}_{\partial^2\pi(\partial\pi)^2} \equiv \frac{H^8}{A_1^3(c_s)^6}\left(\frac{1}{3}\delta_3H^4-\frac{1}{2}\left(\bar{M}_1^3H+\bar{M}_2^2H^2+2\bar{M}_3^2H^2\right)\right) \tag{4.87}$$

$$\tilde{q}_{\dot{\pi}(\partial\pi)^2} \equiv \frac{H^8}{A_1^3(c_s)^6}\left(-\delta_3H^4+9\bar{M}_4H^3-2M_2^4\right) \tag{4.88}$$

$$\tilde{q}_iI(k_1,k_2,k_3) \equiv \frac{4\pi^2A_1^2}{H^8c_s^2}B_I(k_1,k_2,k_3) \tag{4.89}$$

we obtain the equation for f_{NL} in terms of I:

$$f_{NL}^{(i)} = -\frac{10}{3}\frac{\prod_i k_i^3}{\sum_i k_i^3}\frac{1}{\gamma_s^2}\tilde{q}_iI(k_1,k_2,k_3), \tag{4.90}$$

where we used the relation $\Delta_\zeta = \gamma_s\frac{1}{4\pi^2}\frac{H^4}{A_1c_s}$ to write in terms of γ_s, which we discussed in section (**??**). Now we can numerically compute

$$\frac{f_{NL}^{(i)}}{\tilde{q}_i} = -\frac{10}{3}\frac{\prod_i k_i^3}{\sum_i k_i^3}\frac{1}{\gamma_s}I(k_1,k_2,k_3). \tag{4.91}$$

For convenience, we take the ratio of the wavenumber k such that $k_2\to k_2/k_1=\lambda$ and $k_3\to k_3/k_1=\theta$. Then the above equation becomes

$$\frac{f_{NL}^{(i)}}{\tilde{q}_i} = -\frac{10}{3}\frac{k_1^6\lambda^3\theta^3}{1+\lambda^3+\theta^3}\frac{1}{\gamma_s}3I(k_1,\lambda,\theta), \tag{4.92}$$

or

$$f_{NL}^{(i)} = \tilde{q}_i \times \left\{ -\frac{10}{3} \frac{k_1^6 \lambda^3 \theta^3}{1+\lambda^3+\theta^3} \frac{1}{\gamma_s} I(k_1, \lambda, \theta) \right\}. \tag{4.93}$$

To make the connection with observations, the most recent CMB observation by Planck collaboration gives a bound on the size of the equilateral non-Gaussianity of the order $f_{NL} \simeq -26 \pm 47$ [51]. I calculated the left hand side of the equation (4.92) can be computed numerically, setting the bound on $\tilde{q}$.

4.6 Results

In section 4.3.3, we had numerically computed the value of canonical mode function $u(x)$, $x = c_s k\tau$. The computation depends on values of α_0 and β_0 which themselves are compositions of other parameters in EEFToI action. We found empirically that the amplification to the power spectrum γ_s was the largest within the region

$$-0.5 \leq \alpha_0 \leq -0.1 \quad \text{and} \quad 0 \leq \frac{\alpha_0^2}{4} \leq \beta_0 \leq \frac{\alpha_0^2}{3}. \tag{4.94}$$

In fact, when setting $\alpha_0 = -0.18$ and $\beta_0 = \alpha_0^2/4$ we obtained the largest values ($\gamma_s \geq 14.6$) compared to other values of α_0 and β_0 within that region. Next, substituting our numerically computed $u_k(x)$ in equations 4.76 and 4.80, we proceeded to numerically calculate the contributions to bispectrum from these terms.

From physics point of view, a more interesting applications of the EEFToI and EFToI is when they result in larger values of γ_s or significant deviations from the Bunch Davis initial conditions.

In order to numerically set the initial conditions in our calculations in the regime where k^6 term dominates, we chose the value of $x_{initial}$ to be where $\beta_0 x^4$ is far greater than $\alpha_0 x^2$ ($x_{initial} \sim -50|\alpha_0/\beta_0|^{1/2}$). For the upper limit of the integration, we choose $x_{final} = -0.00001$[9].

Without loss of generality, we set the value of $k_1 = 1$[10]. We explored the triangle shapes in the region of $0.2 \leq \lambda \leq 1$ and $0.2 \leq \theta \leq 1$. The choice of the lower bound of 0.2 for λ and θ were due to the limitation of our numerical method. For all the values of u_{k_i} to be far enough into the past such that $x_{initial} \sim -50|\alpha_0/\beta_0|^{1/2}$, we took the values of λ and θ such that their ratios varied within 0.2 and 5. However, since the power of λ in the numerator and the denominator of (4.92) are both 3, we don't expect the right hand side to diverge as $\lambda \to 0$. Due to the symmetry similar argument applies to when $\theta \to 0$.

The figure (4.8) displays the contributions to non-Gaussianity from the two potentially dangerous operators that we have discussed before with fixed k_1 and varying λ and θ. As it can

[9]This corresponds to choosing different values of τ_f for different k, but such that they have exited the horizon. Also, the result of the computation by changing $x_{initial}$ further into the past and x_{final} into the present resulted in negligible difference for the value of γ_s.

[10]Since $I(k_1, k_2, k_3)$ has k_1^{-3} and the coefficients in (4.92) has k_1^6, the final result is independent of the value of k_1.

seen that the value of $f_{NL}/\tilde{q}_i \sim \pm 10^4$ for both operators and it is not diverging. Interestingly the values with larger magnitudes correspond to what is known in literature as flattened triangles. This is in agreement with some earlier results that point out excited states at initial conditions can result to enhancement of non-Gaussianities for these shapes [21]. With setting the conservative observational bound of $f_{NL} \lesssim 10$ we get a bound of $|\tilde{q}_i| \sim 10^{-3}$.

Finally, we can ask what do all these constraint mean in terms of the original couplings and coefficients in EEFToI action, and whether there are corners of the parameter space that lead to scenarios we have explored. The table 4.6 shows the list of conditions and constraints we have considered within the EEFToI. The primary parameters we included in EEFToI were $M_2, \bar{M}_1, \bar{M}_2, \bar{M}_3, \bar{M}_4, \delta_3, H, M_{\rm pl}^2 \dot{H}$.

Constraints	Note
$\alpha_0 < 0$	Regions where the power spectrum is enhanced. Note that for $\alpha_0 > 0$ the power spectrum is suppressed (not interesting)
$\beta_0 > 0$	To avoid tachyonic instabilities (Note $\delta_3 :> 0$)
$\Delta_\zeta^{B.S} \sim 10^{-9}$	The constraint from power spectrum of the CMB observation. Note that $\gamma \sim 10$ at most.
$H > \frac{\sqrt{A_1}}{M_{pl}}$	Decoupling limit
$0 \leq c_{s,h}^2 \leq 1$	Speed of sound for the tensor modes (Note: $\bar{M}_3^2 < 0$)
$0 \leq c_s^2 = \frac{F_1}{A_1} \leq 1$	To avoid superluminality in the regime $\omega^2 \sim k^6$
$A_1 \geq 0$	To avoid ghosts at leading order
$\dot{H} < 0$	To satisfy the null energy condition
$\tilde{q}_i \leq 10^{-3}$	Constraints on f_{NL} from the observations

The figure 4.9 displays the result of a search algorithm we performed to find valid values of parameters of EEFToI imposing conditions 4.6. I also have imposed an additional cutoff on all the mass dimension parameters to be below the Planck scale, since we do not expect semi-classical gravity to be valid above that scale. As one can see in the figure 4.9, the result of the search algorithm indicates that there exists values of parameters that are allowed under the above constraints. In these regions, we have a sensible description of the extended effective field theory of inflation, which can rise from different initial conditions with a dispersion relations $k^6 \sim \omega^2$[21].

4.7 Conclusions

In this work we extended the formalism of the Effective Field Theory of Inflation, proposed earlier in [50], by including in the unitary gauge Lagrangian operators with mass dimensions three and

four. There is a healthy combination of operators in this extended theory that allows sixth order correction to the dispersion relation for scalar perturbations. Modified dispersion relations are known to give rise to interesting effects on CMB observables due to non-Bunch-Davies initial conditions [21].

In this chapter we provided a theoretical framework to motivate the emergence of modified dispersion relations. In particular, we discussed the conditions under which the Extended Effective Field Theory of Inflation is weakly coupled all the way from low energy to the UV region where the dispersion relation becomes dominated by the sextic term. In this situation, the evolution of the modes can be consistently followed from deep inside the horizon to super-horizon scales.

We also analysed the phenomenological implications of our EEFToI for the fluctuations around a quasi de Sitter background. We found that the tensor perturbations are untouched. On the other hand, various scenarios for the scalar perturbations can occur, depending on the parameters of the dispersion relation. If the coefficients of the quartic and the sextic dispersion relation are positive, the scalar power spectrum is suppressed. However, if the quartic coefficient is negative, even for the case where the mode does not become tachyonic before crossing the only turning point, the scalar power spectrum can be enhanced. This in turn leads to a suppression of r with respect to models with Lorentzian dispersion relation.

We proceeded to compute the bispectrum and the size of the non-Gaussianity to constrain the parameters of EEFToI. With the computed power spectrum, we set some constraints on the parameters by computing the non-Gaussianity of the theory. Since the observations have set very small bound on non-Gaussianity with $f_{NL} \sim -26 \pm 47$, and the computed value of $f_{NL}/\tilde{q}_i$ were up to orders of 10^4, we set a constraint on values of $\tilde{q} \leq 10^{-3}$. We found that there is an allowed region of parameters in the action where we do have a sensible description of the EEFToI, with initial conditions set with dispersion relations $k^6 \sim \omega^2$. In future, it would be interesting to see if we can have parameters and operators that will allow for orders higher than k^6 within the framework of EEFToI.

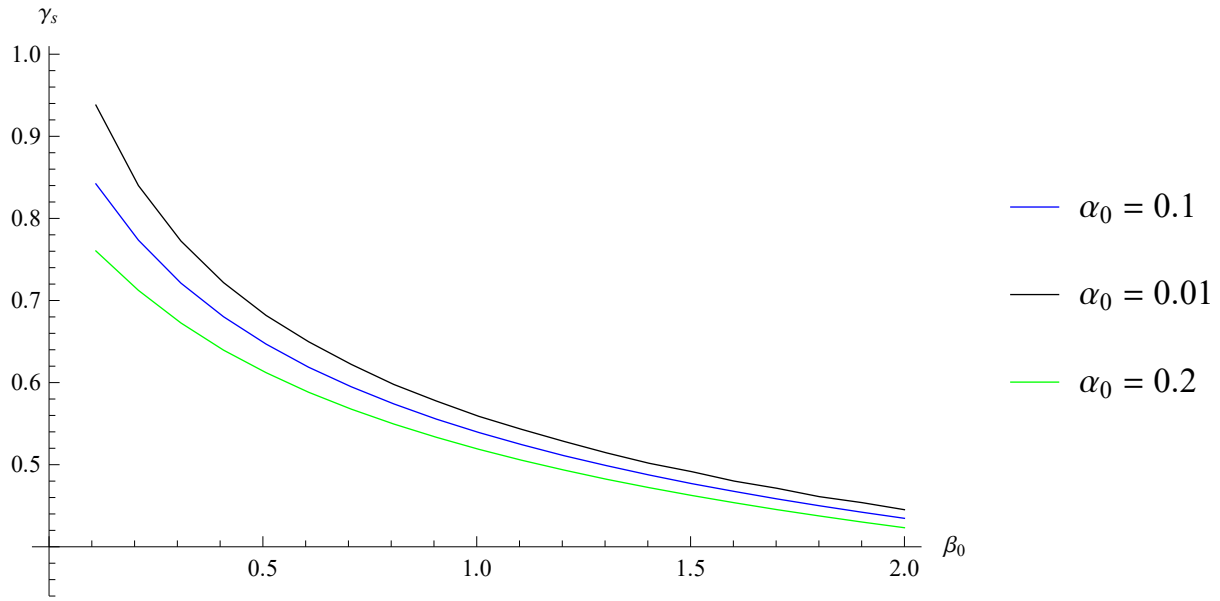

Figure 4.1: Plot of γ_s as a function of β_0 when α_0 and β_0 are both positive and $0.01 \leq \alpha_0 < 1$ with $0 \leq \beta_0 \leq 2$.

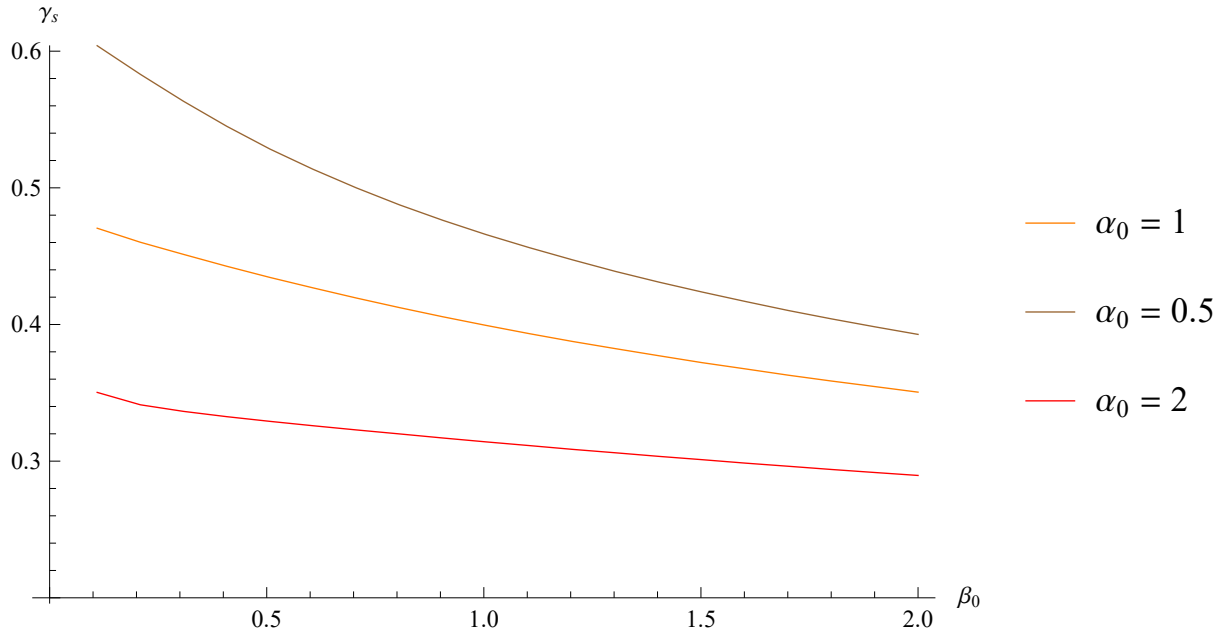

Figure 4.2: Plot of γ_s as a function of β_0 when α_0 and β_0 are both positive and $1 \leq \alpha_0 \leq 2$ with $0 \leq \beta_0 \leq 2$.

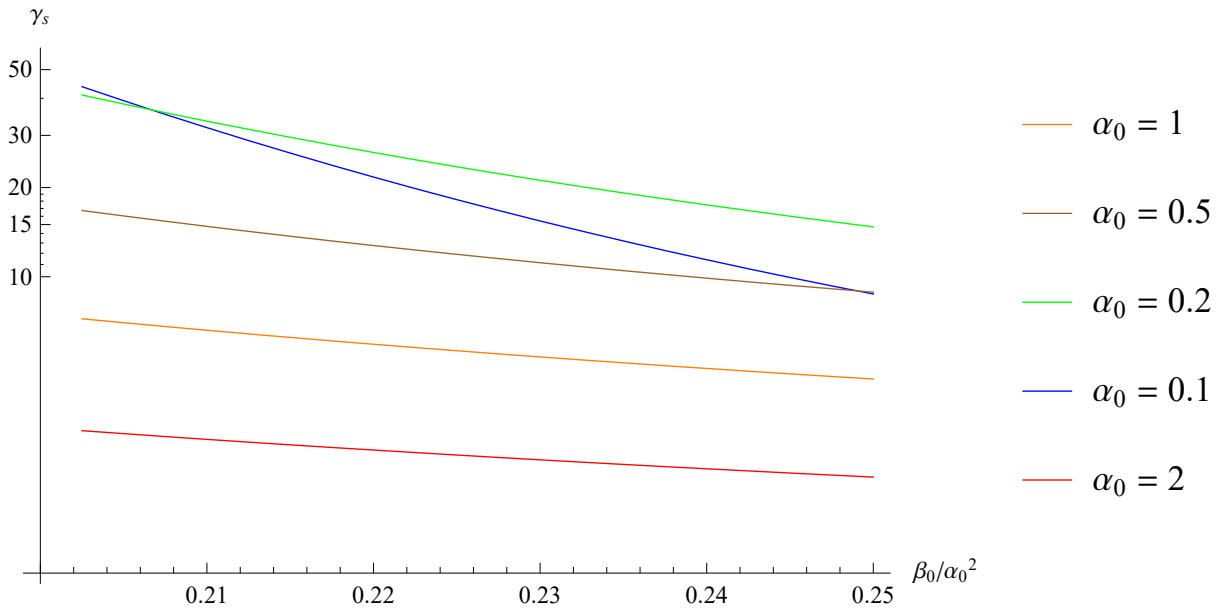

Figure 4.3: Log plot of γ_s as a function of β_0/α_0^2 when α_0 is big and negative ($0.1 \leq |\alpha_0| \leq 2$) and $\frac{\alpha_0^2}{5} \leq \beta_0 \leq \frac{\alpha_0^2}{4}$.

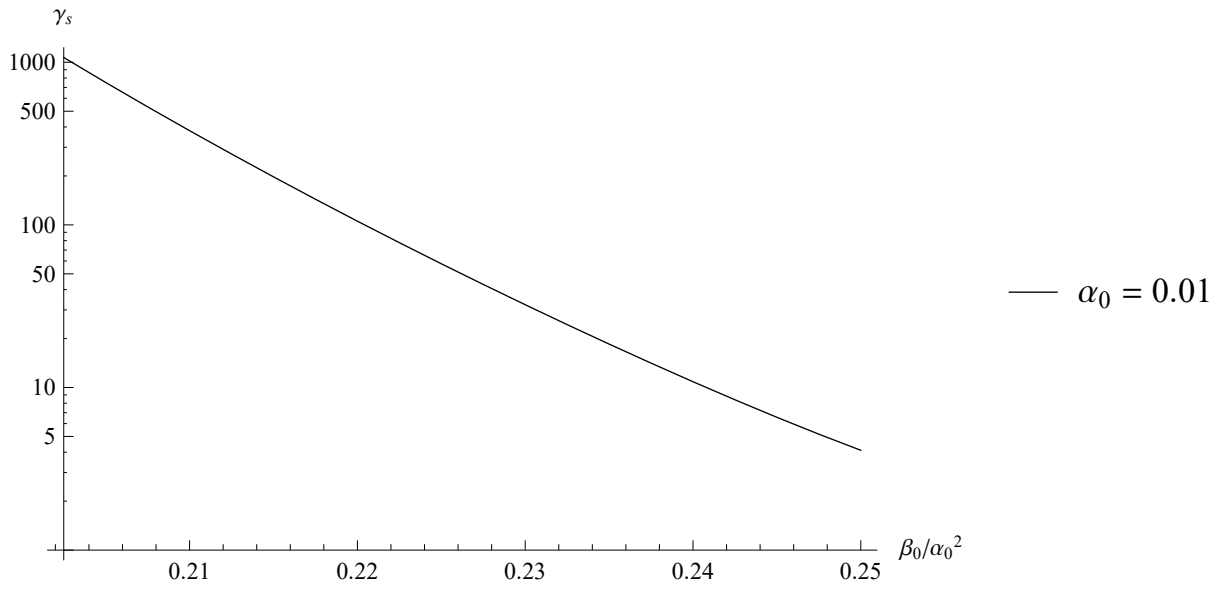

Figure 4.4: Log plot of γ_s as a function of β_0/α_0^2 when α_0 is small and negative ($|\alpha_0| = 0.01$) and $\frac{\alpha_0^2}{5} \leq \beta_0 \leq \frac{\alpha_0^2}{4}$.

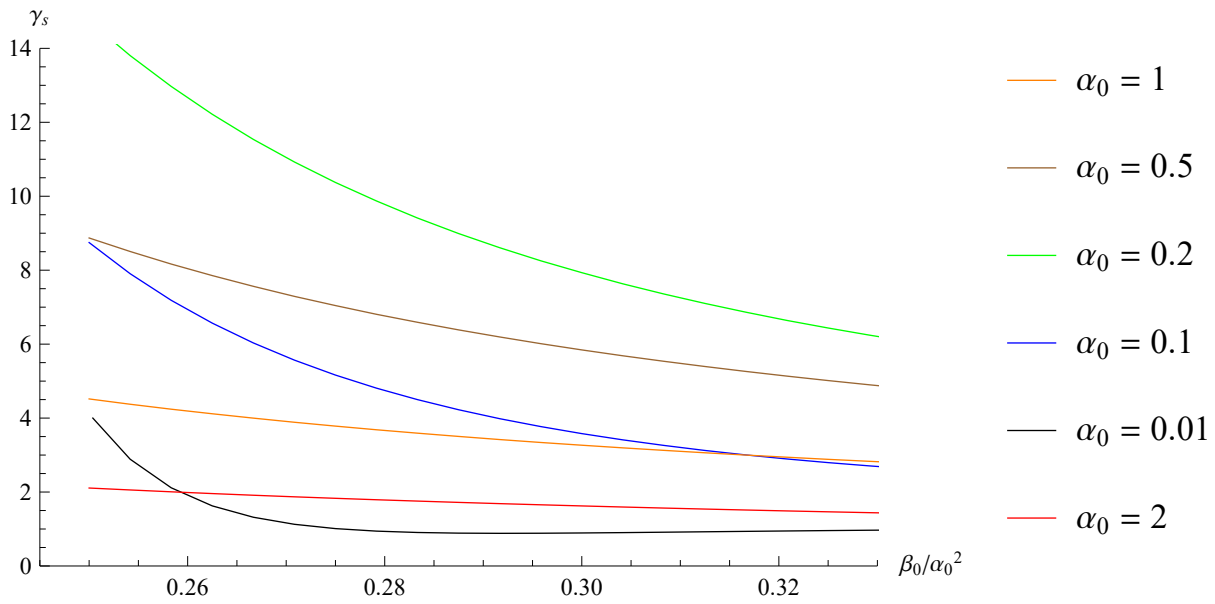

Figure 4.5: γ_s as a function of β_0/α_0^2 when $\alpha_0 < 0$ and $\beta_0 > 0$ and $0.01 \leq |\alpha_0| \leq 2$ and $\frac{\alpha^2}{4} \leq \beta_0 \leq \frac{\alpha^2}{3}$.

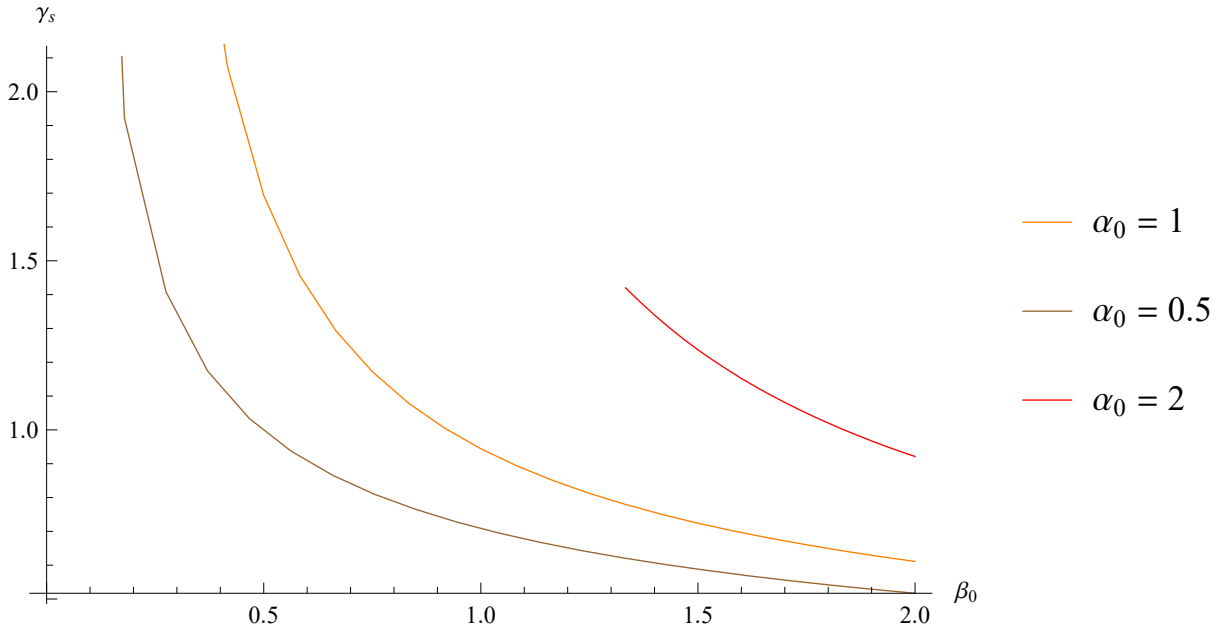

Figure 4.6: γ_s for big values of α_0 (0.5, 1, 2) as a function of β_0 when $\alpha_0 < 0$ and $\beta_0 > 0$ and $\frac{\alpha^2}{3} \leq \beta_0 \leq 2$.

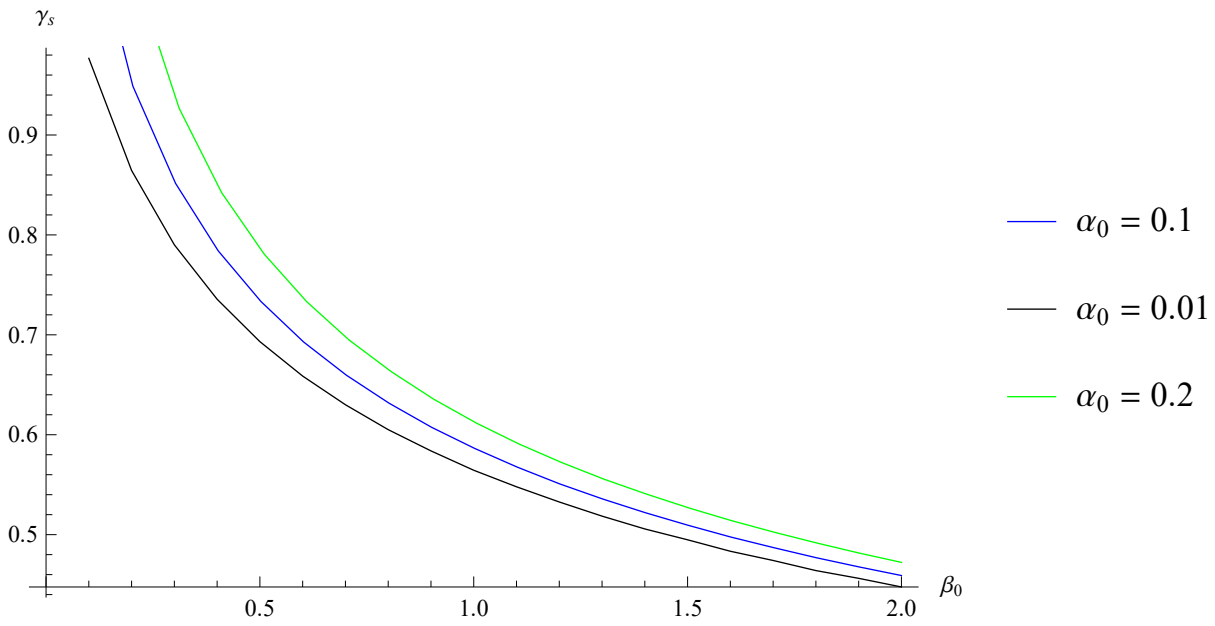

Figure 4.7: γ_s for small values of α_0 (0.01, 0.1, 0.2) as a function of β_0 when $\alpha_0 < 0$ and $\beta_0 > 0$ and $\frac{\alpha^2}{3} \leq \beta_0 \leq 2$.

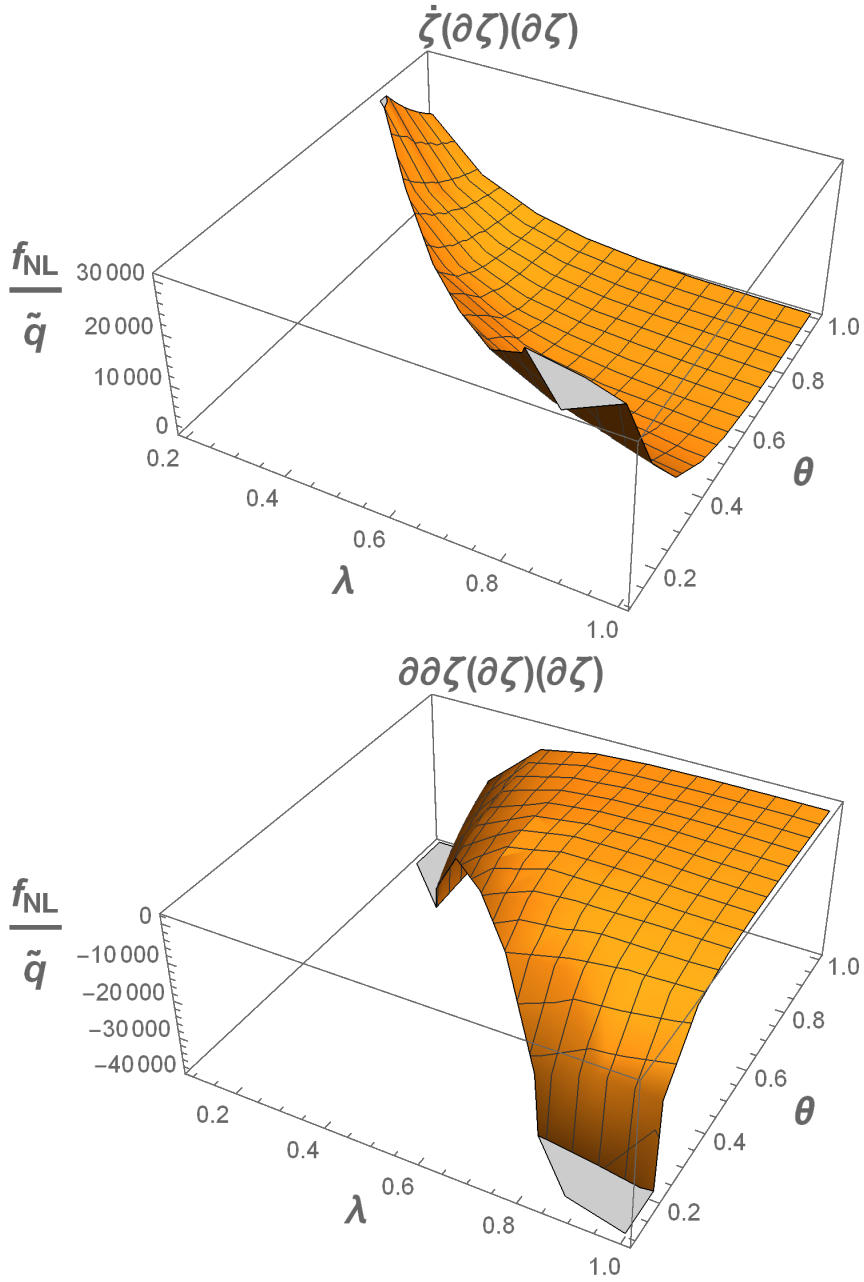

Figure 4.8: Calculation of the quantity $f_{nl}/\tilde{q}_i$ for the terms $\dot{\zeta}(\partial\zeta)^2$ (above) and $\partial^2\zeta(\partial\zeta)^2$ (below)

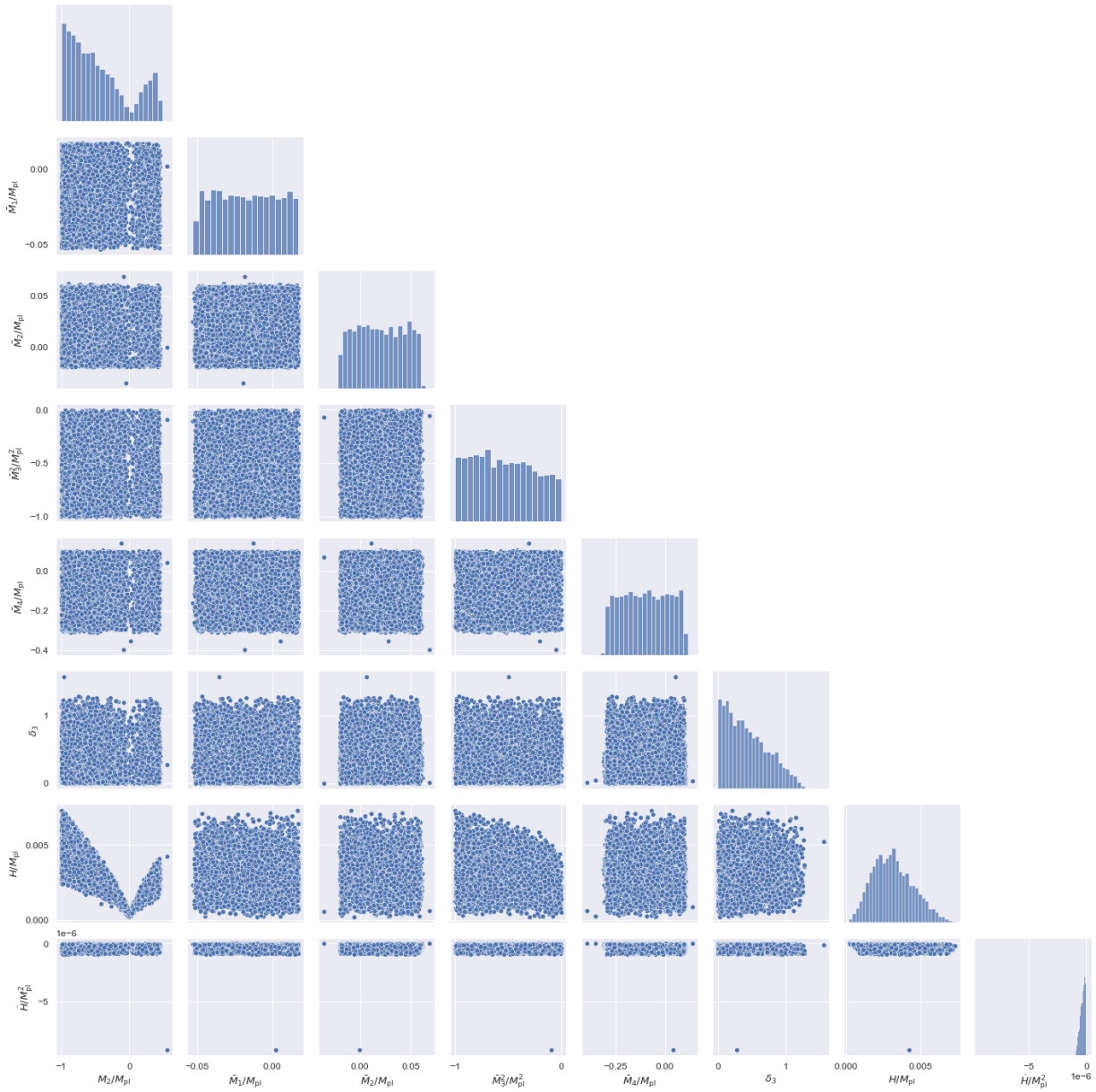

Figure 4.9: Parameters search of EEFToI model under the constraints listed in table 4.6. We searched for allowed values of $M_2, \bar{M}_1, \bar{M}_2, \bar{M}_3^2, \bar{M}_4, \delta_3, H, \dot{H}$. Furthermore, we set an additional cutoff at $1M_{\rm pl}$, except for δ_3 which is dimensionless. Although the points in the plots are scattered, this is due to the method I carried out for searching through parameters. Instead of searching the entire grid, which would take enormous computation time, I took a random search method. Note that the histogram does not represent the probability of each parameter. It just means that the algorithm searched in those respective regions more frequently.

Part II

Reconstructing the Expansion History of the Universe from Observations

Chapter 5

Model Independent Approach to ΛCDM

5.1 Introduction

The discovery of the acceleration of the expansion of the Universe [124, 119] led to the emergence of the ΛCDM paradigm, further supported by the study of the cosmological microwave background [33, 120] and the large-scale structures of the Universe [71, 10]. In this paradigm, gravity is described by general relativity (GR), and the energy budget is dominated by the cosmological constant as dark energy (DE), responsible for the acceleration of the expansion, and a smooth, cold dark matter component. However, the nature of DE is one of the biggest mysteries of modern physics, and the simplest candidate, the cosmological constant, poses theoretical problems [149, 118]. Alternatively, general relativity may not be the correct theory to describe gravity, and the acceleration may reflect departure from GR.

At the background level, for a flat universe, the expansion of the smooth Universe $h(z) = H(z)/H_0$ follows

$$h^2(z) = \Omega_{\rm m}(1+z)^3 + \Omega_{\rm DE}(z), \tag{5.1}$$

where H_0 is the Hubble constant today, $\Omega_{\rm m}$ the matter energy density today,

$$\Omega_{\rm DE}(z) = (1-\Omega_{\rm m}) \exp\left(3\int_0^z \frac{1+w(z')}{1+z'}{\rm d}z'\right), \tag{5.2}$$

the DE contribution to the energy density, and $w(z) = P_{\rm DE}/\rho_{\rm DE}$ is the DE equation of state. For a cosmological constant Λ, $w \equiv -1$ and $\Omega_{\rm DE}(z) = \Omega_\Lambda \equiv 1 - \Omega_{\rm m}$, but current data do not rule out models such as quintessence or dynamical DE models [116, 150].

Meanwhile, at the perturbation level, the growth rate f is defined as

$$f(z) = \frac{{\rm d}\ln\delta}{{\rm d}\ln a} \simeq \Omega_{\rm m}^{\gamma}(z), \tag{5.3}$$

where γ is the growth index [105, 107, 106], and

$$\Omega_{\rm m}(z) = \frac{\Omega_{\rm m}(1+z)^3}{h^2(z)} \tag{5.4}$$

is the matter contribution to the energy density at a given redshift.

Observationally, redshift-space distortion measures

$$f\sigma_8(z) \simeq \sigma_8(0)\Omega_{\rm m}^{\gamma}(z)\exp\left(-\int_0^z \Omega_{\rm m}^{\gamma}(z')\frac{{\rm d}z'}{1+z'}\right), \tag{5.5}$$

where $\sigma_8^2(z)$ is the mass variance in a $8\,h^{-1}$ Mpc sphere. For simplicity, we will denote $\sigma_8 = \sigma_8(0)$ when there is no ambiguity.

From eq. (5.4) and (5.5), it is clear that $f\sigma_8$ depends on $(\Omega_{\rm m}, \gamma, \sigma_8)$ as well as the expansion history $h(z)$. In general relativity (GR), $\gamma \simeq 0.55$, while modified theories of gravity such as $f(R)$ [59] or DGP [67] predict different (possibly scale-dependent) values of γ [107]. Therefore, $f\sigma_8$ is a powerful probe of gravity. Moreover, joined measurements of $h(z)$ and $f\sigma_8$ can help break degeneracies between modified gravity theories and dark energy [105, 106]. Therefore, it has been used to test the ΛCDM model or alternative gravitys theories [113, 32, 29, 138, 77, 129, 110, 114, 142].

In this chapter, we aim to constrain some key cosmological parameters, namely, $\Omega_{\rm m}$, σ_8, and γ, by fitting the growth data using model-independent expansion histories that do not assume any DE model.

§ 5.2 describes the data and method, our results are shown in § 5.3. § 5.4 explores the effects of restricting the DE density to be positive at all redshift, and our conclusions are drawn in § 5.5.

5.2 Method

We used reconstructed expansion histories from the Joint Lightcurve Analysis [34] and combined them with growth measurements.

5.2.1 Model-independent reconstructions of the expansion history

We reconstructed the expansion history from the joint light-curve analysis (JLA) compilation (unbinned data with full covariance matrix) using the iterative model-independent smoothing method [137, 136, 99]. Starting from some initial guess $\hat{\mu}_0(z)$, we calculate the smooth distance modulus at any redshift z at iteration $n+1$ as

$$\hat{\mu}_{n+1}(z) = \hat{\mu}_n(z) + N(z)\sum_i \frac{\mu(z_i) - \hat{\mu}_n(z_i)}{\sigma_i^2}\exp\left(-\frac{\ln^2\left(\frac{1+z_i}{1+z}\right)}{2\Delta^2}\right), \tag{5.6}$$

where

$$N^{-1}(z) = \sum_i \frac{1}{\sigma_i^2} \exp\left(-\frac{\ln^2\left(\frac{1+z_i}{1+z}\right)}{2\Delta^2}\right) \tag{5.7}$$

is a normalization factor, $\mu(z_i)$ and σ_i are the measured distance modulus and its associated error at redshift z_i, and $\Delta = 0.3$ is the smoothing length.

We then obtain the smooth luminosity distances

$$d_{\rm L}(z) = 10^{\mu/5-5}{\rm Mpc}. \tag{5.8}$$

Assuming a flat universe, we can calculate

$$h(z) = \frac{c}{H_0}\left[\frac{\rm d}{{\rm d}z}\left(\frac{d_{\rm L}(z)}{1+z}\right)\right]^{-1}. \tag{5.9}$$

Varying the initial guess $\hat{\mu}_0$, we end up with few thousands reconstructions and calculate their χ^2 as

$$\chi^2_{{\rm SN},n} = \boldsymbol{\delta\mu}_n^{\rm T}\mathbf{C}^{-1}\boldsymbol{\delta\mu}_n, \tag{5.10}$$

where

$$\boldsymbol{\delta\mu}_n = \hat{\boldsymbol{\mu}}_n - \boldsymbol{\mu}_i \tag{5.11}$$

is the residual vector for a given reconstruction n and $\mathbf{C}$ is the covariance matrix provided by [34]. We then only keep reconstructions such that $\chi^2_{\rm SN} < \chi^2_{{\rm SN},\Lambda{\rm CDM}}$. These reconstructions represent a non-exhaustive sample of plausible expansion histories.

We should note that the method of smoothing we used in this work is in fact insensitive to the initial conditions and choice of the smoothing scale [137, 136]: whatever the initial conditions, the method converges to the solution preferred by the data. However, they will approach this final solution via different paths. The central idea of using the iterative smoothing in this work is to come with a *non-exhaustive* sample of plausible expansion histories of the Universe directly reconstructed from the data, therefore we start the procedure with several initial conditions and combine the results at the end.

5.2.2 Combining the likelihoods

For each reconstructed $h_n(z)$, we can calculate $f\sigma_8$ for some $(\Omega_{\rm m}, \gamma, \sigma_8)$ by computing the integral in eq. (5.5). We can thus explore the parameter space, and compare to growth measurements to obtain a χ^2 for the growth data. We used a compilation of growth data points from 2dFGRS

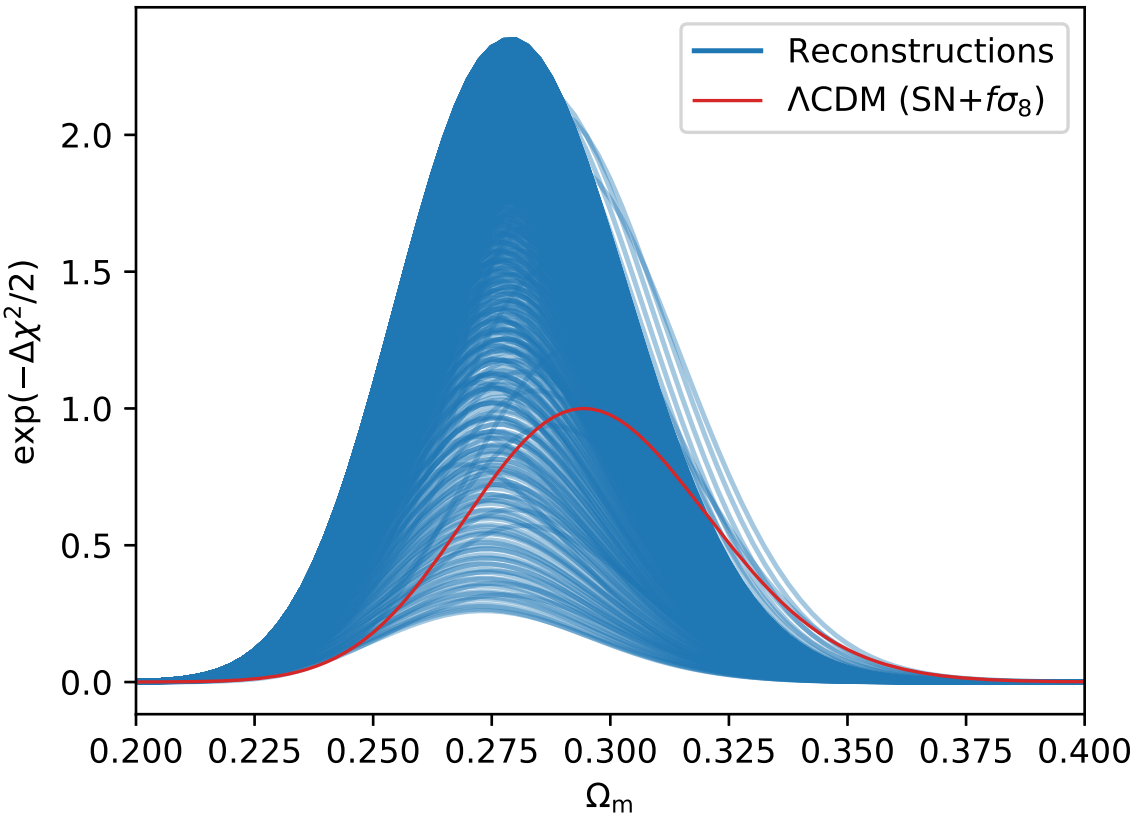

Figure 5.1: $\exp(-\Delta\chi^2/2)$ (with respect to the best-fit ΛCDM model) versus Ω_m for each reconstruction, fixing $(\gamma, \sigma_8) = (0.55, 0.80)$. The red line shows the ΛCDM case.

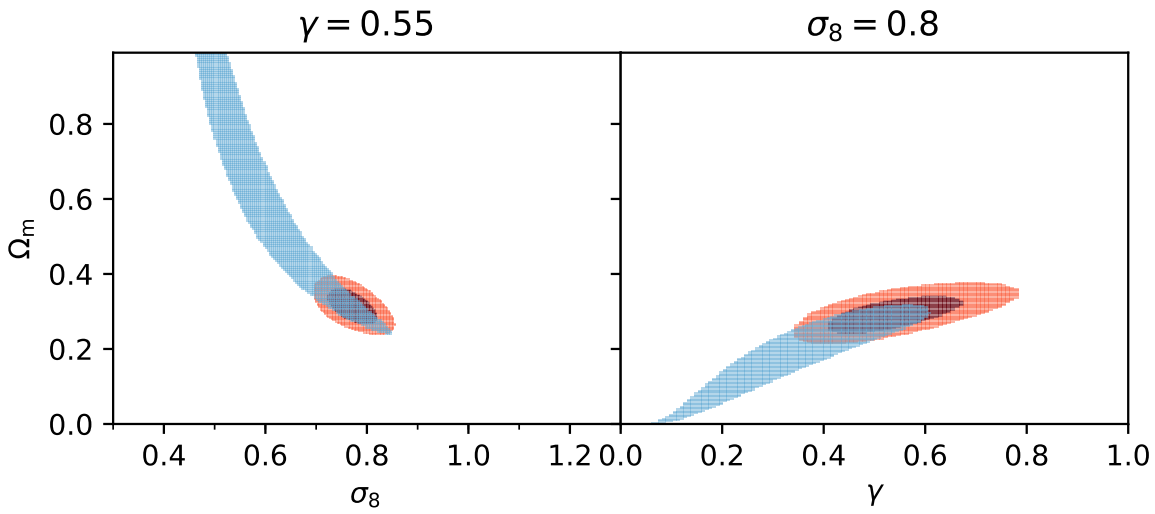

Figure 5.2: Superposition of the $\Delta\chi^2 < 0$ (with respect to the best-fit ΛCDM model) regions for $\gamma = 0.55$ (left) and $\sigma_8 = 0.80$ (right) in the model-independent case in blue. We also show in red the 1σ and 2σ regions of the ΛCDM model.

[143], WiggleZ [37], 6dFGRS [35], the VIPERS [60], the SDSS Main galaxy sample [84], 2MTF [85], and BOSS DR12 [75]. We did not include the FastSound data [115] at $z = 1.4$, since our smooth reconstructions do not reach that redshift.

Since both datasets are independent, we can multiply the likelihood, or equivalently sum the χ^2. Since the growth data are mutually independent, their χ^2 is simply defined as

$$\chi^2_{f\sigma_8} = \sum_i \left(\frac{f\hat{\sigma}_8(z_i|\gamma, \Omega_m, \sigma_8) - f\sigma_{8,i}}{\sigma_{f\sigma_8,i}} \right)^2 . \tag{5.12}$$

The total χ^2_n for reconstruction n is thus $\chi^2_n = \chi^2_{\mathrm{SN},n} + \chi^2_{f\sigma_8,n}$. We can then find the parameters that minimize the χ^2, and their associated confidence intervals.

5.3 Results

Using the reconstructed expansion histories $h(z)$, we calculate the χ^2 as defined in § 5.2.2. First, we fixed $(\gamma, \sigma_8) = (0.55, 0.80)$, and allow Ω_m to vary. Since the reconstructed $h(z)$ were obtained assuming a flat universe, Ω_m is allowed to vary between 0 and 1. For reference, we calculate the χ^2 of the ΛCDM model, and find its minimum $\chi^2_{\mathrm{min,\Lambda CDM}}$. We are interested in $\Delta\chi^2 = \chi^2 - \chi^2_{\mathrm{min,\Lambda CDM}}$, the difference with respect to the best-fit ΛCDM case. Fig. 5.1 shows $\mathcal{L} = \exp(-\Delta\chi^2/2)$ as a function of Ω_m for each reconstruction (in blue). Therefore, combinations

of h and Ω_m with a better χ^2 than the best-fit ΛCDM model ($\Delta\chi^2 < 0$), have a likelihood larger than one. For comparison, we also show in red $\mathcal{L}_{\Lambda CDM} = \exp(-\Delta\chi^2/2)$ for the ΛCDM case. The model-independent reconstructions seem to favour slightly lower Ω_m with respect to the ΛCDM case. However, they are fully consistent with the ΛCDM case.

We then allow γ or σ_8 to vary together with Ω_m, while fixing the third parameter to its fiducial value ($\sigma_8 = 0.80$ or $\gamma = 0.55$). In both cases, we calculate χ^2 for the ΛCDM case, and find the regions where $\Delta\chi^2 < 2.3$ and $\Delta\chi^2 < 6.18$, corresponding to 1σ and 2σ for two degrees of freedom. Fig. 5.2 shows in red the 1σ and 2σ regions of the ΛCDM case. For each model-independent reconstruction, we then calculate the χ^2 of the model-independent case, and find the regions in the (σ_8, Ω_m) and (γ, Ω_m) planes where the reconstruction give a better χ^2 than the best-fit ΛCDM, namely, $\Delta\chi^2 < 0$. Fig. 5.2 shows in blue the superposition of these regions over all reconstructions in the (Ω_m, σ_8) (left) and (Ω_m, γ) (right) planes. Therefore, if a point (σ_8, Ω_m) (or (γ, Ω_m)) is located in the blue region, there exists at least one reconstruction that, combined with (σ_8, Ω_m) (or (γ, Ω_m)), yields a better χ^2 than the best-fit ΛCDM model.

Fixing $\gamma = 0.55$ yields higher preferred values for Ω_m, while fixing $\sigma_8 = 0.80$ yields lower preferred values. However, the model-independent approach is fully consistent with ΛCDM. Moreover, it can be seen that, when $h(z)$ is not restricted to ΛCDM, there is a stronger degeneracy in the parameters. Namely, it is possible to find expansions histories that, coupled with low values of Ω_m and γ, or with high values of Ω_m and σ_8, give a better fit to the combined data. The degeneracy in the parameters can be understood from eq. 5.5: for fixed σ_8, Ω_m^γ should stay roughly constant, , therefore lower Ω_m are compensated by lower γ. Similarly, for fixed γ, $\Omega_m\sigma_8$ should stay constant, therefore lower Ω_m demand higher higher σ_8. This is consistent with the results of [138], with slightly tighter constraints.

Finally, we vary all three parameters $(\Omega_m, \gamma, \sigma_8)$ simultaneously. Fig. 5.3 shows in red the projections of the $\Delta\chi^2 < 3.53$ and 8.02 regions of the ΛCDM case, corresponding to 1σ and 2σ for three degrees of freedom, onto the (σ_8, γ) (top-left), (σ_8, Ω_m) (bottom-left), and (γ, Ω_m) (bottom-right). For the model-independent case, we proceed as in Fig. 5.2, and find the $\Delta\chi^2 < 0$ regions for each reconstruction. We then show in blue the projection onto the three planes of the superposition of the $\Delta\chi^2 < 0$ regions over all reconstruction. Again, the blue region shows the region of the parameter-space where there is at least one model-independent reconstruction that yields a better χ^2 than the best-fit ΛCDM model.

The model-independent joint constraints on $(\Omega_m, \gamma, \sigma_8)$ are now very broad. They are fully consistent with the ΛCDM model. The $\Delta\chi^2 < 0$ region is consistent with both $\Omega_m = 0$ and $\Omega_m = 1$, while it allows γ between about 0.1 and 1, and σ_8 between 0.25 and 1.25.

5.4 Dark energy constraints

In the previous section, we considered all combinations of $(\Omega_m, h(z))$, with the only restriction $\Omega_m < 1$, since the $h(z)$ were obtained assuming a flat universe. Rewriting equation (5.2) as

$$\Omega_{de}(z) = h^2(z) - \Omega_m(1+z)^3, \tag{5.13}$$

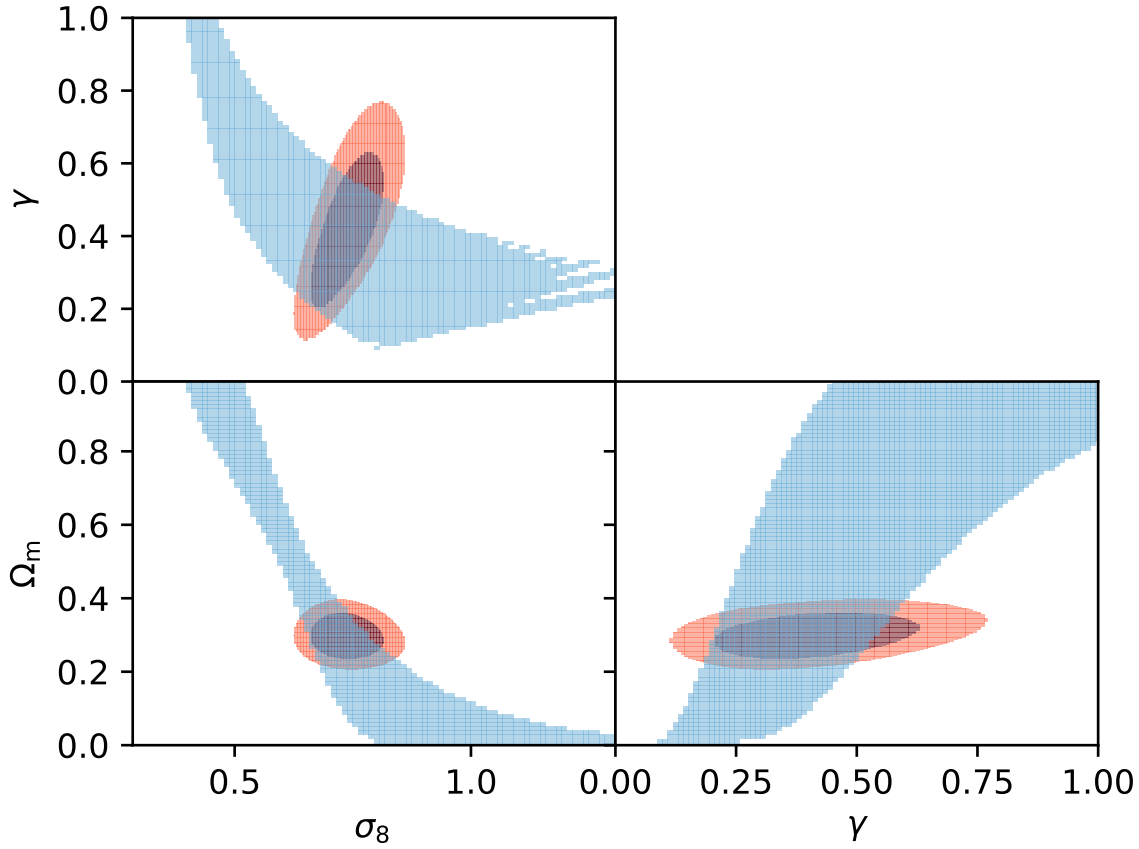

Figure 5.3: Superposition of the $\Delta\chi^2 < 0$ (with respect to the best-fit ΛCDM model) regions for $(\Omega_m, \gamma, \sigma_8)$ for the model-independent case (blue). In red we show the 1σ and 2σ regions for the ΛCDM case.

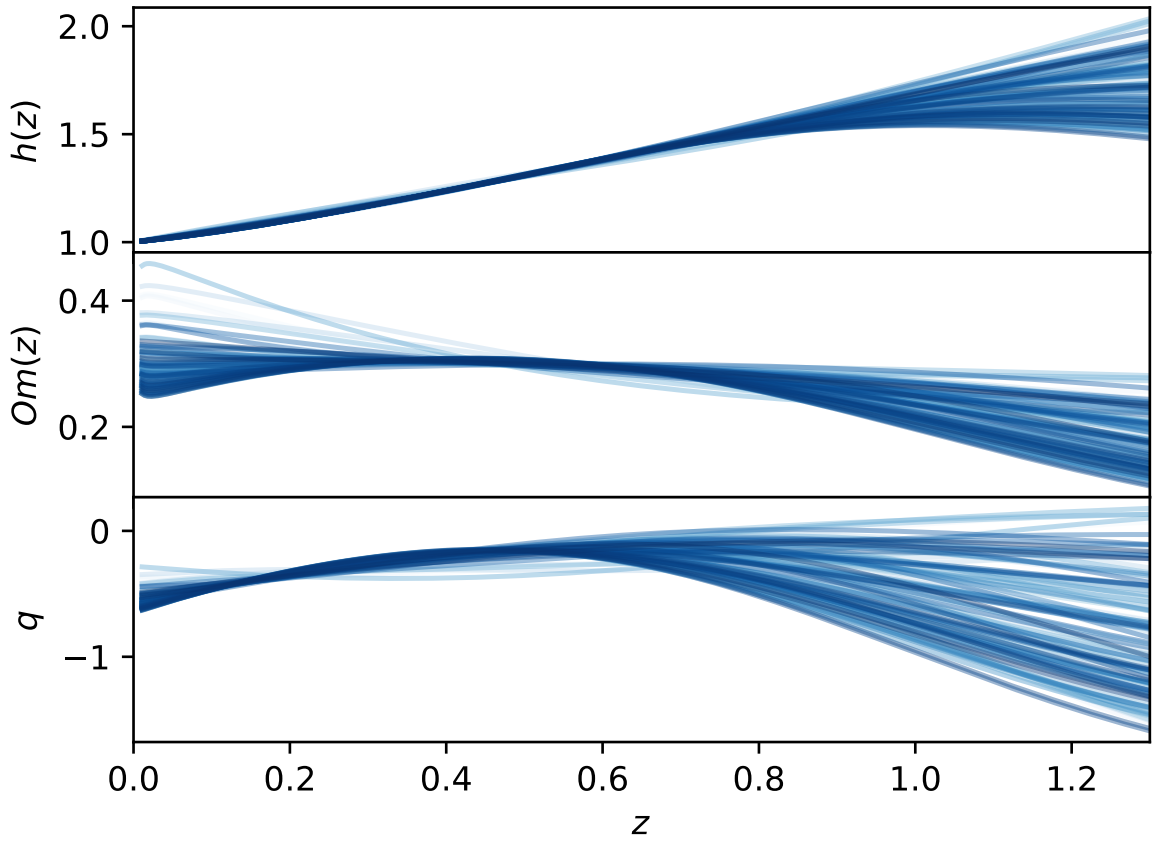

Figure 5.4: Reconstructed $h(z)$, $Om(z)$, and $q(z)$. The colour-code shows the index of the reconstruction.

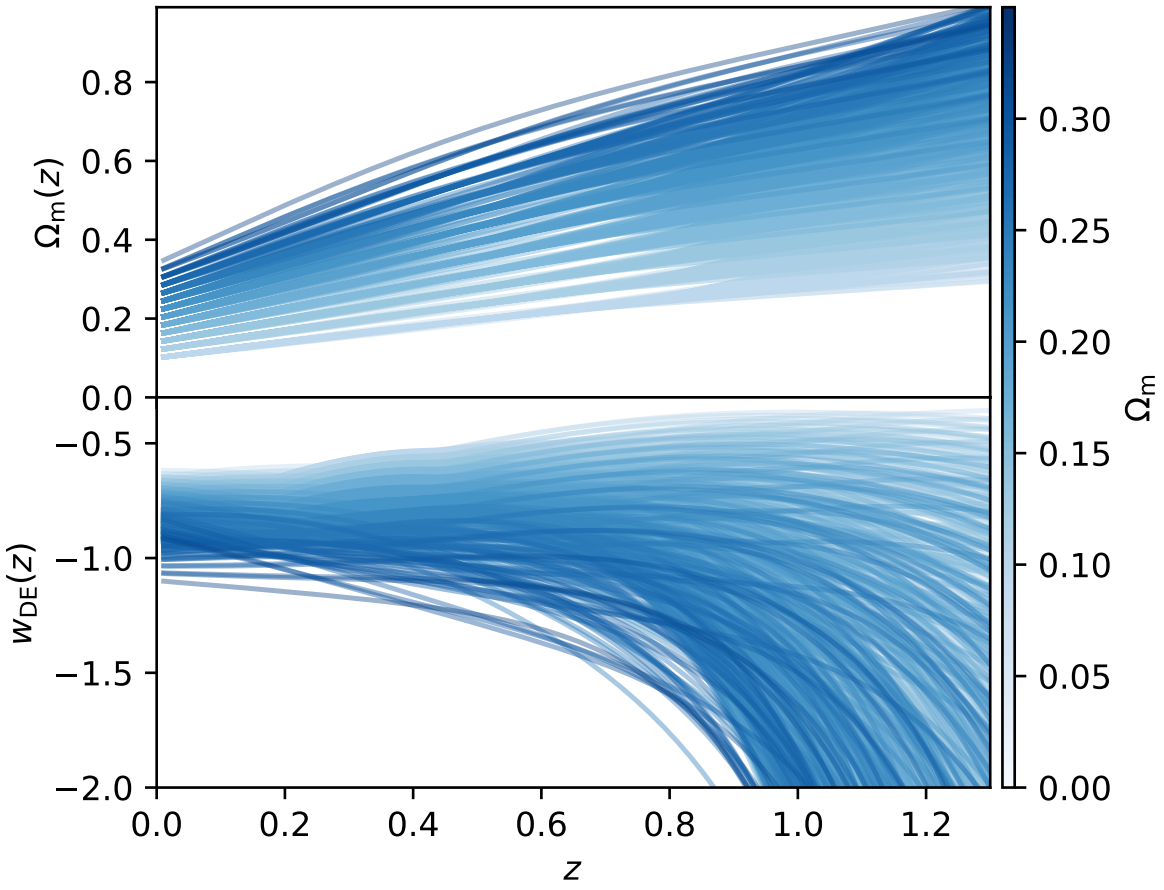

Figure 5.5: Reconstructed $\Omega_m(z)$ (top) and $w(z)$ (bottom) for different Ω_m and $h(z)$. All lines here verify eq. (5.14).

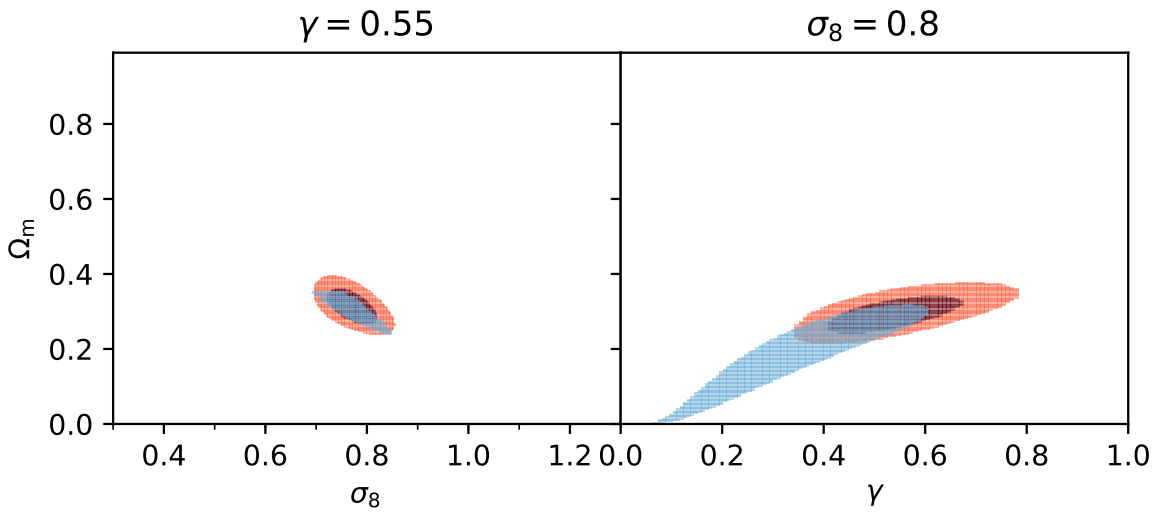

Figure 5.6: Blue: Truncation of the $\Delta\chi^2 < 0$ (with respect to the best-fit ΛCDM model) regions for $\gamma = 0.55$ (left) and $\sigma_8 = 0.80$ (right) in the model-independent case using eq. (5.14) as a hard prior. Red: 1σ and 2σ regions of the ΛCDM model.

another constraint arises. Namely, the equation of state w is well defined, i.e., does not have a singularity, if $\Omega_{\rm DE}(z) > 0$ at all redshift.

Therefore, even though some models can have negative DE density [132, 130], in this section, we only consider combinations of $h(z)$ and $\Omega_{\rm m}$ respecting the positivity condition

$$h^2(z) - \Omega_{\rm m}\,(1+z)^3 \geq 0 \tag{5.14}$$

for all z.

We can then use this to reconstruct the dark energy equation of state

$$\begin{aligned} w_{\rm de}(z) &= \frac{\frac{2}{3}(1+z)\frac{h'(z)}{h(z)} - 1}{1 - \Omega_{\rm m}(1+z)^3 h^{-2}} \\ &= \frac{1}{3}\frac{2q-1}{1-\Omega_{\rm m}(z)}, \end{aligned} \tag{5.15}$$

where

$$q(z) = (1+z)\frac{h'(z)}{h(z)} - 1 \tag{5.16}$$

is the deceleration parameter.

The top-, middle-, and bottom panels of Fig. 5.4 show the expansion history $h(z)$, the Om parameter [131]

$$Om(z) = \frac{h^2(z) - 1}{(1+z)^3 - 1}, \tag{5.17}$$

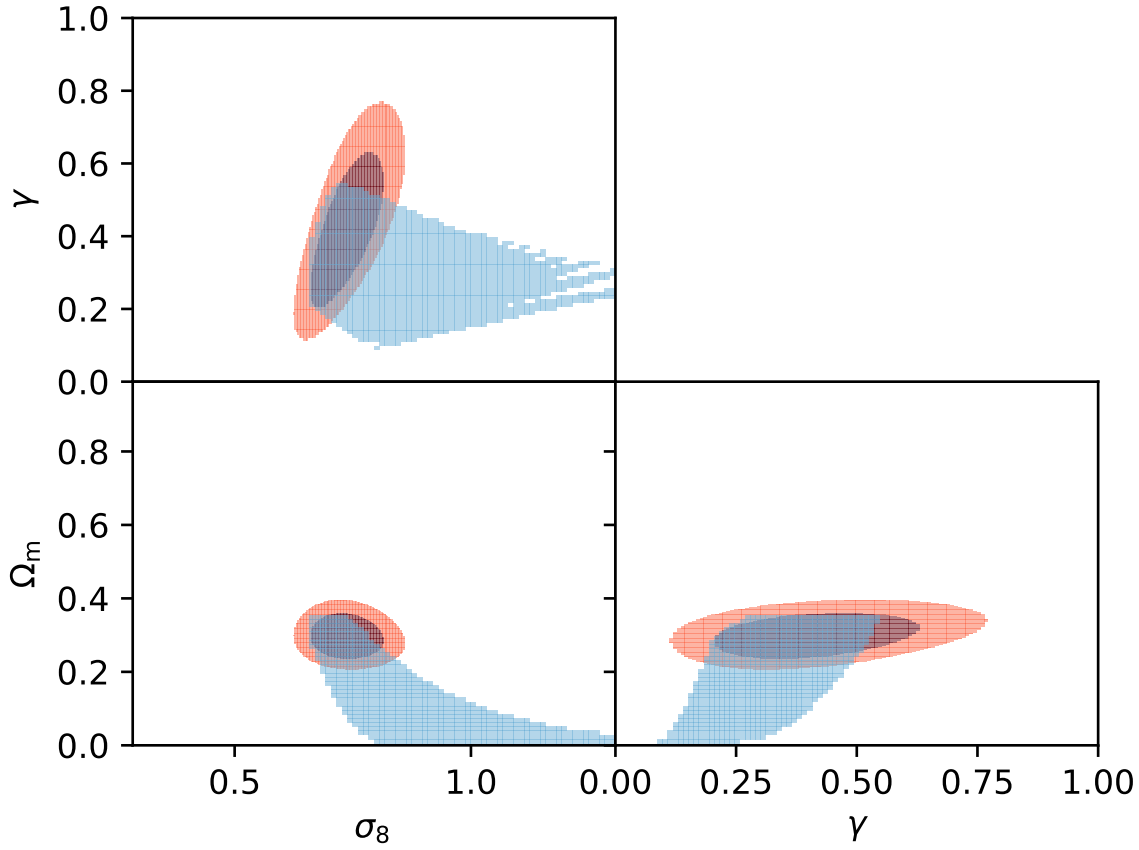

Figure 5.7: Blue: Truncation of the $\Delta\chi^2 < 0$ (with respect to the best-fit ΛCDM model) regions for $(\Omega_m, \gamma, \sigma_8)$ for the model-independent case using eq. (5.14) as a hard prior. Red: 1σ and 2σ regions of the ΛCDM case.

and the deceleration parameter $q(z)$ for a random choice of about 5% of the reconstructions. For a flat ΛCDM Universe, $Om(z) \equiv \Omega_m$, thus Om is a litmus test for flat ΛCDM.

The top and bottom panels of Fig. 5.5 respectively show the matter density $\Omega_m(z)$ and the equation of state of DE for some combination of $(\Omega_m, h(z))$ verifying the positivity condition (5.14), colour-coded by the index of the reconstruction. The expansion histories that are closer from ΛCDM have a Om parameter close to constant, and their $q(z)$ can cross 0, while some reconstructions further from ΛCDM do not cross 0. When $\Omega_m(z)$ crosses 1, eq. (5.14) ceases to be valid, therefore none of the lines shown here crosses 1.

We can now add the positivity condition (5.14) as a hard prior on Ω_m in the previous analysis. Indeed, large values of Ω_m combined with some reconstructions can lead to negative DE density, and these combinations should thus be rejected. Figs. 5.6 and 5.7 show in blue the superposition over all reconstructions verifying equation (5.14) of the projected $\Delta\chi^2 < 0$ regions of the parameter space. The red contours are unchanged with respect to Figs 5.2 and 5.3.

In Fig. 5.6, while the $\sigma_8 = 0.8$ case (right-hand panel) is not affected much, since it preferred lower values of Ω_m, the allowed region for the $\gamma = 0.55$ case is drastically reduced, and only a small space of the original $\Delta\chi^2 < 0$ regions (that is, before applying eq. (5.14)) is allowed. This region is located in the 2σ region of the ΛCDM case.

In Fig. 5.7, the $\Delta\chi^2 < 0$ regions in each projection are also truncated with respect to Fig. 5.3, restricting the lower range of σ_8 and the higher range of γ and Ω_m.

The positivity condition (5.14) is thus a very strong constraint on the cosmological parameters, since it forbids large values of $\Omega_m \gtrsim 0.4$. Indeed, for these values, the DE density crosses zero within our data range, therefore these values are not allowed here. On the other hand, for low enough values, $\Omega_{DE}(z)$ never crosses zero.

5.5 Discussion and conclusion

Using model-independent reconstructions of the expansion history from type Ia supernovae data, we fit the growth data and obtain constraints on $(\Omega_m, \gamma, \sigma_8)$. These model-independent constraints on the cosmological parameters are broader than the ΛCDM ones, but fully consistent. When all three cosmological parameter are let free, they are not well constrained, and it is possible to find expansion histories with cosmological parameters that are far from the ΛCDM constraints that give a reasonable fit to the data.

However, when restricting the combinations of Ω_m and the reconstructed expansion histories $h(z)$ that yield a positive dark energy density parameter ($h^2(z) - \Omega_m(1+z)^3 > 0$), the constraints on the cosmological parameters become stronger. Moreover, when imposing GR, i.e., fixing $\gamma = 0.55$, the model-independent contours are truncated and fully contained within the ΛCDM ones, showing strong evidence in favour of ΛCDM. That is, combinations of large Ω_m with expansion histories that are too different from ΛCDM are excluded. It should be noted that in [105], γ depends on w following $\gamma(w) = 0.55 + 0.05w(z = 1)$, therefore fixing $\gamma = 0.55$ is not completely model-independent. However, we expect it to have little influence on the results presented here.

Our constraints are more stringent than [138] thanks to the better quality of the data and the introduction of the DE density positivity condition. The results are consistent with a flat-ΛCDM Universe and gravity described by general relativity, although modified theories of gravity predicting different growth index cannot be ruled out at this stage. The combined χ^2 being currently dominated by the supernovae data, better growth measurements are needed to further constrain gravity theory.

Future surveys such as the Dark Energy Spectroscopic Instrument [64] will bring down the errors on the growth measurements, while surveys such as the Wide Field Infrared Survey Telescope [144] and the Large Synoptic Survey Telescope [88] are expected to observe thousands of supernovae, increasing the quality of the data and covering a larger redshift range.

Acknowledgements

We thank Eric Linder for useful discussions, and Teppei Okumura for providing us with the $f\sigma_8$ data. The computations were performed by using the high performance computing cluster Polaris at the Korea Astronomy and Space Science Institute. A.S. would like to acknowledge the support of the National Research Foundation of Korea (NRF-2016R1C1B2016478). The authors thank the Yukawa Institute for Theoretical Physics at Kyoto University. Discussions during the CosKASI-ICG-NAOC-YITP joint workshop YITP-T-17-03 were useful to complete this work.

5.6 Data visualization

For visualization purpose, Fig. 5.8 shows some reconstructed $f\sigma_8$ verifying eq. (5.14) and with $\chi^2 < \chi^2_{\Lambda\mathrm{CDM}}$.

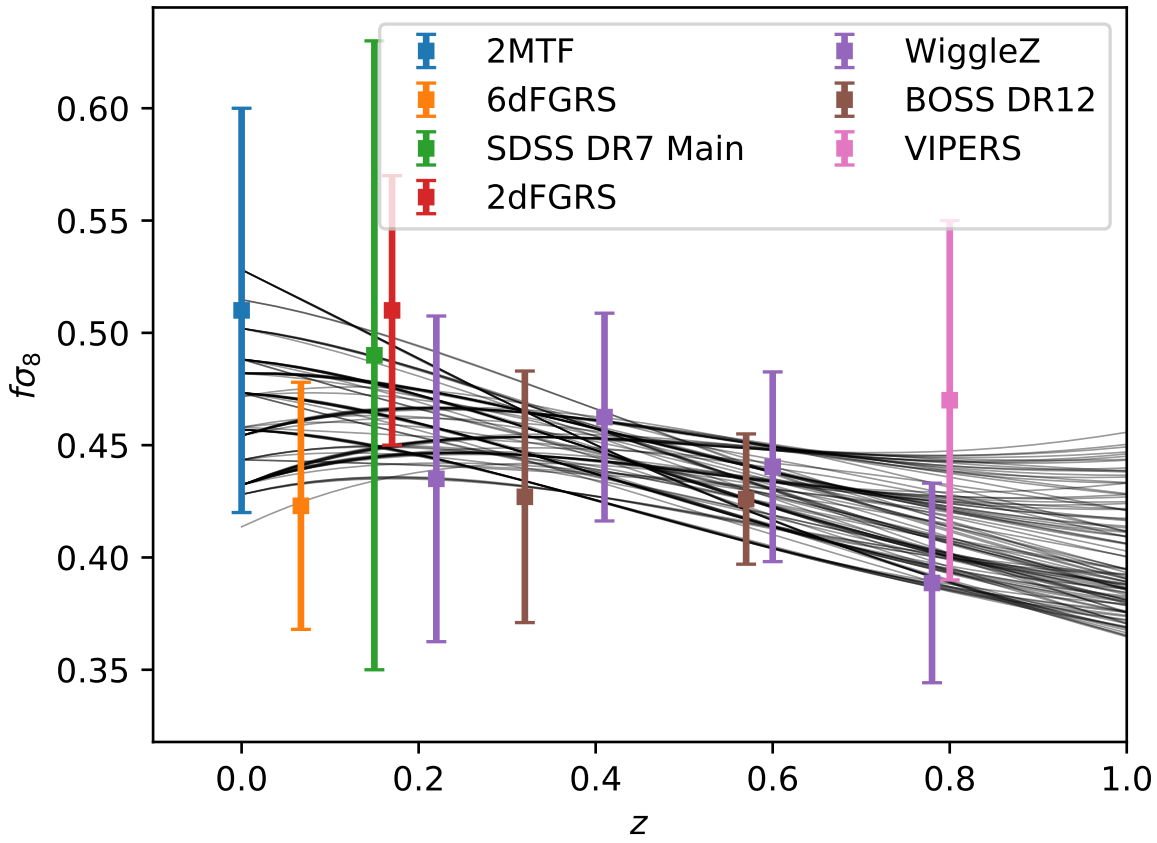

Figure 5.8: $f\sigma_8$ data and reconstructed $f\sigma_8$ with free $(\Omega_m, \gamma, \sigma_8)$. All lines shown here have $\chi^2 < \chi^2_{\Lambda CDM}$.

Chapter 6

Summary

In this thesis, we have explored different theories and approaches to addressing some of the puzzles in cosmology. Specifically, in part I, we focused on the aspect of the early universe. We introduced two different approaches to understanding very early era of the expansion history of universe. In chapter 2, we introduced Cuscuton gravity, a form of modified gravity via an auxiliary field without its own dynamics. By studying the evolution of perturbations given a toy model of Cuscuton gravity, we showed that a non-singular bouncing universe can be realized without having any catastrophic instabilities. There are other important steps for the theory such as matching with the observational values of the amplitude and scale invariance of the power spectrum. In fact, recently the analysis of power spectrum for both scalar modes and the tensor modes have been studied in [93].

In chapters 3, I briefly reviewed the effective field theory approach to inflation (EFToI). We first write down the most generic action that satisfies 3-diff invariance, and then restore the time symmetry. Different models of single field inflationary scenarios, including the canonical slow-roll inflation, can be realized through this approach. In chapter 4 we extended the formalism of the EFToI to include the terms that produce $k^6 \sim \omega^2$ dispersion relations. These terms were previously excluded in the original studies of the EFToI since k^6 dispersion relations would be strongly coupled at low energy scales. However, it has been shown that in certain regions of parameter space, the theory remains weakly coupled throughout the history of its evolution. We compute the power spectrum and the non-Gaussianity of the theory to constrain these possible regions of parameter space, and show that there exists some domain where the theory is valid.

In part II, we switch our focus to the observables of the late universe. From the supernova type Ia data, we reconstruct the expansion history of the universe and then fit the growth rate measurements to the reconstructed history. We then put a model independent cosmological constraints on some of the key observable parameters of ΛCDM, including the mass density parameter Ω_m. The constraints generally agree with the concordance model, but the precision of the data is not yet sufficient to rule out some theories of modified gravity. Furthermore, when we require that the dark energy density be positive at all redshift, the constraints seems to be in favor of ΛCDM model over other theories of gravity and universe. Stronger equipment and

more precise observation will provide us with a stronger restrictions and constraints on possible models of the universe. For example, surveys such as the Wide Field Infrared Survey and the Large Synoptic Survey Telescope are expected to give us the improved quality of the data from the supernovae observations.

Overall, with more novel ideas being conjectured every day and advancing technologies to back up the theories with data, we one day hope to have more complete understanding of the history of the universe from the very early era to the present.

References

[1] Allan Adams, Nima Arkani-Hamed, Sergei Dubovsky, Alberto Nicolis, and Riccardo Rattazzi. Causality, analyticity and an IR obstruction to UV completion. *JHEP*, 10:014, 2006.

[2] P. A. R. Ade et al. Planck 2013 Results. XXIV. Constraints on primordial non-Gaussianity. *Astron. Astrophys.*, 571:A24, 2014.

[3] Peter Adshead, Diego Blas, C. P. Burgess, Peter Hayman, and Subodh P Patil. Magnon Inflation: Slow Roll with Steep Potentials. *JCAP*, 1611(11):009, 2016.

[4] Niayesh Afshordi. Cuscuton and low energy limit of Horava-Lifshitz gravity. *Phys. Rev.*, D80:081502, 2009.

[5] Niayesh Afshordi, Daniel J.H. Chung, Michael Doran, and Ghazal Geshnizjani. Cuscuton Cosmology: Dark Energy meets Modified Gravity. *Phys.Rev.*, D75:123509, 2007.

[6] Niayesh Afshordi, Daniel J.H. Chung, and Ghazal Geshnizjani. Cuscuton: A Causal Field Theory with an Infinite Speed of Sound. *Phys.Rev.*, D75:083513, 2007.

[7] N. Aghanim, Y. Akrami, M. Ashdown, J. Aumont, C. Baccigalupi, M. Ballardini, A. J. Banday, R. B. Barreiro, N. Bartolo, and et al. Planck 2018 results. *Astronomy & Astrophysics*, 641:A6, Sep 2020.

[8] Ivan Agullo and Leonard Parker. Non-gaussianities and the Stimulated creation of quanta in the inflationary universe. *Phys. Rev.*, D83:063526, 2011.

[9] Y. Akrami, M. Ashdown, J. Aumont, C. Baccigalupi, M. Ballardini, A. J. Banday, R. B. Barreiro, N. Bartolo, S. Basak, and et al. Planck2018 results. *Astronomy & Astrophysics*, 641:A7, Sep 2020.

[10] Shadab Alam, Metin Ata, Stephen Bailey, Florian Beutler, Dmitry Bizyaev, Jonathan A. Blazek, Adam S. Bolton, Joel R. Brownstein, Angela Burden, Chia-Hsun Chuang, Johan Comparat, Antonio J. Cuesta, Kyle S. Dawson, Daniel J. Eisenstein, Stephanie Escoffier, Héctor Gil-Marín, Jan Niklas Grieb, Nick Hand, Shirley Ho, Karen Kinemuchi, David Kirkby, Francisco Kitaura, Elena Malanushenko, Viktor Malanushenko, Claudia Maraston, Cameron K. McBride, Robert C. Nichol, Matthew D. Olmstead, Daniel Oravetz,

Nikhil Padmanabhan, Nathalie Palanque-Delabrouille, Kaike Pan, Marcos Pellejero-Ibanez, Will J. Percival, Patrick Petitjean, Francisco Prada, Adrian M. Price-Whelan, Beth A. Reid, Sergio A. Rodríguez-Torres, Natalie A. Roe, Ashley J. Ross, Nicholas P. Ross, Graziano Rossi, Jose Alberto Rubiño-Martín, Shun Saito, Salvador Salazar-Albornoz, Lado Samushia, Ariel G. Sánchez, Siddharth Satpathy, David J. Schlegel, Donald P. Schneider, Claudia G. Scóccola, Hee-Jong Seo, Erin S. Sheldon, Audrey Simmons, Anže Slosar, Michael A. Strauss, Molly E. C. Swanson, Daniel Thomas, Jeremy L. Tinker, Rita Tojeiro, Mariana Vargas Magaña, Jose Alberto Vazquez, Licia Verde, David A. Wake, Yuting Wang, David H. Weinberg, Martin White, W. Michael Wood-Vasey, Christophe Yèche, Idit Zehavi, Zhongxu Zhai, and Gong-Bo Zhao. The clustering of galaxies in the completed SDSS-III Baryon Oscillation Spectroscopic Survey: cosmological analysis of the DR12 galaxy sample. MNRAS, 470(3):2617–2652, September 2017.

[11] Mohsen Alishahiha, Eva Silverstein, and David Tong. DBI in the sky. *Phys. Rev.*, D70:123505, 2004.

[12] Nima Arkani-Hamed, Paolo Creminelli, Shinji Mukohyama, and Matias Zaldarriaga. Ghost inflation. *JCAP*, 0404:001, 2004.

[13] C. Armendariz-Picon, T. Damour, and Viatcheslav F. Mukhanov. k - inflation. *Phys. Lett.*, B458:209–218, 1999.

[14] C. Armendariz-Picon, T. Damour, and Viatcheslav F. Mukhanov. k - inflation. *Phys. Lett.*, B458:209–218, 1999.

[15] C. Armendariz-Picon, Viatcheslav F. Mukhanov, and Paul J. Steinhardt. A Dynamical solution to the problem of a small cosmological constant and late time cosmic acceleration. *Phys. Rev. Lett.*, 85:4438–4441, 2000.

[16] C. Armendariz-Picon, Viatcheslav F. Mukhanov, and Paul J. Steinhardt. Essentials of k essence. *Phys. Rev.*, D63:103510, 2001.

[17] Richard L. Arnowitt, Stanley Deser, and Charles W. Misner. Dynamical Structure and Definition of Energy in General Relativity. *Phys. Rev.*, 116:1322–1330, 1959.

[18] Frederico Arroja and Misao Sasaki. A note on the equivalence of a barotropic perfect fluid with a K-essence scalar field. *Phys.Rev.*, D81:107301, 2010.

[19] Amjad Ashoorioon. Non-Unitary Evolution in the General Extended EFT of Inflation \& Excited Initial States. *JHEP*, 12:012, 2018.

[20] Amjad Ashoorioon, Roberto Casadio, Michele Cicoli, Ghazal Geshnizjani, and Hyung J. Kim. Extended Effective Field Theory of Inflation. *JHEP*, 02:172, 2018.

[21] Amjad Ashoorioon, Roberto Casadio, Ghazal Geshnizjani, and Hyung J. Kim. Getting Super-Excited with Modified Dispersion Relations. *JCAP*, 1709(09):008, 2017.

[22] Amjad Ashoorioon, Diego Chialva, and Ulf Danielsson. Effects of Nonlinear Dispersion Relations on Non-Gaussianities. *JCAP*, 1106:034, 2011.

[23] Amjad Ashoorioon, Konstantinos Dimopoulos, M. M. Sheikh-Jabbari, and Gary Shiu. Non-Bunch?Davis initial state reconciles chaotic models with BICEP and Planck. *Phys. Lett.*, B737:98–102, 2014.

[24] Amjad Ashoorioon, Konstantinos Dimopoulos, M. M. Sheikh-Jabbari, and Gary Shiu. Reconciliation of High Energy Scale Models of Inflation with Planck. *JCAP*, 1402:025, 2014.

[25] Amjad Ashoorioon and Gary Shiu. A Note on Calm Excited States of Inflation. *JCAP*, 1103:025, 2011.

[26] Eugeny Babichev, Viatcheslav Mukhanov, and Alexander Vikman. k-Essence, superluminal propagation, causality and emergent geometry. *JHEP*, 02:101, 2008.

[27] Nicola Bartolo, Matteo Fasiello, Sabino Matarrese, and Antonio Riotto. Large non-gaussianities in the effective field theory approach to single-field inflation: the bispectrum. *Journal of Cosmology and Astroparticle Physics*, 2010(08):008–008, Aug 2010.

[28] Nicola Bartolo, Matteo Fasiello, Sabino Matarrese, and Antonio Riotto. Large non-Gaussianities in the Effective Field Theory Approach to Single-Field Inflation: the Bispectrum. *JCAP*, 1008:008, 2010.

[29] Spyros Basilakos. The ΛCDM Growth Rate of Structure Revisited. *International Journal of Modern Physics D*, 21(7):1250064, July 2012.

[30] Daniel Baumann and Daniel Green. Equilateral Non-Gaussianity and New Physics on the Horizon. *JCAP*, 1109:014, 2011.

[31] Rachel Bean, Daniel J.H. Chung, and Ghazal Geshnizjani. Reconstructing a general inflationary action. *Phys.Rev.*, D78:023517, 2008.

[32] Rachel Bean and Matipon Tangmatitham. Current constraints on the cosmic growth history. Phys. Rev. D, 81(8):083534, April 2010.

[33] C. L. Bennett, M. Halpern, G. Hinshaw, N. Jarosik, A. Kogut, M. Limon, S. S. Meyer, L. Page, D. N. Spergel, G. S. Tucker, and et al. First-year wilkinson microwave anisotropy probe (wmap) observations: Preliminary maps and basic results. *The Astrophysical Journal Supplement Series*, 148(1):1–27, Sep 2003.

[34] M. Betoule, R. Kessler, J. Guy, J. Mosher, D. Hardin, R. Biswas, P. Astier, P. El-Hage, M. Konig, S. Kuhlmann, J. Marriner, R. Pain, N. Regnault, C. Balland, B. A. Bassett, P. J. Brown, H. Campbell, R. G. Carlberg, F. Cellier-Holzem, D. Cinabro, A. Conley, C. B. D'Andrea, D. L. DePoy, M. Doi, R. S. Ellis, S. Fabbro, A. V. Filippenko, R. J.

Foley, J. A. Frieman, D. Fouchez, L. Galbany, A. Goobar, R. R. Gupta, G. J. Hill, R. Hlozek, C. J. Hogan, I. M. Hook, D. A. Howell, S. W. Jha, L. Le Guillou, G. Leloudas, C. Lidman, J. L. Marshall, A. Möller, A. M. Mourão, J. Neveu, R. Nichol, M. D. Olmstead, N. Palanque-Delabrouille, S. Perlmutter, J. L. Prieto, C. J. Pritchet, M. Richmond, A. G. Riess, V. Ruhlmann-Kleider, M. Sako, K. Schahmaneche, D. P. Schneider, M. Smith, J. Sollerman, M. Sullivan, N. A. Walton, and C. J. Wheeler. Improved cosmological constraints from a joint analysis of the SDSS-II and SNLS supernova samples. A&A, 568:A22, August 2014.

[35] Florian Beutler, Chris Blake, Matthew Colless, D. Heath Jones, Lister Staveley-Smith, Gregory B. Poole, Lachlan Campbell, Quentin Parker, Will Saunders, and Fred Watson. The 6dF Galaxy Survey: z$\approx$ 0 measurements of the growth rate and σ_8. MNRAS, 423(4):3430–3444, July 2012.

[36] N. D. Birrell and P. C. W. Davies. Quantum fields in curved space. 1982.

[37] Chris Blake, Sarah Brough, Matthew Colless, Carlos Contreras, Warrick Couch, Scott Croom, Tamara Davis, Michael J. Drinkwater, Karl Forster, David Gilbank, Mike Gladders, Karl Glazebrook, Ben Jelliffe, Russell J. Jurek, I. Hui Li, Barry Madore, D. Christopher Martin, Kevin Pimbblet, Gregory B. Poole, Michael Pracy, Rob Sharp, Emily Wisnioski, David Woods, Ted K. Wyder, and H. K. C. Yee. The WiggleZ Dark Energy Survey: the growth rate of cosmic structure since redshift z=0.9. MNRAS, 415(3):2876–2891, August 2011.

[38] Arvind Borde, Alan H. Guth, and Alexander Vilenkin. Inflationary space-times are incompletein past directions. *Phys. Rev. Lett.*, 90:151301, 2003.

[39] Arvind Borde, Alan H. Guth, and Alexander Vilenkin. Inflationary spacetimes are incomplete in past directions. *Physical Review Letters*, 90(15), Apr 2003.

[40] Supranta S. Boruah, Hyung J. Kim, and Ghazal Geshnizjani. Theory of Cosmological Perturbations with Cuscuton. *JCAP*, 1707(07):022, 2017.

[41] Supranta S. Boruah, Hyung J. Kim, Michael Rouben, and Ghazal Geshnizjani. Cuscuton bounce. *Journal of Cosmology and Astroparticle Physics*, 2018(08):031–031, Aug 2018.

[42] Robert H. Brandenberger. Introduction to Early Universe Cosmology. *PoS*, ICFI2010:001, 2010.

[43] Robert H. Brandenberger, H. Feldman, and Viatcheslav F. Mukhanov. Classical and quantum theory of perturbations in inflationary universe models. pages 19–30, 1993.

[44] C. P. Burgess and M. Williams. Who you gonna call? runaway ghosts, higher derivatives and time-dependence in efts. *Journal of High Energy Physics*, 2014(8), Aug 2014.

[45] Yi-Fu Cai, Damien A. Easson, and Robert Brandenberger. Towards a Nonsingular Bouncing Cosmology. *JCAP*, 1208:020, 2012.

[46] Yi-Fu Cai, Evan McDonough, Francis Duplessis, and Robert H. Brandenberger. Two Field Matter Bounce Cosmology. *JCAP*, 1310:024, 2013.

[47] Yong Cai, Hai-Guang Li, Taotao Qiu, and Yun-Song Piao. The Effective Field Theory of nonsingular cosmology: II. *Eur. Phys. J.*, C77(6):369, 2017.

[48] Yong Cai, Youping Wan, Hai-Guang Li, Taotao Qiu, and Yun-Song Piao. The Effective Field Theory of nonsingular cosmology. *JHEP*, 01:090, 2017.

[49] Yong Cai, Yu-Tong Wang, and Yun-Song Piao. Is there an effect of a nontrivial c_T during inflation? *Phys. Rev.*, D93(6):063005, 2016.

[50] Clifford Cheung, Paolo Creminelli, A. Liam Fitzpatrick, Jared Kaplan, and Leonardo Senatore. The Effective Field Theory of Inflation. *JHEP*, 03:014, 2008.

[51] Planck Collaboration, Y. Akrami, F. Arroja, M. Ashdown, J. Aumont, C. Baccigalupi, M. Ballardini, A. J. Banday, R. B. Barreiro, N. Bartolo, S. Basak, K. Benabed, J. P. Bernard, M. Bersanelli, P. Bielewicz, J. R. Bond, J. Borrill, F. R. Bouchet, M. Bucher, C. Burigana, R. C. Butler, E. Calabrese, J. F. Cardoso, B. Casaponsa, A. Challinor, H. C. Chiang, L. P. L. Colombo, C. Combet, B. P. Crill, F. Cuttaia, P. de Bernardis, A. de Rosa, G. de Zotti, J. Delabrouille, J. M. Delouis, E. Di Valentino, J. M. Diego, O. Doré, M. Douspis, A. Ducout, X. Dupac, S. Dusini, G. Efstathiou, F. Elsner, T. A. Enßlin, H. K. Eriksen, Y. Fantaye, J. Fergusson, R. Fernandez-Cobos, F. Finelli, M. Frailis, A. A. Fraisse, E. Franceschi, A. Frolov, S. Galeotta, K. Ganga, R. T. Génova-Santos, M. Gerbino, J. González-Nuevo, K. M. Górski, S. Gratton, A. Gruppuso, J. E. Gudmundsson, J. Hamann, W. Handley, F. K. Hansen, D. Herranz, E. Hivon, Z. Huang, A. H. Jaffe, W. C. Jones, G. Jung, E. Keihänen, R. Keskitalo, K. Kiiveri, J. Kim, N. Krachmalnicoff, M. Kunz, H. Kurki-Suonio, J. M. Lamarre, A. Lasenby, M. Lattanzi, C. R. Lawrence, M. Le Jeune, F. Levrier, A. Lewis, M. Liguori, P. B. Lilje, V. Lindholm, M. López-Caniego, Y. Z. Ma, J. F. Macías-Pérez, G. Maggio, D. Maino, N. Mandolesi, A. Marcos-Caballero, M. Maris, P. G. Martin, E. Martínez-González, S. Matarrese, N. Mauri, J. D. McEwen, P. D. Meerburg, P. R. Meinhold, A. Melchiorri, A. Mennella, M. Migliaccio, M. A. Miville-Deschênes, D. Molinari, A. Moneti, L. Montier, G. Morgante, A. Moss, M. Münchmeyer, P. Natoli, F. Oppizzi, L. Pagano, D. Paoletti, B. Partridge, G. Patanchon, F. Perrotta, V. Pettorino, F. Piacentini, G. Polenta, J. L. Puget, J. P. Rachen, B. Racine, M. Reinecke, M. Remazeilles, A. Renzi, G. Rocha, J. A. Rubiño-Martín, B. Ruiz-Granados, L. Salvati, M. Savelainen, D. Scott, E. P. S. Shellard, M. Shiraishi, C. Sirignano, G. Sirri, K. Smith, L. D. Spencer, L. Stanco, R. Sunyaev, A. S. Suur-Uski, J. A. Tauber, D. Tavagnacco, M. Tenti, L. Toffolatti, M. Tomasi, T. Trombetti, J. Valiviita, B. Van Tent, P. Vielva, F. Villa, N. Vittorio, B. D. Wandelt, I. K. Wehus, A. Zacchei, and A. Zonca. Planck 2018 results. ix. constraints on primordial non-gaussianity, 2019.

[52] Paolo Creminelli, Jérôme Gleyzes, Jorge Noreña, and Filippo Vernizzi. Resilience of the standard predictions for primordial tensor modes. *Phys. Rev. Lett.*, 113(23):231301, 2014.

[53] Paolo Creminelli, Kurt Hinterbichler, Justin Khoury, Alberto Nicolis, and Enrico Trincherini. Subluminal Galilean Genesis. *JHEP*, 02:006, 2013.

[54] Paolo Creminelli, Markus A. Luty, Alberto Nicolis, and Leonardo Senatore. Starting the Universe: Stable Violation of the Null Energy Condition and Non-standard Cosmologies. *JHEP*, 12:080, 2006.

[55] Paolo Creminelli, Markus A. Luty, Alberto Nicolis, and Leonardo Senatore. Starting the Universe: Stable Violation of the Null Energy Condition and Non-standard Cosmologies. *JHEP*, 12:080, 2006.

[56] Paolo Creminelli, Alberto Nicolis, and Enrico Trincherini. Galilean Genesis: An Alternative to inflation. *JCAP*, 1011:021, 2010.

[57] Paolo Creminelli, David Pirtskhalava, Luca Santoni, and Enrico Trincherini. Stability of Geodesically Complete Cosmologies. *JCAP*, 1611(11):047, 2016.

[58] G. D'Amico, C. de Rham, S. Dubovsky, G. Gabadadze, D. Pirtskhalava, and A. J. Tolley. Massive Cosmologies. *Phys. Rev.*, D84:124046, 2011.

[59] Antonio De Felice and Shinji Tsujikawa. f(R) Theories. *Living Reviews in Relativity*, 13(1):3, June 2010.

[60] Sylvain de la Torre and John A. Peacock. Reconstructing the distribution of haloes and mock galaxies below the resolution limit in cosmological simulations. MNRAS, 435(1):743–748, October 2013.

[61] Claudia de Rham and Scott Melville. Unitary null energy condition violation in P(X) cosmologies. *Phys. Rev.*, D95(12):123523, 2017.

[62] F.J. de Urries and J. Julve. Ostrogradski formalism for higher derivative scalar field theories. *J.Phys.*, A31:6949–6964, 1998.

[63] Cedric Deffayet, Oriol Pujolas, Ignacy Sawicki, and Alexander Vikman. Imperfect Dark Energy from Kinetic Gravity Braiding. *JCAP*, 1010:026, 2010.

[64] DESI Collaboration, Amir Aghamousa, Jessica Aguilar, Steve Ahlen, Shadab Alam, Lori E. Allen, Carlos Allende Prieto, James Annis, Stephen Bailey, Christophe Balland, Otger Ballester, Charles Baltay, Lucas Beaufore, Chris Bebek, Timothy C. Beers, Eric F. Bell, José Luis Bernal, Robert Besuner, Florian Beutler, Chris Blake, Hannes Bleuler, Michael Blomqvist, Robert Blum, Adam S. Bolton, Cesar Briceno, David Brooks, Joel R. Brownstein, Elizabeth Buckley-Geer, Angela Burden, Etienne Burtin, Nicolas G. Busca, Robert N. Cahn, Yan-Chuan Cai, Laia Cardiel-Sas, Raymond G. Carlberg, Pierre-Henri Carton, Ricard Casas, Francisco J. Castander, Jorge L. Cervantes-Cota, Todd M. Claybaugh, Madeline Close, Carl T. Coker, Shaun Cole, Johan Comparat, Andrew P. Cooper, M. C. Cousinou, Martin Crocce, Jean-Gabriel Cuby, Daniel P. Cunningham,

Tamara M. Davis, Kyle S. Dawson, Axel de la Macorra, Juan De Vicente, Timothée Delubac, Mark Derwent, Arjun Dey, Govinda Dhungana, Zhejie Ding, Peter Doel, Yutong T. Duan, Anne Ealet, Jerry Edelstein, Sarah Eftekharzadeh, Daniel J. Eisenstein, Ann Elliott, Stéphanie Escoffier, Matthew Evatt, Parker Fagrelius, Xiaohui Fan, Kevin Fanning, Arya Farahi, Jay Farihi, Ginevra Favole, Yu Feng, Enrique Fernandez, Joseph R. Findlay, Douglas P. Finkbeiner, Michael J. Fitzpatrick, Brenna Flaugher, Samuel Flender, Andreu Font-Ribera, Jaime E. Forero-Romero, Pablo Fosalba, Carlos S. Frenk, Michele Fumagalli, Boris T. Gaensicke, Giuseppe Gallo, Juan Garcia-Bellido, Enrique Gaztanaga, Nicola Pietro Gentile Fusillo, Terry Gerard, Irena Gershkovich, Tommaso Giannantonio, Denis Gillet, Guillermo Gonzalez-de-Rivera, Violeta Gonzalez-Perez, Shelby Gott, Or Graur, Gaston Gutierrez, Julien Guy, Salman Habib, Henry Heetderks, Ian Heetderks, Katrin Heitmann, Wojciech A. Hellwing, David A. Herrera, Shirley Ho, Stephen Holland, Klaus Honscheid, Eric Huff, Timothy A. Hutchinson, Dragan Huterer, Ho Seong Hwang, Joseph Maria Illa Laguna, Yuzo Ishikawa, Dianna Jacobs, Niall Jeffrey, Patrick Jelinsky, Elise Jennings, Linhua Jiang, Jorge Jimenez, Jennifer Johnson, Richard Joyce, Eric Jullo, Stéphanie Juneau, Sami Kama, Armin Karcher, Sonia Karkar, Robert Kehoe, Noble Kennamer, Stephen Kent, Martin Kilbinger, Alex G. Kim, David Kirkby, Theodore Kisner, Ellie Kitanidis, Jean-Paul Kneib, Sergey Koposov, Eve Kovacs, Kazuya Koyama, Anthony Kremin, Richard Kron, Luzius Kronig, Andrea Kueter-Young, Cedric G. Lacey, Robin Lafever, Ofer Lahav, Andrew Lambert, Michael Lampton, Martin Landriau, Dustin Lang, Tod R. Lauer, Jean-Marc Le Goff, Laurent Le Guillou, Auguste Le Van Suu, Jae Hyeon Lee, Su-Jeong Lee, Daniela Leitner, Michael Lesser, Michael E. Levi, Benjamin L'Huillier, Baojiu Li, Ming Liang, Huan Lin, Eric Linder, Sarah R. Loebman, Zarija Lukić, Jun Ma, Niall MacCrann, Christophe Magneville, Laleh Makarem, Marc Manera, Christopher J. Manser, Robert Marshall, Paul Martini, Richard Massey, Thomas Matheson, Jeremy McCauley, Patrick McDonald, Ian D. McGreer, Aaron Meisner, Nigel Metcalfe, Timothy N. Miller, Ramon Miquel, John Moustakas, Adam Myers, Milind Naik, Jeffrey A. Newman, Robert C. Nichol, Andrina Nicola, Luiz Nicolati da Costa, Jundan Nie, Gustavo Niz, Peder Norberg, Brian Nord, Dara Norman, Peter Nugent, Thomas O'Brien, Minji Oh, Knut A. G. Olsen, Cristobal Padilla, Hamsa Padmanabhan, Nikhil Padmanabhan, Nathalie Palanque-Delabrouille, Antonella Palmese, Daniel Pappalardo, Isabelle Pâris, Changbom Park, Anna Patej, John A. Peacock, Hiranya V. Peiris, Xiyan Peng, Will J. Percival, Sandrine Perruchot, Matthew M. Pieri, Richard Pogge, Jennifer E. Pollack, Claire Poppett, Francisco Prada, Abhishek Prakash, Ronald G. Probst, David Rabinowitz, Anand Raichoor, Chang Hee Ree, Alexandre Refregier, Xavier Regal, Beth Reid, Kevin Reil, Mehdi Rezaie, Constance M. Rockosi, Natalie Roe, Samuel Ronayette, Aaron Roodman, Ashley J. Ross, Nicholas P. Ross, Graziano Rossi, Eduardo Rozo, Vanina Ruhlmann-Kleider, Eli S. Rykoff, Cristiano Sabiu, Lado Samushia, Eusebio Sanchez, Javier Sanchez, David J. Schlegel, Michael Schneider, Michael Schubnell, Aurélia Secroun, Uros Seljak, Hee-Jong Seo, Santiago Serrano, Arman Shafieloo, Huanyuan Shan, Ray Sharples, Michael J. Sholl, William V. Shourt, Joseph H. Silber, David R. Silva, Martin M. Sirk, Anze Slosar, Alex Smith, George F. Smoot, Debopam Som, Yong-Seon Song, David Sprayberry, Ryan Staten,

Andy Stefanik, Gregory Tarle, Suk Sien Tie, Jeremy L. Tinker, Rita Tojeiro, Francisco Valdes, Octavio Valenzuela, Monica Valluri, Mariana Vargas-Magana, Licia Verde, Alistair R. Walker, Jiali Wang, Yuting Wang, Benjamin A. Weaver, Curtis Weaverdyck, Risa H. Wechsler, David H. Weinberg, Martin White, Qian Yang, Christophe Yeche, Tianmeng Zhang, Gong-Bo Zhao, Yi Zheng, Xu Zhou, Zhimin Zhou, Yaling Zhu, Hu Zou, and Ying Zu. The DESI Experiment Part I: Science,Targeting, and Survey Design. *arXiv e-prints*, page arXiv:1611.00036, October 2016.

[65] David A. Dobre, Andrei V. Frolov, José T. Gálvez Ghersi, Sabir Ramazanov, and Alexander Vikman. Unbraiding the Bounce: Superluminality around the Corner. *JCAP*, 1803:020, 2018.

[66] S. Dubovsky, T. Gregoire, A. Nicolis, and R. Rattazzi. Null energy condition and superluminal propagation. *JHEP*, 03:025, 2006.

[67] G. Dvali, G. Gabadadze, and M. Porrati. 4D gravity on a brane in 5D Minkowski space. *Physics Letters B*, 485(1-3):208–214, July 2000.

[68] Damien A. Easson, Ignacy Sawicki, and Alexander Vikman. G-Bounce. *JCAP*, 1111:021, 2011.

[69] Damien A. Easson, Ignacy Sawicki, and Alexander Vikman. When Matter Matters. *JCAP*, 1307:014, 2013.

[70] Damien A. Easson and Alexander Vikman. The Phantom of the New Oscillatory Cosmological Phase. 2016.

[71] Daniel J. Eisenstein, Idit Zehavi, David W. Hogg, Roman Scoccimarro, Michael R. Blanton, Robert C. Nichol, Ryan Scranton, Hee-Jong Seo, Max Tegmark, Zheng Zheng, Scott F. Anderson, Jim Annis, Neta Bahcall, Jon Brinkmann, Scott Burles, Francisco J. Castander, Andrew Connolly, Istvan Csabai, Mamoru Doi, Masataka Fukugita, Joshua A. Frieman, Karl Glazebrook, James E. Gunn, John S. Hendry, Gregory Hennessy, Zeljko Ivezić, Stephen Kent, Gillian R. Knapp, Huan Lin, Yeong-Shang Loh, Robert H. Lupton, Bruce Margon, Timothy A. McKay, Avery Meiksin, Jeffery A. Munn, Adrian Pope, Michael W. Richmond, David Schlegel, Donald P. Schneider, Kazuhiro Shimasaku, Christopher Stoughton, Michael A. Strauss, Mark SubbaRao, Alexander S. Szalay, István Szapudi, Douglas L. Tucker, Brian Yanny, and Donald G. York. Detection of the Baryon Acoustic Peak in the Large-Scale Correlation Function of SDSS Luminous Red Galaxies. ApJ, 633(2):560–574, November 2005.

[72] Angelika Fertig, Jean-Luc Lehners, and Enno Mallwitz. Conflation: a new type of accelerated expansion. *JCAP*, 1608(08):073, 2016.

[73] Jaume Garriga and Viatcheslav F. Mukhanov. Perturbations in k-inflation. *Phys. Lett.*, B458:219–225, 1999.

[74] Jaume Garriga and Viatcheslav F. Mukhanov. Perturbations in k-inflation. *Phys.Lett.*, B458:219–225, 1999.

[75] Héctor Gil-Marín, Will J. Percival, Licia Verde, Joel R. Brownstein, Chia-Hsun Chuang, Francisco-Shu Kitaura, Sergio A. Rodríguez-Torres, and Matthew D. Olmstead. The clustering of galaxies in the SDSS-III Baryon Oscillation Spectroscopic Survey: RSD measurement from the power spectrum and bispectrum of the DR12 BOSS galaxies. MNRAS, 465(2):1757–1788, February 2017.

[76] Henrique Gomes and Daniel C. Guariento. Hamiltonian analysis of the cuscuton. *Phys. Rev.*, D95(10):104049, 2017.

[77] Adrià Gómez-Valent, Joan Solà, and Spyros Basilakos. Dynamical vacuum energy in the expanding Universe confronted with observations: a dedicated study. J. Cosmology Astropart. Phys., 2015(1):004, January 2015.

[78] Garrett Goon and Kurt Hinterbichler. Superluminality, black holes and EFT. *JHEP*, 02:134, 2017.

[79] Michel Goossens, Frank Mittelbach, and Alexander Samarin. *The LaTeX Companion*. Addison-Wesley, Reading, Massachusetts, 1994.

[80] Alan H. Guth. Inflationary universe: A possible solution to the horizon and flatness problems. *Phys. Rev. D*, 23:347–356, Jan 1981.

[81] S. W. Hawking and G. F. R. Ellis. *The Large Scale Structure of Space-Time*. Cambridge Monographs on Mathematical Physics. Cambridge University Press, 1973.

[82] R. Holman and Andrew J. Tolley. Enhanced Non-Gaussianity from Excited Initial States. *JCAP*, 0805:001, 2008.

[83] Petr Horava. Quantum Gravity at a Lifshitz Point. *Phys.Rev.*, D79:084008, 2009.

[84] Cullan Howlett, Ashley J. Ross, Lado Samushia, Will J. Percival, and Marc Manera. The clustering of the SDSS main galaxy sample - II. Mock galaxy catalogues and a measurement of the growth of structure from redshift space distortions at z = 0.15. MNRAS, 449(1):848–866, May 2015.

[85] Cullan Howlett, Lister Staveley-Smith, Pascal J. Elahi, Tao Hong, Tom H. Jarrett, D. Heath Jones, Bärbel S. Koribalski, Lucas M. Macri, Karen L. Masters, and Christopher M. Springob. 2MTF - VI. Measuring the velocity power spectrum. MNRAS, 471(3):3135–3151, November 2017.

[86] Anna Ijjas and Paul J. Steinhardt. Classically stable nonsingular cosmological bounces. *Phys. Rev. Lett.*, 117(12):121304, 2016.

[87] Anna Ijjas and Paul J. Steinhardt. Fully stable cosmological solutions with a non-singular classical bounce. *Phys. Lett.*, B764:289–294, 2017.

[88] Željko Ivezić, Steven M. Kahn, J. Anthony Tyson, Bob Abel, Emily Acosta, Robyn Allsman, David Alonso, Yusra AlSayyad, Scott F. Anderson, John Andrew, James Roger P. Angel, George Z. Angeli, Reza Ansari, Pierre Antilogus, Constanza Araujo, Robert Armstrong, Kirk T. Arndt, Pierre Astier, Éric Aubourg, Nicole Auza, Tim S. Axelrod, Deborah J. Bard, Jeff D. Barr, Aurelian Barrau, James G. Bartlett, Amanda E. Bauer, Brian J. Bauman, Sylvain Baumont, Ellen Bechtol, Keith Bechtol, Andrew C. Becker, Jacek Becla, Cristina Beldica, Steve Bellavia, Federica B. Bianco, Rahul Biswas, Guillaume Blanc, Jonathan Blazek, Roger D. Blandford, Josh S. Bloom, Joanne Bogart, Tim W. Bond, Michael T. Booth, Anders W. Borgland, Kirk Borne, James F. Bosch, Dominique Boutigny, Craig A. Brackett, Andrew Bradshaw, William Nielsen Brandt, Michael E. Brown, James S. Bullock, Patricia Burchat, David L. Burke, Gianpietro Cagnoli, Daniel Calabrese, Shawn Callahan, Alice L. Callen, Jeffrey L. Carlin, Erin L. Carlson, Srinivasan Chandrasekharan, Glenaver Charles-Emerson, Steve Chesley, Elliott C. Cheu, Hsin-Fang Chiang, James Chiang, Carol Chirino, Derek Chow, David R. Ciardi, Charles F. Claver, Johann Cohen-Tanugi, Joseph J. Cockrum, Rebecca Coles, Andrew J. Connolly, Kem H. Cook, Asantha Cooray, Kevin R. Covey, Chris Cribbs, Wei Cui, Roc Cutri, Philip N. Daly, Scott F. Daniel, Felipe Daruich, Guillaume Daubard, Greg Daues, William Dawson, Francisco Delgado, Alfred Dellapenna, Robert de Peyster, Miguel de Val-Borro, Seth W. Digel, Peter Doherty, Richard Dubois, Gregory P. Dubois-Felsmann, Josef Durech, Frossie Economou, Tim Eifler, Michael Eracleous, Benjamin L. Emmons, Angelo Fausti Neto, Henry Ferguson, Enrique Figueroa, Merlin Fisher-Levine, Warren Focke, Michael D. Foss, James Frank, Michael D. Freemon, Emmanuel Gangler, Eric Gawiser, John C. Geary, Perry Gee, Marla Geha, Charles J. B. Gessner, Robert R. Gibson, D. Kirk Gilmore, Thomas Glanzman, William Glick, Tatiana Goldina, Daniel A. Goldstein, Iain Goodenow, Melissa L. Graham, William J. Gressler, Philippe Gris, Leanne P. Guy, Augustin Guyonnet, Gunther Haller, Ron Harris, Patrick A. Hascall, Justine Haupt, Fabio Hernandez, Sven Herrmann, Edward Hileman, Joshua Hoblitt, John A. Hodgson, Craig Hogan, James D. Howard, Dajun Huang, Michael E. Huffer, Patrick Ingraham, Walter R. Innes, Suzanne H. Jacoby, Bhuvnesh Jain, Fabrice Jammes, M. James Jee, Tim Jenness, Garrett Jernigan, Darko Jevremović, Kenneth Johns, Anthony S. Johnson, Margaret W. G. Johnson, R. Lynne Jones, Claire Juramy-Gilles, Mario Jurić, Jason S. Kalirai, Nitya J. Kallivayalil, Bryce Kalmbach, Jeffrey P. Kantor, Pierre Karst, Mansi M. Kasliwal, Heather Kelly, Richard Kessler, Veronica Kinnison, David Kirkby, Lloyd Knox, Ivan V. Kotov, Victor L. Krabbendam, K. Simon Krughoff, Petr Kubánek, John Kuczewski, Shri Kulkarni, John Ku, Nadine R. Kurita, Craig S. Lage, Ron Lambert, Travis Lange, J. Brian Langton, Laurent Le Guillou, Deborah Levine, Ming Liang, Kian-Tat Lim, Chris J. Lintott, Kevin E. Long, Margaux Lopez, Paul J. Lotz, Robert H. Lupton, Nate B. Lust, Lauren A. MacArthur, Ashish Mahabal, Rachel Mandelbaum, Thomas W. Markiewicz, Darren S. Marsh, Philip J. Marshall, Stuart Marshall, Morgan May, Robert McKercher, Michelle McQueen, Joshua Meyers, Myriam Migliore, Michelle Miller, David J. Mills, Connor Miraval, Joachim Moeyens, Fred E.

Moolekamp, David G. Monet, Marc Moniez, Serge Monkewitz, Christopher Montgomery, Christopher B. Morrison, Fritz Mueller, Gary P. Muller, Freddy Muñoz Arancibia, Douglas R. Neill, Scott P. Newbry, Jean-Yves Nief, Andrei Nomerotski, Martin Nordby, Paul O'Connor, John Oliver, Scot S. Olivier, Knut Olsen, William O'Mullane, Sandra Ortiz, Shawn Osier, Russell E. Owen, Reynald Pain, Paul E. Palecek, John K. Parejko, James B. Parsons, Nathan M. Pease, J. Matt Peterson, John R. Peterson, Donald L. Petravick, M. E. Libby Petrick, Cathy E. Petry, Francesco Pierfederici, Stephen Pietrowicz, Rob Pike, Philip A. Pinto, Raymond Plante, Stephen Plate, Joel P. Plutchak, Paul A. Price, Michael Prouza, Veljko Radeka, Jayadev Rajagopal, Andrew P. Rasmussen, Nicolas Regnault, Kevin A. Reil, David J. Reiss, Michael A. Reuter, Stephen T. Ridgway, Vincent J. Riot, Steve Ritz, Sean Robinson, William Roby, Aaron Roodman, Wayne Rosing, Cecille Roucelle, Matthew R. Rumore, Stefano Russo, Abhijit Saha, Benoit Sassolas, Terry L. Schalk, Pim Schellart, Rafe H. Schindler, Samuel Schmidt, Donald P. Schneider, Michael D. Schneider, William Schoening, German Schumacher, Megan E. Schwamb, Jacques Sebag, Brian Selvy, Glenn H. Sembroski, Lynn G. Seppala, Andrew Serio, Eduardo Serrano, Richard A. Shaw, Ian Shipsey, Jonathan Sick, Nicole Silvestri, Colin T. Slater, J. Allyn Smith, R. Chris Smith, Shahram Sobhani, Christine Soldahl, Lisa Storrie-Lombardi, Edward Stover, Michael A. Strauss, Rachel A. Street, Christopher W. Stubbs, Ian S. Sullivan, Donald Sweeney, John D. Swinbank, Alexander Szalay, Peter Takacs, Stephen A. Tether, Jon J. Thaler, John Gregg Thayer, Sandrine Thomas, Adam J. Thornton, Vaikunth Thukral, Jeffrey Tice, David E. Trilling, Max Turri, Richard Van Berg, Daniel Vanden Berk, Kurt Vetter, Francoise Virieux, Tomislav Vucina, William Wahl, Lucianne Walkowicz, Brian Walsh, Christopher W. Walter, Daniel L. Wang, Shin-Yawn Wang, Michael Warner, Oliver Wiecha, Beth Willman, Scott E. Winters, David Wittman, Sidney C. Wolff, W. Michael Wood-Vasey, Xiuqin Wu, Bo Xin, Peter Yoachim, and Hu Zhan. LSST: From Science Drivers to Reference Design and Anticipated Data Products. ApJ, 873(2):111, March 2019.

[89] Theodore Jacobson. Black hole evaporation and ultrashort distances. *Phys. Rev.*, D44:1731–1739, 1991.

[90] A. H. Jaffe, P. A. R. Ade, A. Balbi, J. J Bock, J. R. Bond, J. Borrill, A. Boscaleri, K. Coble, B. P. Crill, P. de Bernardis, and et al. Cosmology from maxima-1, boomerang, and cobe dmr cosmic microwave background observations. *Physical Review Letters*, 86(16):3475–3479, Apr 2001.

[91] Justin Khoury, Burt A. Ovrut, Paul J. Steinhardt, and Neil Turok. The Ekpyrotic universe: Colliding branes and the origin of the hot big bang. *Phys. Rev.*, D64:123522, 2001.

[92] Justin Khoury and Paul J. Steinhardt. Adiabatic Ekpyrosis: Scale-Invariant Curvature Perturbations from a Single Scalar Field in a Contracting Universe. *Phys.Rev.Lett.*, 104:091301, 2010.

[93] J. Leo Kim and Ghazal Geshnizjani. Spectrum of cuscuton bounce. *Journal of Cosmology and Astroparticle Physics*, 2021(03):104, Mar 2021.

[94] Donald Knuth. *The TEXbook*. Addison-Wesley, Reading, Massachusetts, 1986.

[95] E. Komatsu et al. Seven-Year Wilkinson Microwave Anisotropy Probe (WMAP) Observations: Cosmological Interpretation. *Astrophys. J. Suppl.*, 192:18, 2011.

[96] Eiichiro Komatsu and David N. Spergel. Acoustic signatures in the primary microwave background bispectrum. *Physical Review D*, 63(6), Feb 2001.

[97] Leslie Lamport. *LATEX — A Document Preparation System*. Addison-Wesley, Reading, Massachusetts, second edition, 1994.

[98] L.D. Landau and E.M. Lifshitz. TEXTBOOK ON THEORETICAL PHYSICS. VOL. 6: FLUID MECHANICS. 1987.

[99] Benjamin L'Huillier and Arman Shafieloo. Model-independent test of the FLRW metric, the flatness of the Universe, and non-local estimation of H_0 r_d. J. Cosmology Astropart. Phys., 2017(1):015, January 2017.

[100] Benjamin L'Huillier, Arman Shafieloo, and Hyungjin Kim. Model-independent cosmological constraints from growth and expansion. *Mon. Not. Roy. Astron. Soc.*, 476(3):3263–3268, 2018.

[101] Andrew R. Liddle and David H. Lyth. COBE, gravitational waves, inflation and extended inflation. *Phys. Lett.*, B291:391–398, 1992.

[102] Chunshan Lin, Jerome Quintin, and Robert H. Brandenberger. Massive gravity and the suppression of anisotropies and gravitational waves in a matter-dominated contracting universe. *JCAP*, 1801:011, 2018.

[103] A. Linde, V. Mukhanov, and A. Vikman. On adiabatic perturbations in the ekpyrotic scenario. *JCAP*, 1002:006, 2010.

[104] Andrei D. Linde. A New Inflationary Universe Scenario: A Possible Solution of the Horizon, Flatness, Homogeneity, Isotropy and Primordial Monopole Problems. *Phys. Lett. B*, 108:389–393, 1982.

[105] Eric V. Linder. Cosmic growth history and expansion history. Phys. Rev. D, 72(4):043529, August 2005.

[106] Eric V. Linder. Cosmic growth and expansion conjoined. *Astroparticle Physics*, 86:41–45, January 2017.

[107] Eric V. Linder and Robert N. Cahn. Parameterized beyond-Einstein growth. *Astroparticle Physics*, 28(4-5):481–488, December 2007.

[108] Joao Magueijo. Speedy sound and cosmic structure. *Phys.Rev.Lett.*, 100:231302, 2008.

[109] Jerome Martin and Robert H. Brandenberger. The TransPlanckian problem of inflationary cosmology. *Phys. Rev.*, D63:123501, 2001.

[110] Eva-Maria Mueller, Will Percival, Eric Linder, Shadab Alam, Gong-Bo Zhao, Ariel G. Sánchez, Florian Beutler, and Jon Brinkmann. The clustering of galaxies in the completed SDSS-III Baryon Oscillation Spectroscopic Survey: constraining modified gravity. MNRAS, 475(2):2122–2131, April 2018.

[111] Viatcheslav F. Mukhanov and Alexander Vikman. Enhancing the tensor-to-scalar ratio in simple inflation. *JCAP*, 0602:004, 2006.

[112] Viatcheslav F. Mukhanov and Alexander Vikman. Enhancing the tensor-to-scalar ratio in simple inflation. *JCAP*, 0602:004, 2006.

[113] S. Nesseris and L. Perivolaropoulos. Testing ΛCDM with the growth function δ(a): Current constraints. Phys. Rev. D, 77(2):023504, January 2008.

[114] Savvas Nesseris, George Pantazis, and Leandros Perivolaropoulos. Tension and constraints on modified gravity parametrizations of G_{eff}(z) from growth rate and Planck data. Phys. Rev. D, 96(2):023542, July 2017.

[115] Teppei Okumura, Chiaki Hikage, Tomonori Totani, Motonari Tonegawa, Hiroyuki Okada, Karl Glazebrook, Chris Blake, Pedro G. Ferreira, Surhud More, Atsushi Taruya, Shinji Tsujikawa, Masayuki Akiyama, Gavin Dalton, Tomotsugu Goto, Takashi Ishikawa, Fumihide Iwamuro, Takahiko Matsubara, Takahiro Nishimichi, Kouji Ohta, Ikkoh Shimizu, Ryuichi Takahashi, Naruhisa Takato, Naoyuki Tamura, Kiyoto Yabe, and Naoki Yoshida. The Subaru FMOS galaxy redshift survey (FastSound). IV. New constraint on gravity theory from redshift space distortions at z ~ 1.4. PASJ, 68(3):38, June 2016.

[116] Junpei Ooba, Bharat Ratra, and Naoshi Sugiyama. Planck 2015 Constraints on the Non-flat XCDM Inflation Model. ApJ, 869(1):34, December 2018.

[117] M. Ostrogradski. Memoires sur les equations differentielles relatives au probleme des isoperimetre. *Mem. Ac. St. Petersbourg*, VI 4:385, 1850.

[118] P. J. Peebles and Bharat Ratra. The cosmological constant and dark energy. *Reviews of Modern Physics*, 75(2):559–606, April 2003.

[119] S. Perlmutter, G. Aldering, G. Goldhaber, R. A. Knop, P. Nugent, P. G. Castro, S. Deustua, S. Fabbro, A. Goobar, D. E. Groom, I. M. Hook, A. G. Kim, M. Y. Kim, J. C. Lee, N. J. Nunes, R. Pain, C. R. Pennypacker, R. Quimby, C. Lidman, R. S. Ellis, M. Irwin, R. G. McMahon, P. Ruiz-Lapuente, N. Walton, B. Schaefer, B. J. Boyle, A. V. Filippenko, T. Matheson, A. S. Fruchter, N. Panagia, H. J. M. Newberg, W. J. Couch, and The Supernova Cosmology Project. Measurements of Ω and Λ from 42 High-Redshift Supernovae. ApJ, 517(2):565–586, June 1999.

[120] Planck Collaboration, P. A. R. Ade, N. Aghanim, M. Arnaud, M. Ashdown, J. Aumont, C. Baccigalupi, A. J. Banday, R. B. Barreiro, J. G. Bartlett, N. Bartolo, E. Battaner, R. Battye, K. Benabed, A. Benoît, A. Benoit-Lévy, J. P. Bernard, M. Bersanelli, P. Bielewicz, J. J. Bock, A. Bonaldi, L. Bonavera, J. R. Bond, J. Borrill, F. R. Bouchet, F. Boulanger, M. Bucher, C. Burigana, R. C. Butler, E. Calabrese, J. F. Cardoso, A. Catalano, A. Challinor, A. Chamballu, R. R. Chary, H. C. Chiang, J. Chluba, P. R. Christensen, S. Church, D. L. Clements, S. Colombi, L. P. L. Colombo, C. Combet, A. Coulais, B. P. Crill, A. Curto, F. Cuttaia, L. Danese, R. D. Davies, R. J. Davis, P. de Bernardis, A. de Rosa, G. de Zotti, J. Delabrouille, F. X. Désert, E. Di Valentino, C. Dickinson, J. M. Diego, K. Dolag, H. Dole, S. Donzelli, O. Doré, M. Douspis, A. Ducout, J. Dunkley, X. Dupac, G. Efstathiou, F. Elsner, T. A. Enßlin, H. K. Eriksen, M. Farhang, J. Fergusson, F. Finelli, O. Forni, M. Frailis, A. A. Fraisse, E. Franceschi, A. Frejsel, S. Galeotta, S. Galli, K. Ganga, C. Gauthier, M. Gerbino, T. Ghosh, M. Giard, Y. Giraud-Héraud, E. Giusarma, E. Gjerløw, J. González-Nuevo, K. M. Górski, S. Gratton, A. Gregorio, A. Gruppuso, J. E. Gudmundsson, J. Hamann, F. K. Hansen, D. Hanson, D. L. Harrison, G. Helou, S. Henrot-Versillé, C. Hernández-Monteagudo, D. Herranz, S. R. Hildebrandt, E. Hivon, M. Hobson, W. A. Holmes, A. Hornstrup, W. Hovest, Z. Huang, K. M. Huffenberger, G. Hurier, A. H. Jaffe, T. R. Jaffe, W. C. Jones, M. Juvela, E. Keihänen, R. Keskitalo, T. S. Kisner, R. Kneissl, J. Knoche, L. Knox, M. Kunz, H. Kurki-Suonio, G. Lagache, A. Lähteenmäki, J. M. Lamarre, A. Lasenby, M. Lattanzi, C. R. Lawrence, J. P. Leahy, R. Leonardi, J. Lesgourgues, F. Levrier, A. Lewis, M. Liguori, P. B. Lilje, M. Linden-Vørnle, M. López-Caniego, P. M. Lubin, J. F. Macías-Pérez, G. Maggio, D. Maino, N. Mandolesi, A. Mangilli, A. Marchini, M. Maris, P. G. Martin, M. Martinelli, E. Martínez-González, S. Masi, S. Matarrese, P. McGehee, P. R. Meinhold, A. Melchiorri, J. B. Melin, L. Mendes, A. Mennella, M. Migliaccio, M. Millea, S. Mitra, M. A. Miville-Deschênes, A. Moneti, L. Montier, G. Morgante, D. Mortlock, A. Moss, D. Munshi, J. A. Murphy, P. Naselsky, F. Nati, P. Natoli, C. B. Netterfield, H. U. Nørgaard-Nielsen, F. Noviello, D. Novikov, I. Novikov, C. A. Oxborrow, F. Paci, L. Pagano, F. Pajot, R. Paladini, D. Paoletti, B. Partridge, F. Pasian, G. Patanchon, T. J. Pearson, O. Perdereau, L. Perotto, F. Perrotta, V. Pettorino, F. Piacentini, M. Piat, E. Pierpaoli, D. Pietrobon, S. Plaszczynski, E. Pointecouteau, G. Polenta, L. Popa, G. W. Pratt, G. Prézeau, S. Prunet, J. L. Puget, J. P. Rachen, W. T. Reach, R. Rebolo, M. Reinecke, M. Remazeilles, C. Renault, A. Renzi, I. Ristorcelli, G. Rocha, C. Rosset, M. Rossetti, G. Roudier, B. Rouillé d'Orfeuil, M. Rowan-Robinson, J. A. Rubiño-Martín, B. Rusholme, N. Said, V. Salvatelli, L. Salvati, M. Sandri, D. Santos, M. Savelainen, G. Savini, D. Scott, M. D. Seiffert, P. Serra, E. P. S. Shellard, L. D. Spencer, M. Spinelli, V. Stolyarov, R. Stompor, R. Sudiwala, R. Sunyaev, D. Sutton, A. S. Suur-Uski, J. F. Sygnet, J. A. Tauber, L. Terenzi, L. Toffolatti, M. Tomasi, M. Tristram, T. Trombetti, M. Tucci, J. Tuovinen, M. Türler, G. Umana, L. Valenziano, J. Valiviita, F. Van Tent, P. Vielva, F. Villa, L. A. Wade, B. D. Wandelt, I. K. Wehus, M. White, S. D. M. White, A. Wilkinson, D. Yvon, A. Zacchei, and A. Zonca. Planck 2015 results. XIII. Cosmological parameters. A&A, 594:A13, September 2016.

[121] Vivian Poulin, Tristan L. Smith, Tanvi Karwal, and Marc Kamionkowski. Early Dark

Energy Can Resolve The Hubble Tension. *Phys. Rev. Lett.*, 122(22):221301, 2019.

[122] Taotao Qiu, Jarah Evslin, Yi-Fu Cai, Mingzhe Li, and Xinmin Zhang. Bouncing Galileon Cosmologies. *JCAP*, 1110:036, 2011.

[123] Adam G. Riess, Alexei V. Filippenko, Peter Challis, Alejandro Clocchiatti, Alan Diercks, Peter M. Garnavich, Ron L. Gilliland, Craig J. Hogan, Saurabh Jha, Robert P. Kirshner, and et al. Observational evidence from supernovae for an accelerating universe and a cosmological constant. *The Astronomical Journal*, 116(3):1009–1038, Sep 1998.

[124] Adam G. Riess, Alexei V. Filippenko, Peter Challis, Alejandro Clocchiatti, Alan Diercks, Peter M. Garnavich, Ron L. Gilliland, Craig J. Hogan, Saurabh Jha, Robert P. Kirshner, B. Leibundgut, M. M. Phillips, David Reiss, Brian P. Schmidt, Robert A. Schommer, R. Chris Smith, J. Spyromilio, Christopher Stubbs, Nicholas B. Suntzeff, and John Tonry. Observational Evidence from Supernovae for an Accelerating Universe and a Cosmological Constant. AJ, 116(3):1009–1038, September 1998.

[125] Antonio Enea Romano. General background conditions for K-bounce and adiabaticity. *Eur. Phys. J.*, C77(3):147, 2017.

[126] V. A. Rubakov. The Null Energy Condition and its violation. *Phys. Usp.*, 57:128–142, 2014. [Usp. Fiz. Nauk184,no.2,137(2014)].

[127] V. A. Rubakov. Can Galileons support Lorentzian wormholes? *Teor. Mat. Fiz.*, 187(2):338–349, 2016. [Theor. Math. Phys.187,no.2,743(2016)].

[128] V. A. Rubakov. More about wormholes in generalized Galileon theories. *Theor. Math. Phys.*, 188(2):1253–1258, 2016. [Teor. Mat. Fiz.188,no.2,337(2016)].

[129] Eduardo J. Ruiz and Dragan Huterer. Testing the dark energy consistency with geometry and growth. Phys. Rev. D, 91(6):063009, March 2015.

[130] V. Sahni, A. Shafieloo, and A. A. Starobinsky. Model-independent Evidence for Dark Energy Evolution from Baryon Acoustic Oscillations. ApJ, 793(2):L40, October 2014.

[131] Varun Sahni, Arman Shafieloo, and Alexei A. Starobinsky. Two new diagnostics of dark energy. Phys. Rev. D, 78(10):103502, November 2008.

[132] Varun Sahni and Yuri Shtanov. Braneworld models of dark energy. J. Cosmology Astropart. Phys., 2003(11):014, November 2003.

[133] Ignacy Sawicki and Alexander Vikman. Hidden Negative Energies in Strongly Accelerated Universes. *Phys. Rev.*, D87(6):067301, 2013.

[134] Bernard F. JR. Schutz. Perfect fluids in general relativity: velocity Potentials and variational principle. *Phys.Rev.*, D2:2762–2773, 1970.

[135] Leonardo Senatore, Kendrick M. Smith, and Matias Zaldarriaga. Non-Gaussianities in Single Field Inflation and their Optimal Limits from the WMAP 5-year Data. *JCAP*, 1001:028, 2010.

[136] Arman Shafieloo. Model-independent reconstruction of the expansion history of the Universe and the properties of dark energy. MNRAS, 380(4):1573–1580, October 2007.

[137] Arman Shafieloo, Ujjaini Alam, Varun Sahni, and Alexei A. Starobinsky. Smoothing supernova data to reconstruct the expansion history of the Universe and its age. MNRAS, 366(3):1081–1095, March 2006.

[138] Arman Shafieloo, Alex G. Kim, and Eric V. Linder. Model independent tests of cosmic growth versus expansion. Phys. Rev. D, 87(2):023520, January 2013.

[139] Sarah E. Shandera and S. H. Henry Tye. Observing brane inflation. *JCAP*, 0605:007, 2006.

[140] Gary Shiu and Bret Underwood. Observing the Geometry of Warped Compactification via Cosmic Inflation. *Phys. Rev. Lett.*, 98:051301, 2007.

[141] V. M. Slipher. Radial velocity observations of spiral nebulae. *The Observatory*, 40:304–306, August 1917.

[142] Joan Solà, Adrià Gómez-Valent, and Javier de Cruz Pérez. Dynamical dark energy: Scalar fields and running vacuum. *Modern Physics Letters A*, 32(9):1750054–144, March 2017.

[143] Yong-Seon Song and Will J. Percival. Reconstructing the history of structure formation using redshift distortions. J. Cosmology Astropart. Phys., 2009(10):004, October 2009.

[144] D. Spergel, N. Gehrels, C. Baltay, D. Bennett, J. Breckinridge, M. Donahue, A. Dressler, B. S. Gaudi, T. Greene, O. Guyon, C. Hirata, J. Kalirai, N. J. Kasdin, B. Macintosh, W. Moos, S. Perlmutter, M. Postman, B. Rauscher, J. Rhodes, Y. Wang, D. Weinberg, D. Benford, M. Hudson, W. S. Jeong, Y. Mellier, W. Traub, T. Yamada, P. Capak, J. Colbert, D. Masters, M. Penny, D. Savransky, D. Stern, N. Zimmerman, R. Barry, L. Bartusek, K. Carpenter, E. Cheng, D. Content, F. Dekens, R. Demers, K. Grady, C. Jackson, G. Kuan, J. Kruk, M. Melton, B. Nemati, B. Parvin, I. Poberezhskiy, C. Peddie, J. Ruffa, J. K. Wallace, A. Whipple, E. Wollack, and F. Zhao. Wide-Field InfrarRed Survey Telescope-Astrophysics Focused Telescope Assets WFIRST-AFTA 2015 Report. *arXiv e-prints*, page arXiv:1503.03757, March 2015.

[145] A. A. Starobinsky. Cosmic Background Anisotropy Induced by Isotropic Flat-Spectrum Gravitational-Wave Perturbations. *Sov. Astron. Lett.*, 11:133, 1985.

[146] Alexei A. Starobinsky. A New Type of Isotropic Cosmological Models Without Singularity. *Phys. Lett. B*, 91:99–102, 1980.

[147] Virginia Trimble. Existence and nature of dark matter in the universe. ARA&A, 25:425–472, January 1987.

[148] Alexander Vikman. Can dark energy evolve to the phantom? *Phys. Rev.*, D71:023515, 2005.

[149] Steven Weinberg. The cosmological constant problem. *Reviews of Modern Physics*, 61(1):1–23, January 1989.

[150] Gong-Bo Zhao, Marco Raveri, Levon Pogosian, Yuting Wang, Robert G. Crittenden, Will J. Handley, Will J. Percival, Florian Beutler, Jonathan Brinkmann, Chia-Hsun Chuang, Antonio J. Cuesta, Daniel J. Eisenstein, Francisco-Shu Kitaura, Kazuya Koyama, Benjamin L'Huillier, Robert C. Nichol, Matthew M. Pieri, Sergio Rodriguez-Torres, Ashley J. Ross, Graziano Rossi, Ariel G. Sánchez, Arman Shafieloo, Jeremy L. Tinker, Rita Tojeiro, Jose A. Vazquez, and Hanyu Zhang. Dynamical dark energy in light of the latest observations. *Nature Astronomy*, 1:627–632, August 2017.

APPENDICES

Appendix A

The Interaction Lagrangian for the EEFToI

From the terms in (4.2), we have set $\delta_1 = \delta_2 = 0$. In this Appendix I give the full expansion of the $\bar{M}_4$, δ_3 and δ_4 terms of order π^3

The contributions from the $\bar{M}_4$ **term** to the π^3 Lagrangian: $a^3\nabla^\mu\delta g^{00}\nabla^\nu\delta K_{\mu\nu}$

$$= \frac{6H\partial_i\pi\partial_j\partial_j\pi\partial_i\dot{\pi}}{a} - \frac{2H^2\partial_i\pi^2\partial_j^2\pi}{a} + 18aH^3\dot{\pi}\partial_i\pi^2 - 14aH^2\dot{\pi}\partial_i\pi\partial_i\dot{\pi} - 8aH\dot{\pi}\ddot{\pi}\partial_i^2\pi + 18a^3H^2\dot{\pi}^2\ddot{\pi}$$
$$+ \frac{\partial_j\pi\partial_i\partial_j\pi\partial_i\partial_k^2\pi}{a^3} + \frac{\partial_i\pi\partial_i\partial_j\pi\partial_k^2\partial_j\pi}{a^3} + \frac{2\ddot{\pi}\partial_i\partial_j\pi^2}{a} + \frac{\partial_j\pi\partial_i\dot{\pi}\partial_i\partial_j\dot{\pi}}{a} + \frac{5\partial_i\dot{\pi}\partial_i\partial_j\pi\partial_j\dot{\pi}}{a} + \frac{\partial_i\pi\partial_i\dot{\pi}\partial_j\partial_j\dot{\pi}}{a} \tag{A.1}$$

The contributions from the δ_3 **term** to the π^3 Lagrangian: $a^3\nabla^\mu\delta K_{\nu\mu}\nabla^\nu\delta K^\sigma{}_\sigma$

$$
\begin{aligned}
&= 3a(t)\dot\pi\left(\partial_i(\pi)\right)^2H(t)^4 + 18a(t)^3\left(\dot\pi\right)^2\ddot\pi H(t)^3 - 21a(t)\dot\pi\partial_i(\pi)\partial_i\left(\dot\pi\right)H(t)^3 + 6a(t)\left(\dot\pi\right)^2\partial_i^2(\pi)H(t)^3 \\
&- \frac{\left(\partial_i(\pi)\right)^2\partial_j^2(\pi)H(t)^3}{a(t)} + 3a(t)\dot\pi\partial_i(\pi)\partial_i\left(\ddot\pi\right)H(t)^2 + \frac{4\dot\pi\partial_i(\pi)\partial_i\left(\partial_j^2(\pi)\right)H(t)^2}{a(t)} \\
&- 6a(t)\dot\pi\ddot\pi\partial_i^2(\pi)H(t)^2 - 3a(t)\left(\dot\pi\right)^2\partial_i^2\left(\dot\pi\right)H(t)^2 + \frac{2\partial_i\left(\dot\pi\right)\partial_i\left(\partial_j(\pi)\right)\partial_j(\pi)H(t)^2}{a(t)} \\
&+ \frac{9\partial_i^2(\pi)\partial_j(\pi)\partial_j\left(\dot\pi\right)H(t)^2}{a(t)} - \frac{4\dot\pi\partial_i^2(\pi)\partial_j^2(\pi)H(t)^2}{a(t)} + 18a(t)^3\left(\dot\pi\right)^3\dot H(t)H(t)^2 \\
&- \frac{3}{2}a(t)\dot\pi\left(\partial_i(\pi)\right)^2\dot H(t)H(t)^2 + \frac{3\ddot\pi\left(\partial_i\left(\partial_j(\pi)\right)\right)^2H(t)}{a(t)} + \frac{3\partial_i^2(\pi)\left(\partial_j\left(\dot\pi\right)\right)^2H(t)}{2a(t)} \\
&+ \frac{5\dot\pi\partial_i\left(\dot\pi\right)\partial_i\left(\partial_j^2(\pi)\right)H(t)}{a(t)} + \frac{5\partial_i\left(\dot\pi\right)\partial_i\left(\partial_j\left(\dot\pi\right)\right)\partial_j(\pi)H(t)}{2a(t)} + \frac{17\partial_i\left(\dot\pi\right)\partial_i\left(\partial_j(\pi)\right)\partial_j\left(\dot\pi\right)H(t)}{2a(t)} \\
&+ \frac{3\partial_i^2\left(\dot\pi\right)\partial_j(\pi)\partial_j\left(\dot\pi\right)H(t)}{2a(t)} - \frac{4\partial_i^2(\pi)\partial_j(\pi)\partial_j\left(\partial_k^2(\pi)\right)H(t)}{a(t)^3} - \frac{\partial_i(\pi)\partial_i\left(\ddot\pi\right)\partial_j^2(\pi)H(t)}{a(t)} \\
&- \frac{\ddot\pi\partial_i^2(\pi)\partial_j^2(\pi)H(t)}{a(t)} + \frac{2\dot\pi\partial_i^2(\pi)\partial_j^2\left(\dot\pi\right)H(t)}{a(t)} + \frac{4\partial_i^2(\pi)\partial_j\left(\partial_k(\pi)\right)\partial_k\left(\partial_j(\pi)\right)H(t)}{a(t)^3} \\
&+ \frac{2\left(\partial_i\left(\partial_j(\pi)\right)\right)^2\partial_k^2(\pi)H(t)}{a(t)^3} - \frac{2\partial_i(\pi)\partial_i\left(\partial_j^2(\pi)\right)\partial_k^2(\pi)H(t)}{a(t)^3} - 27a(t)\left(\dot\pi\right)^2\partial_i^2(\pi)\dot H(t)H(t) \\
&+ \frac{3\left(\partial_i(\pi)\right)^2\partial_j^2(\pi)\dot H(t)H(t)}{2a(t)} - \frac{4\dot\pi\partial_i\left(\partial_j^2(\pi)\right)\partial_i\left(\partial_k^2(\pi)\right)}{a(t)^3} - \frac{7\partial_i\left(\partial_j(\pi)\right)\partial_i\left(\partial_k^2(\pi)\right)\partial_j\left(\dot\pi\right)}{2a(t)^3} \\
&- \frac{3\partial_i(\pi)\partial_i\left(\partial_k\left(\dot\pi\right)\right)\partial_j^2\left(\partial_k(\pi)\right)}{2a(t)^3} - \frac{\partial_i^2\left(\dot\pi\right)\partial_j^2\left(\partial_k(\pi)\right)\partial_k(\pi)}{a(t)^3} - \frac{2\partial_i^2\left(\dot\pi\right)\partial_j\left(\partial_k(\pi)\right)\partial_k\left(\partial_j(\pi)\right)}{a(t)^3} \\
&- \frac{3\partial_i^2\left(\partial_j(\pi)\right)\partial_j\left(\dot\pi\right)\partial_k^2(\pi)}{2a(t)^3} - \frac{\left(\partial_i\left(\partial_j(\pi)\right)\right)^2\partial_k^2\left(\dot\pi\right)}{a(t)^3} - \frac{\partial_i^2\left(\partial_j(\pi)\right)\partial_j(\pi)\partial_k^2\left(\dot\pi\right)}{2a(t)^3} \\
&- \frac{2\dot\pi\partial_i^2\left(\partial_j(\pi)\right)\partial_k^2\left(\partial_j(\pi)\right)}{a(t)^3} + \frac{6\dot\pi\left(\partial_i\left(\partial_j(\pi)\right)\right)^2\dot H(t)}{a(t)} + \frac{9\dot\pi\partial_i\left(\partial_j(\pi)\right)\partial_j\left(\partial_i(\pi)\right)\dot H(t)}{a(t)}
\end{aligned}
$$

The contributions from the δ_4 **term** to the π^3 Lagrangian: $: a^3 \nabla_\mu \delta K^\mu{}_\nu \nabla_\gamma \delta K^{\gamma\nu}$

$$
\begin{aligned}
= & \frac{2H(t)\partial_j^2(\pi)\left(\partial_i\left(\partial_k(\pi)\right)\right)^2}{a(t)^3} - \frac{2H(t)\partial_i(\pi)\partial_j^2(\pi)\partial_i\left(\partial_k^2(\pi)\right)}{a(t)^3} - \frac{6\dot{\pi}H(t)^2\left(\partial_i\left(\partial_j(\pi)\right)\right)^2}{a(t)} \\
& + \frac{4H(t)^2\partial_i(\pi)\partial_j^2(\pi)\partial_i(\dot{\pi})}{a(t)} - \frac{2\dot{\pi}H(t)^2\partial_i^2(\pi)\partial_j^2(\pi)}{a(t)} + \frac{4\dot{\pi}H(t)\partial_i\left(\partial_j^2(\pi)\right)\partial_i(\dot{\pi})}{a(t)} \\
& + \frac{H(t)\partial_j(\pi)\partial_i(\dot{\pi})\,\partial_i\left(\partial_j(\dot{\pi})\right)}{a(t)} + \frac{5H(t)\partial_i\left(\partial_j(\pi)\right)\partial_i(\dot{\pi})\,\partial_j(\dot{\pi})}{a(t)} + \frac{H(t)\partial_j^2(\pi)\left(\partial_i(\dot{\pi})\right)^2}{a(t)} \\
& + \frac{H(t)\partial_i(\pi)\partial_i(\dot{\pi})\,\partial_j^2(\dot{\pi})}{a(t)} - \frac{H(t)^3\left(\partial_i(\pi)\right)^2\partial_j^2(\pi)}{a(t)} + 3\dot{\pi}a(t)H(t)^4\left(\partial_i(\pi)\right)^2 \\
& - 6\dot{\pi}a(t)H(t)^3\partial_i(\pi)\partial_i(\dot{\pi}) + 12\left(\dot{\pi}\right)^2 a(t)H(t)^3\partial_i^2(\pi) - 2\dot{\pi}a(t)H(t)^2\left(\partial_i(\dot{\pi})\right)^2 \\
& - \frac{2\dot{\pi}\partial_i\left(\partial_j^2(\pi)\right)\partial_i\left(\partial_k^2(\pi)\right)}{a(t)^3} - \frac{\partial_j(\pi)\partial_i\left(\partial_k^2(\pi)\right)\partial_i\left(\partial_j(\dot{\pi})\right)}{a(t)^3} - \frac{5\partial_i\left(\partial_j(\pi)\right)\partial_i\left(\partial_k^2(\pi)\right)\partial_j(\dot{\pi})}{a(t)^3} \\
& - \frac{\partial_j^2(\pi)\partial_i\left(\partial_k^2(\pi)\right)\partial_i(\dot{\pi})}{a(t)^3} - \frac{\partial_j(\pi)\partial_i^2\left(\partial_j(\pi)\right)\partial_k^2(\dot{\pi})}{a(t)^3} + 18\left(\dot{\pi}\right)^3 a(t)^3 H(t)^4
\end{aligned}
\tag{A.2}
$$

Appendix B

f_{NL} Calculations for the local-type non-Gaussianity

For the local-type NG, we can paremetrize the size of the non-Gaussianty (f_{NL}) as

$$\zeta(x) = \zeta_L(x) - \frac{3}{5} f_{NL} \zeta_L^2(x), \tag{B.1}$$

with

$$\langle \zeta_L(x) \rangle = 0. \tag{B.2}$$

The Fourier transform of ζ_L is

$$\zeta_L(x) = \frac{1}{(2\pi)^{3/2}} \int d^3k \; e^{ikx} \zeta_L(\mathbf{k}) \tag{B.3}$$

$$\zeta(\mathbf{k}) = \frac{1}{(2\pi)^{3/2}} \int d^3x \; e^{-ikx} \zeta(x) = \int d^3x \; e^{-ikx} \left(\zeta_L(x) - \frac{3}{5} f_{NL} \zeta_L^2(x) \right) \tag{B.4}$$

$$= \int d^3x \; e^{-ikx} \left(\int d^3\tilde{k} \; e^{i\tilde{k}x} \zeta_L(\tilde{\mathbf{k}}) - \frac{3}{5} f_{NL} \frac{1}{(2\pi)^3} \int d^3\tilde{k} \; e^{i\tilde{k}x} \zeta_L(\tilde{\mathbf{k}}) \int d^3k' \; e^{ik'x} \zeta_L(\mathbf{k}') \right) \tag{B.5}$$

$$= \left(\int d^3\tilde{k} \; \delta^3(\mathbf{k} - \tilde{\mathbf{k}}) \zeta_L(\tilde{\mathbf{k}}) - \frac{3}{5} f_{NL} \frac{1}{(2\pi)^3} \int d^3\tilde{k} d^3k' \; \delta^3(\mathbf{k} - \mathbf{k}' - \tilde{\mathbf{k}}) \zeta_L(\tilde{\mathbf{k}}) \; \zeta_L(\mathbf{k}') \right) \tag{B.6}$$

$$\zeta(\mathbf{k}) = \left(\zeta_L(\mathbf{k}) - \frac{3}{5} f_{NL} \frac{1}{(2\pi)^3} \int d^3k' \; \zeta_L(\mathbf{k} - \mathbf{k}') \; \zeta_L(\mathbf{k}') \right) \tag{B.7}$$

$$\langle \zeta(\mathbf{k}_1) \zeta(\mathbf{k}_2) \zeta(\mathbf{k}_3) \rangle = \langle \zeta_L(\mathbf{k}_1) \zeta_L(\mathbf{k}_2) \zeta_L(\mathbf{k}_3) \rangle - \frac{3}{5} f_{NL} \frac{1}{(2\pi)^3} \left\langle \zeta_L(\mathbf{k}_1) \zeta_L(\mathbf{k}_2) \int d^3k' \; \zeta_L(\mathbf{k}_3 - \mathbf{k}') \; \zeta_L(\mathbf{k}') \right\rangle \ldots \tag{B.8}$$

Using Isserlis' theorem, the first term becomes

$$\langle \zeta_L(\mathbf{k}_1)\zeta_L(\mathbf{k}_2)\zeta_L(\mathbf{k}_3)\rangle = \langle \zeta_L(\mathbf{k}_1)\rangle \langle \zeta_L(\mathbf{k}_2)\zeta_L(\mathbf{k}_3)\rangle \ldots = 0 \tag{B.9}$$

The second term can also be calculated using Wick's theorem

$$\left\langle \zeta_L(\mathbf{k}_1)\zeta_L(\mathbf{k}_2)\int d^3k'\ \zeta_L(\mathbf{k}_3-\mathbf{k}')\ \zeta_L(\mathbf{k}')\right\rangle = \int d^3k'\ \langle \zeta_L(\mathbf{k}_1)\zeta_L(\mathbf{k}_2)\zeta_L(\mathbf{k}_3-\mathbf{k}')\ \zeta_L(\mathbf{k}')\rangle$$

$$= \int d^3k'\ \langle \zeta_L(\mathbf{k}_1)\zeta_L(\mathbf{k}_2)\rangle \langle \zeta_L(\mathbf{k}_3-\mathbf{k}')\ \zeta_L(\mathbf{k}')\rangle \tag{B.10}$$

$$+ \int d^3k'\ \langle \zeta_L(\mathbf{k}_1)\zeta_L(\mathbf{k}')\rangle \langle \zeta_L(\mathbf{k}_2)\zeta_L(\mathbf{k}_3-\mathbf{k}')\rangle \tag{B.11}$$

$$+ \int d^3k'\ \langle \zeta_L(\mathbf{k}_2)\zeta_L(\mathbf{k}')\rangle \langle \zeta_L(\mathbf{k}_1)\zeta_L(\mathbf{k}_3-\mathbf{k}')\rangle \tag{B.12}$$

We have

$$\langle \zeta_L(\mathbf{k}_1)\zeta_L(\mathbf{k}_2)\rangle = (2\pi)^3\delta^3(\mathbf{k}_1+\mathbf{k}_2)P_\zeta(k_1)$$

and

$$\langle \zeta_L(\mathbf{k}_3-\mathbf{k}')\ \zeta_L(\mathbf{k}')\rangle = (2\pi)^3\delta^3(\mathbf{k}_3)P_\zeta(k').$$

This means that the first term

$$\int d^3k'\ \langle \zeta_L(\mathbf{k}_1)\zeta_L(\mathbf{k}_2)\rangle \langle \zeta_L(\mathbf{k}_3-\mathbf{k}')\ \zeta_L(\mathbf{k}')\rangle = \int d^3k'\ (2\pi)^6\delta^3(\mathbf{k}_1+\mathbf{k}_2)\delta^3(\mathbf{k}_3)P(k_1)P(k') \tag{B.13}$$

does not contribute to three point function for $k_3 \neq 0$. The second and the third terms

$$\int d^3k'\ \langle \zeta_L(\mathbf{k}_1)\zeta_L(\mathbf{k}')\rangle \langle \zeta_L(\mathbf{k}_2)\zeta_L(\mathbf{k}_3-\mathbf{k}')\rangle = \int d^3k'\ (2\pi)^6\delta^3(\mathbf{k}_1+\mathbf{k}')P(k_1)\delta^3(\mathbf{k}_2+\mathbf{k}_3-\mathbf{k}')P(k_2)$$
$$= (2\pi)^6 P(k_1)\delta^3(\mathbf{k}_2+\mathbf{k}_3+\mathbf{k}_1)P(k_2)$$

$$\int d^3k'\ \langle \zeta_L(\mathbf{k}_2)\zeta_L(\mathbf{k}')\rangle \langle \zeta_L(\mathbf{k}_1)\zeta_L(\mathbf{k}_3-\mathbf{k}')\rangle = \int d^3k'\ (2\pi)^6\delta^3(\mathbf{k}_2+\mathbf{k}')P(k_2)\delta^3(\mathbf{k}_1+\mathbf{k}_3-\mathbf{k}')P(k_1)$$
$$= (2\pi)^6 P(k_1)\delta^3(\mathbf{k}_2+\mathbf{k}_3+\mathbf{k}_1)P(k_2)$$

Finally adding everything we have

$$\langle \zeta(\mathbf{k}_1)\zeta(\mathbf{k}_2)\zeta(\mathbf{k}_3)\rangle = -\frac{3}{5}f_{NL}\frac{1}{(2\pi)^3}\left\langle \zeta_L(\mathbf{k}_1)\zeta_L(\mathbf{k}_2)\int d^3k'\ \zeta_L(\mathbf{k}_3-\mathbf{k}')\ \zeta_L(\mathbf{k}')\right\rangle + \text{sym} \tag{B.14}$$

$$= -\frac{6}{5}(2\pi)^3\delta^3(\mathbf{k}_1+\mathbf{k}_2+\mathbf{k}_3)f_{NL}\Big(P(k_1)P(k_2)+P(k_3)P(k_2)+P(k_1)P(k_3)\Big) \tag{B.15}$$

Now dimensionless power spectrum is defined as $\Delta(k) = P(k)\frac{k^3}{2\pi^2}$ so substituting above we get:

$$\langle\zeta(\mathbf{k}_1)\zeta(\mathbf{k}_2)\zeta(\mathbf{k}_3)\rangle = -\frac{6}{5}(2\pi)^3\delta^3(\mathbf{k}_1+\mathbf{k}_2+\mathbf{k}_3)f_{NL}\left(\Delta(k_1)\Delta(k_2)\frac{4\pi^4}{k_1^3k_2^3}+\Delta(k_3)\Delta(k_2)\frac{4\pi^4}{k_3^3k_2^3}+\Delta(k_1)\Delta(k_3)\frac{4\pi^4}{k_3^3k_1^3}\right).$$

Since $4\pi^4 = (2\pi)^4/4$ then we get

$$\langle\zeta(\mathbf{k}_1)\zeta(\mathbf{k}_2)\zeta(\mathbf{k}_3)\rangle = -\frac{3}{10}(2\pi)^7\delta^3(\mathbf{k}_1+\mathbf{k}_2+\mathbf{k}_3)f_{NL}\left(\Delta(k_1)\Delta(k_2)\frac{1}{k_1^3k_2^3}+\Delta(k_3)\Delta(k_2)\frac{1}{k_3^3k_2^3}+\Delta(k_1)\Delta(k_3)\frac{1}{k_3^3k_1^3}\right)$$

If scale dependence of $\Delta(k)$ is negligible then we get:

$$\langle\zeta(\mathbf{k}_1)\zeta(\mathbf{k}_2)\zeta(\mathbf{k}_3)\rangle = -\frac{3}{10}(2\pi)^7\delta^3(\mathbf{k}_1+\mathbf{k}_2+\mathbf{k}_3)f_{NL}\,[\Delta(k_1)]^2\left(\frac{1}{k_1^3k_2^3}+\frac{1}{k_3^3k_2^3}+\frac{1}{k_3^3k_1^3}\right)$$

$$\langle\zeta(\mathbf{k}_1)\zeta(\mathbf{k}_2)\zeta(\mathbf{k}_3)\rangle = -\frac{3}{10}(2\pi)^7\delta^3(\mathbf{k}_1+\mathbf{k}_2+\mathbf{k}_3)f_{NL}\,[\Delta(k_1)]^2\left(\frac{k_1^3+k_2^3+k_3^3}{k_1^3k_2^3k_3^3}\right)$$

So after reordering

$$\langle\zeta(\mathbf{k}_1)\zeta(\mathbf{k}_2)\zeta(\mathbf{k}_3)\rangle = (2\pi)^7\delta^3(\mathbf{k}_1+\mathbf{k}_2+\mathbf{k}_3)\frac{[\Delta(k_1)]^2}{k_1^3k_2^3k_3^3}\times\left\{-\frac{3}{10}f_{NL}\left(k_1^3+k_2^3+k_3^3\right)\right\}$$

in general we can write different contributions as

$$\langle\zeta(\mathbf{k}_1)\zeta(\mathbf{k}_2)\zeta(\mathbf{k}_3)\rangle = (2\pi)^7\delta^3(\mathbf{k}_1+\mathbf{k}_2+\mathbf{k}_3)\frac{[\Delta(k_1)]^2}{k_1^3k_2^3k_3^3}\times\mathcal{A}(k_1,k_2,k_3)$$

Which means for the particular case of assuming

$$\zeta(x) = \zeta_L(x) - \frac{3}{5}f_{NL}\zeta_L^2(x)$$

we get

$$\mathcal{A}(k_1,k_2,k_3) = -\frac{3}{10}f_{NL}\left(k_1^3+k_2^3+k_3^3\right)$$

Appendix C

Detailed Calculations of the Three Point Functions and Preparing for the Numerical Calculations for JULIA

C.1 Transforming Coefficients

The $\zeta'(\partial\zeta)^2$ term in the original Lagrangian is written in terms of π:

$$\mathcal{L} = \cdots + C_{\dot{\pi}(\partial\pi)^2}\dot{\pi}(\partial\pi)^2 + \ldots. \tag{C.1}$$

Now we take $\pi \rightarrow \zeta = -H\pi$

$$\Rightarrow -\frac{1}{H^3}C_{\dot{\pi}(\partial\pi)^2}\dot{\zeta}(\partial\zeta)^2 \tag{C.2}$$

Then we transform from the cosmic time to the conformal time $dt \rightarrow a\ d\tau$

$$\Rightarrow -\frac{1}{aH^3}C_{\dot{\pi}(\partial\pi)^2}\zeta'(\partial\zeta)^2. \tag{C.3}$$

We now define,

$$C_{\zeta'(\partial\zeta)^2} = -\frac{1}{aH^3}C_{\dot{\pi}(\partial\pi)^2} \tag{C.4}$$

Then the three point contribution for the $\dot{\pi}(\partial\pi)^2$ can be written as

$$\begin{aligned}\langle\zeta(\mathbf{k}_1)\zeta(\mathbf{k}_2)\zeta(\mathbf{k}_3)\rangle_{\dot{\pi}(\partial\pi)^2} = -i\int_{-\infty}^{0} a(\tau')d\tau' C_{\zeta'(\partial\zeta)^2}\ 2(2\pi)^3\delta^3(\mathbf{k}_3+\mathbf{k}_2+\mathbf{k}_1)\times \\ f_{k_1}(t)f_{k_1}^{*}{}'(t')f_{k_2}(t)f_{k_2}^{*}(t')f_{k_3}(t)f_{k_3}^{*}(t')\mathbf{k}_2\cdot\mathbf{k}_3 + sym + c.c,\end{aligned} \tag{C.5}$$

where f is the mode function for ζ. The above procedure also applies for writing the contributions from the $\partial^2\pi(\partial\pi)^2$ term.

C.1.1 Transforming the Integration Variables for Numerical Calculations

We have numerical values for $u_k(x)$, so the integration has to be written in terms of $u_k(x)$ with the variable x. Again, for the contributions from the $\dot{\pi}(\partial\pi)^2$ term, we use the relations

$$\begin{aligned} x_i &= c_s k_i \tau \\ a &= -c_s k_i / H x_i \\ \sqrt{A_1} f &= -\frac{H}{a} u \\ \sqrt{A_1} f' &= -\frac{H}{a}\frac{du}{d\tau} + H^2 u = -c_s k_i \frac{H}{a}\frac{du}{dx_i} + H^2 u = x_i H^2 \frac{du}{dx_i} + H^2 u \end{aligned}$$

to obtain

$$\begin{aligned} \langle \zeta(\mathbf{k}_1)\zeta(\mathbf{k}_2)\zeta(\mathbf{k}_3)\rangle_{\dot{\pi}(\partial\pi)^2} = i \int_{-\infty}^{\tau_f} \left(\frac{H^7 x_1'}{a(\tau_f)^3 a(\tau')^2 A_1^3}\right) d\tau' \; C_{\zeta'(\partial\zeta)^2} \; 4(2\pi)^3 \delta^3(\mathbf{k}_3 + \mathbf{k}_2 + \mathbf{k}_1) \\ u_{k_1}(\tau_f) u_{k_1}^{*\prime}(\tau') u_{k_2}(\tau_f) u_{k_2}^*(\tau') u_{k_3}(\tau_f) u_{k_3}^*(\tau') \mathbf{k}_2 \cdot \mathbf{k}_3 + sym + c.c \\ - i \int_{-\infty}^{\tau_f} \left(\frac{H^7}{a(\tau_f)^3 a(\tau')^2 A_1^3}\right) d\tau' C_{\zeta'(\partial\zeta)^2} \; 4(2\pi)^3 \delta^3(\mathbf{k}_3 + \mathbf{k}_2 + \mathbf{k}_1) \\ u_{k_1}(\tau_f) u_{k_1}^*(\tau') u_{k_2}(\tau_f) u_{k_2}^*(\tau') u_{k_3}(\tau_f) u_{k_3}^*(\tau') \mathbf{k}_2 \cdot \mathbf{k}_3 + sym + c.c. \end{aligned} \tag{C.6}$$

Changing the integration variable to x_n, and substituting a, we have

$$\begin{aligned} \Rightarrow -i4(2\pi)^3 \delta^3(\mathbf{k}_3 + \mathbf{k}_2 + \mathbf{k}_1) \frac{1}{\sqrt{c_s^6 k_a^2 k_2^2 k_3^2}} \frac{H^{12} x_f^3}{(c_s k_1)^5 A_1^3} \int_{-\infty}^{x_f} (x_1')^2 dx_1' \; C_{\zeta'(\partial\zeta)^2} \\ u_{k_1}(\frac{k_3}{k_1} x_f) u_{k_1}^{*\prime}(\frac{k_3}{k_1} x_1') u_{k_2}(\frac{k_2}{k_1} x_f) u_{k_2}^*(\frac{k_2}{k_1} x_1') u_{k_3}(x_f) u_{k_3}^*(x_1') \mathbf{k}_2 \cdot \mathbf{k}_3 + sym + c.c \\ - i4(2\pi)^3 \delta^3(\mathbf{k}_3 + \mathbf{k}_2 + \mathbf{k}_3) \frac{1}{\sqrt{c_s^6 k_a^2 k_2^2 k_3^2}} \frac{H^{12} x_f^3}{(c_s k_1)^5 A_1^3} \int_{-\infty}^{x_f} x_1' dx_1' \; C_{\zeta'(\partial\zeta)^2} \\ u_{k_1}(\frac{k_3}{k_1} x_f) u_{k_1}^*(\frac{k_3}{k_1} x_1') u_{k_2}(\frac{k_2}{k_1} x_f) u_{k_2}^*(\frac{k_2}{k_1} x_1') u_{k_3}(x_f) u_{k_3}^*(x_1') \mathbf{k}_2 \cdot \mathbf{k}_3 + sym + c.c. \end{aligned} \tag{C.7}$$

Using the Cosine Law

$$k_3^2 = k_1^2 + k_2^2 - 2k_1 k_2 \cos(\theta) \Rightarrow \mathbf{k}_1 \mathbf{k}_2 = k_1 k_2 \cos(\theta) = \frac{k_3^2 - k_1^2 - k_2^2}{2}, \tag{C.8}$$

we obtain

$$\Rightarrow \langle\zeta(\mathbf{k}_1)\zeta(\mathbf{k}_2)\zeta(\mathbf{k}_3)\rangle_{\dot{\pi}(\partial\pi)^2} = -i2(2\pi)^3\delta^3(\mathbf{k}_3+\mathbf{k}_2+\mathbf{k}_1)\frac{1}{\sqrt{c_s^6k_a^2k_2^2k_3^2}}\frac{H^{12}x_f^3}{(c_sk_1)^5A_1^3}\int_{-\infty}^{x_f}(x_1')^2dx_1'\ C_{\zeta'(\partial\zeta)^2}$$

$$u_{k_1}(\frac{k_3}{k_1}x_f)u_{k_1}^{*}{}'(\frac{k_3}{k_1}x_1')u_{k_2}(\frac{k_2}{k_1}x_f)u_{k_2}^{*}(\frac{k_2}{k_1}x_1')u_{k_3}(x_f)u_{k_3}^{*}(x_1')(k_1^2-k_3^2-k_2^2)+sym+c.c$$

$$-i2(2\pi)^3\delta^3(\mathbf{k}_3+\mathbf{k}_2+\mathbf{k}_3)\frac{1}{\sqrt{c_s^6k_a^2k_2^2k_3^2}}\frac{H^{12}x_f^3}{(c_sk_1)^5A_1^3}\int_{-\infty}^{x_f}x_1'dx_1'\ C_{\zeta'(\partial\zeta)^2}$$

$$u_{k_1}(\frac{k_3}{k_1}x_f)u_{k_1}^{*}(\frac{k_3}{k_1}x_1')u_{k_2}(\frac{k_2}{k_1}x_f)u_{k_2}^{*}(\frac{k_2}{k_1}x_1')u_{k_3}(x_f)u_{k_3}^{*}(x_1')(k_1^2-k_3^2-k_2^2)+sym+c.c. \tag{C.9}$$